

FACULTY OF SCIENCE
UNIVERSITY OF COPENHAGEN



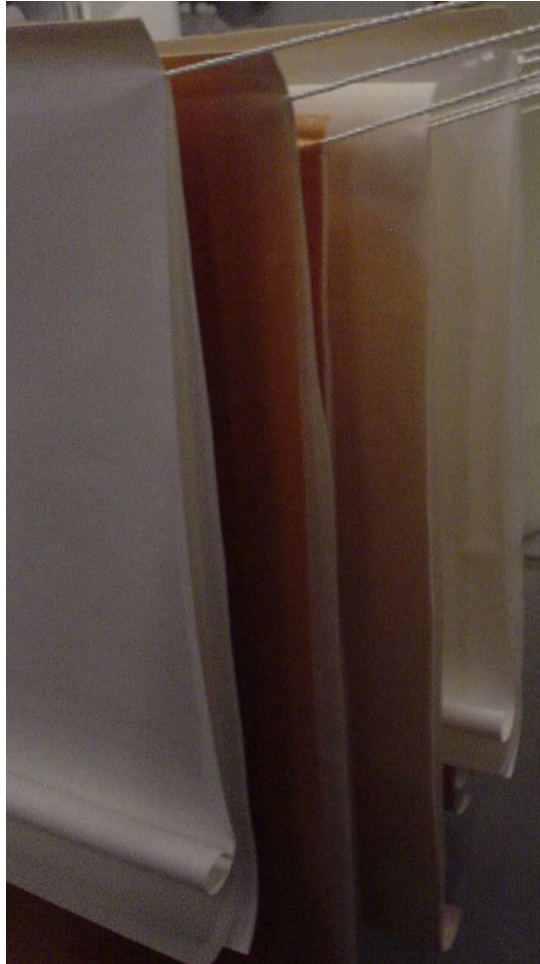
Investigation of Filtration Membranes from the Dairy Protein Industry for Residual Fouling using Infrared Spectroscopy and Chemometrics

PhD Thesis

Jannie Krog Jensen

March 2015

Investigation of Filtration Membranes from the Dairy Protein Industry for Residual Fouling using Infrared Spectroscopy and Chemometrics



PHD Thesis
by
Jannie Krog Jensen

Title

Investigation of Filtration Membranes from the Dairy Protein Industry for Residual Fouling using Infrared Spectroscopy and Chemometrics

Prepared at the Department for Food Science (FOOD), Spectroscopy and Chemometrics section (SPECC) by Jannie Krog Jensen

Submission

March 12th, 2015

Defence

May 28th 2015, 10-13

Supervisors

Assoc. Professor Frans van den Berg

and

Professor Søren Balling Engelsen

University of Copenhagen

Faculty of Science

Department of Food Science, SPECC

Opponents

Assoc. Professor Anna de Juan Capdevila

Chemometrics Group

Department of Analytical Chemistry

University of Barcelona

Per Waaben, PhD

Foss Analytical A/S

Hillerød

Denmark

Professor Rasmus Bro

Spectroscopy and Chemometrics, SPECC

Department of Food Science

Faculty of Science

University of Copenhagen

Cover illustration

Different membranes hanging to dry

PhD Thesis 2015 © Jannie Krog Jensen

Preface

This thesis is the outcome of a collaboration between Spectroscopy and Chemometrics section (SPECC) at the Department of Food Science, Faculty of Life Sciences, University of Copenhagen and Danmark Protein, Arla a/b in Nr. Vium with financial support from The Strategic Research Council through the inSPIRe FOOD consortium as well as the Danish Dairy Research Foundation. The project was supervised by Associate Professor Frans van den Berg and Professor Søren Balling Engelsen from the University of Copenhagen.

I would like to express my gratitude towards my supervisors for giving me the opportunity to do a PhD and for sharing their knowledge and ideas. Their support and inspiration has been very valuable. A special thanks to Frans for always being available and helping me through all phases of my PhD.

I would like to thank the people at Danmark Protein who have been really supportive and have never questioned my intentions when I was asking for more (very expensive) samples. They gave me the opportunity to create a large industrial scale data set that has provided us with new insight about membrane residual fouling.

My colleagues at SPECC have ensured that every day was a good day, and the atmosphere has always been positive, ensuring an inspiring and social work environment. This amazing atmosphere is also the reason why I have spent much time with the department, initially as a laboratory technician trainee and finalizing both my B.sc. and M.sc. before getting the opportunity to start my research career with Frans in his project concerning process water.

A lot of love to my family and friends, you have helped me keep up my good spirit with support and a lot of fun.

And finally a big thank you and a lot of love to my boyfriend Steffen for support and who has reminded me that there is a life outside of the university.

Jannie Krog Jensen,
Frederiksberg, March 2015

Abstract

Ultrafiltration and microfiltration operations are applied intensively in the dairy and water cleaning industries. The main capacity limiting factors of such operations are the flux and efficiency decline by irreversible adsorption of foulants onto the membranes and the efficiency by which the reversible fouling can be removed/cleaned. The aim of this thesis is to investigate the residual fouling that is deposited on ultrafiltration and microfiltration membranes after usage. The membrane surfaces are investigated using infrared spectroscopy with an attenuated reflectance sampling unit and this is thesis work highlights the strengths and weaknesses of using infrared spectroscopy to investigate residual fouling on membranes and in particular the challenges with the infrared penetration depth when layering in the samples occurs.

Real size production membrane cartridges at different stages of use from Danmark Protein, Arla amba were the target of the investigations. However, in order to obtain samples sizes that fit in the sampling interface of the infrared instrument the membranes were dissected into smaller pieces named coupons. In total four ultrafiltration membrane cartridges and two microfiltration membrane cartridges were investigated with Attenuated-Total-Reflection Fourier-Transform-Infrared (ATR FT-IR) to map the residual fouling on both types of cartridges. The height of the characteristic amide peaks from proteins were used to determine the relative concentrations.

The first investigation (Paper I) describes the concentration development over the membrane leaves as a function of the distance from the feed inlet and the distance from the center permeate tube. A non-homogenous concentration distribution of residual fouling was observed with the highest concentration of residual fouling present at the center tube decreasing in concentration outwards in a *flame*-like shape. The relative concentration calculations are based on the height of the amide II peak ($1500\text{-}1550\text{ cm}^{-1}$)

which was chosen because it unlike the amide I band has no interference with adsorbed water and other membrane constituents that can interfere with the computation.

Based on the findings of the first investigation it was decided to develop a new method to evaluate the concentration of the residual fouling on real size production membranes as current best practice methods rely on univariate height measurements that supply only information on the targeted residual fouling peak(s). In a second study (Paper II), it was decided to investigate the infrared data of the membrane by applying multivariate curve resolution (MCR) in order to resolve the residual fouling from the membrane components. Indeed the result showed that the MCR model needed three factors to describe the system, one describing the membrane material (polyethersulfone, PES), and two describing the residual fouling that is present on the membrane. The MCR method improved the interpretation of the models considerably compared to e.g. PCA or the univariate data analysis. However, it also became evident that the penetration depth of the infrared beam creates additional complexity when measuring semi-solid layered samples.

In order to obtain an overview of the different analysis methods and data analysis methods that have been employed by other researchers when studying residual fouling on ultrafiltration and microfiltration membranes a literature review was conducted (Paper III). ATR FT-IR turned out to be a commonly used spectroscopic method to evaluate ultrafiltration membranes. The data analysis is most commonly performed univariate by calculating height of selected peaks along with identification of different chemical entities especially when investigating grafting/grafted membranes. Paper III gives an overview of these different approaches and data analysis methods and their results.

In conclusion, the research in this thesis has shown how the application of multivariate infrared spectroscopy combined with new data analysis methods has augmented the knowledge about residual fouling on real size production membranes. The information obtained can be used to investigate and monitor

residual membrane fouling and help in the design of new membranes and membrane grafting that can be optimized for the purpose.

Resumé

Ultrafiltrerings- og mikrofiltrerings-membraner bliver i høj grad brugt af både mejeriindustri og vandrensningsindustrien. De største begrænsende faktorer for disse enheder er flux og nedgang i effektiviteten som følge af irreversibel fouling på membranerne og samtidig den effektivitet hvormed den reversible fouling kan fjernes/rengøres. Formålet med denne afhandling er at undersøge residual foulingen (tilbageværende protein, fedt og mineraler efter endt rengøring) som er deponeret på ultrafiltrerings- og mikrofiltreringsmembraner efter brug. Membranoverfladerne er undersøgt ved at bruge infrarød spektroskopi i kombination med en attenuated total reflectance prøveenhed. Denne afhandling understreger de styrker og svagheder der opstår når infrarød spektroskopi benyttes til undersøgelse af residual fouling på membraner og i særdeleshed udfordringerne med lysgennemtrængningen af den infrarøde lysstråle når prøverne består af flere lag.

Produktionsmembraner der har været benyttet i forskellige stadier hos Danmark Protein, Arla amla, var målet for vores undersøgelser. For at opnå den korrekte prøvestørrelse der passer ind i prøveinterfacen på det infrarøde spektrofotometer dissekeres membranerne i mindre stykker som herefter kaldes kupper. Fire ultrafiltreringsmembraner og to mikrofiltreringsmembraner blev målt med Attenuated-Total-Reflection Fourier-Transform-Infrared (ATR FT-IR) således at residual foulingen kunne kortlægges. Højden på de karakteristiske amid-toppe der stammer fra protein blev brugt til at bestemme den relative koncentration af fouling.

Den første undersøgelse (Paper I) beskriver hvordan koncentrationen udvikler sig over membranbladene som en funktion af distancen fra føde-tilførslen og distancen fra permeat-centerrøret. En inhomogen fordeling af koncentrationen af residual foulingen blev observeret med den højeste koncentration af residual fouling tættest på centerrøret med en faldende

koncentration udad i en *flamme*-lignende struktur. Den relative koncentrationsberegning bygger på højden af amid II-toppen ($1500\text{-}1550\text{ cm}^{-1}$) som er valgt fordi, i modsætning til amid I-toppen, er der ingen interferens fra absorberet vand eller andre membrankomponenter som kan forstyrre beregningerne.

Baseret på resultaterne fra den første undersøgelse blev det besluttet at benytte en ny metode til at evaluere koncentrationen af residual fouling på produktionsmembranerne. Som det forholder sig på nuværende tidspunkt benyttes univariate metoder hvor højden af toppene måles, hvilket kun giver information om de specifikt udvalgte residual fouling-toppe. I det andet studie (Paper II) blev det besluttet at undersøge data fra de infrarøde målinger på membranerne ved at benytte multivariate curve resolution (MCR) for at kunne adskille residual fouling-toppe fra membranmateriale-toppe. Faktisk viste resultatet at MCR-modellen bruger tre komponenter til at beskrive systemet, en til at beskrive membranmaterialet (polyethersulfone, PES) og to der beskriver den tilbageværende fouling på membranen. MCR metoden forbedrede fortolkningen af modellerne betragteligt sammenlignet med f.eks. PCA eller univariat dataanalyse. Dog blev det tydeliggjort at lysgennemtrængningen af den infrarøde lysstråle tilføjer yderligere kompleksitet når prøverne består af halv-faste lagdelte prøver.

For at danne et overblik over de forskellige analysemetoder og dataanalysemetoder der er blevet benyttet af andre forskere, når residual fouling på ultrafiltrerings- og mikrofiltrerings-membraner er blevet undersøgt, er en litteraturgennemgang blevet udført (Paper III). ATR FT-IR viste sig at være den mest almindelige spektroskopiske metode til at evaluere ultrafiltreringsmembraner. Dataanalysen er mest almindeligt udført univariat ved at beregne højden af udvalgte toppe i kombination med identifikation af forskellige kemiske enheder, særligt når membraner udsat for grafting (kemisk modifikation) undersøges. Paper III giver et overblik over disse forskellige metoder, dataanalysemetoder og resultaterne af disse.

Afslutningsvis, har denne forskning vist hvordan anvendelsen af multivariat infrarød spektroskopi kombineret med nye dataanalysemetoder har øget vores

viden om residual fouling i produktionsmembraner. Informationen kan bruges til at undersøge og overvåge residual fouling og kan bidrage til udformning af nye membraner samt grafting af membraner som kan optimeres til specifikke formål.

List of Publications

Paper I

J.K. Jensen, N. Ottosen, S.B. Engelsen, F. van den Berg (2015), Investigation of UF and MF Membrane Residual Fouling in Full Scale Dairy Production using FT-IR to Quantify Protein and Fat. *International Journal of Food Engineering*, 11(1):1–15

Paper II

J.K. Jensen, J. M. A. Rubio, S. B. Engelsen, F. van den Berg (2015). Protein Residual Fouling identification on UF Membranes using ATR-FT-IR and multivariate curve resolution.
Submitted to Chemometrics and Intelligent Laboratory Systems.

Paper III

J.K. Jensen, S.B. Engelsen, F. van den Berg (2015), Review of ATR FT-IR as Investigative Tool and Quantitative Method for Protein Fouling in Membrane Separation Systems, In preparation, intended for Journal of Applied Spectroscopy.

Additional work by the author

Poster I

C.B. Lyndgaard, J.K. Jensen, S. Knøchel, F. van den Berg (2012), Process Water – Minimizing Industrial Water use by In-process Cleaning Diagnostics. Danish Water Forum (DWF), GEUS, Copenhagen.

Poster II

J.K. Jensen, F. van den Berg (2013), Mapping of UF Membrane Residual-Fouling in Full Scale Dairy Production using FT-IR to Quantify Protein and Fat. Scandinavian Symposium on Chemometrics (SSC13), Stockholm.

Contents

PREFACE	I
ABSTRACT	III
RESUMÉ	VI
LIST OF PUBLICATIONS	IX
1 INTRODUCTION	1
1.1 BACKGROUND	1
1.2 AIMS AND SCOPE OF THE THESIS.....	3
1.3 OUTLINE OF THE THESIS.....	4
2 FILTRATION	5
2.1 MEMBRANE FILTRATION AND CLEANING	5
2.2 PROTEIN RECOVERY BY FILTRATION	6
2.3 FILTRATION MEMBRANES.....	9
2.4 SAMPLE DESCRIPTION	12
2.5 MACRO COMPONENTS IN WHEY AND MEMBRANE FOULING	14
2.6 FOULING	15
2.7 CLEANING IN PLACE (CIP)	16
2.7.1 <i>Membrane Flushing</i>	18
2.7.2 <i>Alkaline treatment</i>	18
2.7.3 <i>Enzyme treatment</i>	18
2.7.4 <i>Acid treatment</i>	19
2.7.5 <i>Disinfectant/sanitizer</i>	20
2.8 GRAFTING OF MEMBRANES	21
2.9 VISUALIZATION OF MEMBRANE FOULING.....	23
3 INFRARED SPECTROSCOPY	27
3.1 ATTENUATED TOTAL REFLECTANCE.....	30
3.2 TOTAL INTERNAL REFLECTION	31

3.3 LAMBERT-BEERS LAW	35
3.4 SPECTRAL RESOLUTION.....	37
3.5 INTERPRETATION OF IR SPECTRUM	37
3.6 THE IR INSTRUMENT.....	40
3.6.1 <i>The dispersive IR spectrometer</i>	40
3.6.2 <i>The FT-IR spectrometer</i>	41
4 DATA ANALYSIS	45
4.1 PRINCIPAL COMPONENT ANALYSIS (PCA).....	47
4.2 MULTIVARIATE CURVE RESOLUTION (MCR)	49
4.2.1 <i>MCR algorithm</i>	49
4.2.2 <i>Rank determination and initial guess</i>	51
4.2.3 <i>Ambiguities</i>	53
4.2.4 <i>MCR constraints</i>	55
4.3 ANALYSIS OF VARIANCE (ANOVA).....	57
4.4 NON-LINEAR REGRESSION	59
5 PROCESS ANALYTICAL TECHNOLOGY	62
6 FLUORESCENCE SPECTROSCOPY	72
7 DISCUSSION AND PERSPECTIVES	77
8 REFERENCES	84

Paper I: Investigation of UF and MF Membrane Residual Fouling in Full Scale Dairy Production using FT-IR to Quantify Protein and Fat

Paper II: Resolving ATR-FT-IR spectra of Protein Residual Fouling on Membranes using MCR

Paper III: Review of ATR-FT-IR as investigative tool and quantitative method for Protein Fouling in Membrane Separation Systems

Poster I: Process Water – Minimizing Industrial Water Use by In-Process Cleaning Diagnostics

Poster II: Mapping of UF Membrane Residual Fouling in Full Scale Dairy Production using FT-IR to Quantify Protein and Fat

Introduction

1.1 Background

The food and the water cleaning industry, along with a smaller but growing area the pharmaceutical industry, represent a significant part in the turnover of the membrane manufacturing industry worldwide (Regula et al., 2014, Maruyama et al., 2001). In food processing, 45% of the applications of membrane units are in the dairy industry (mainly whey protein concentration and milk protein standardization) followed by beverages (wine, beer, fruit juices, etc.) and egg products. The most common membrane application is ultrafiltration (UF). Ultrafiltration is used in the dairy sector to concentrate, fractionate and purify dairy proteins with high functional, biological and nutritional properties. An example is the recovery and the purification of valuable milk constituents, changing a cheap byproduct that was mostly used for animal feed, whey, into a source of high economic gain (Regula et al., 2014).

At Arla amba, the largest Danish dairy processor/producer, whey products make up 3.4% of the total product line and in 2012 Arla produced 2.4 mill tons of whey. As can be seen in Figure 1.1 the volume of whey has steadily increased since 1981 to 2012, and their projection for 2017 is an increase to 5.7 mill tons.

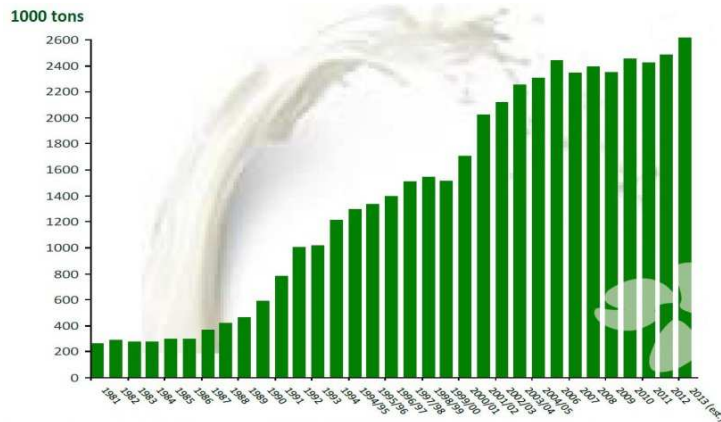


Figure 1.1 – The volume of whey produced 1981-2013 for Arla amba. (<http://www.barjordtilbord.dk>, accessed 24-01-2015).

Organic membranes are the most common type of membranes worldwide and 80-90% of the membrane area installed is organic in nature despite the drawbacks that they have such as limited chemical and temperature resistance and reduced lifetime (2-3 years); the main reason is the price. The annual cost of cleaning in a full scale production is 17-24 €/m² while additional costs for electricity, cooling, heating, water, waste water treatment, man power and membrane wear typically amounts to 33-43 €/m² (Berg, 2014).

Regardless of the industrial fields in which the ultrafiltration membranes are applied fouling remains an inherent problem. Flux decline caused by irreversible adsorption of foulants is the major cause and one of the reasons why it is not used in a wider range of industries (Regula et al., 2014). As a result reduction of fouling and cleaning of fouled membranes has been investigated in various ways since 1980. These studies include optimization of filtering conditions, production of membranes with reduced adsorptive conditions (Ran et al., 2014), backflushing (Tragårdh, 1989), and cleaning and disinfection using harsh chemical agents (Regula et al., 2014)

The process of removal of the fouling – the cleaning - is of great interest due to the considerable volumes of water and chemicals that are used every day. The resources that are used are of course expensive, but the most important factor is the production down time that is required when the systems are cleaned with cleaning-in-place (CIP) procedures. After CIP the used water is

led back to the waste management facility which, depending on the state of the water, can be a costly and energy demanding process as well. In the Danish dairy industries a substantial effort is made to minimize the use of water, time and costs for cleaning – minimizing the so-called *water footprint*. In light of this effort this thesis research will bring increased knowledge on the cleanliness state of the spiral wound (SW) ultrafiltration (UF) and microfiltration (MF) membrane cartridges that are routinely used in the whey processing.

1.2 Aims and scope of the thesis

The main aims of this thesis work are:

- ✓ *To characterize the residual fouling on ultrafiltration and microfiltration real size production membranes with infrared spectroscopy*
- ✓ *To develop novel data analysis methods that better can provide an overview of the residual fouling*
- ✓ *To investigate new spectroscopic methods to measure fouling on real size production membranes*

Analyzing real size production membranes has only been scarcely reported in literature (Kimura et al., 2004, Bégoin et al., 2006a, Bégoin et al., 2006b). Often pilot or lab scale model systems are used which unfortunately do not give the full, and complicated, picture of the ongoing processes during industrial whey filtration. Our wish was to measure fouling as it is happening during full-scale production, but the circumstances around the membrane do not allow for in-situ measurements. Our samples originate from spiral wound membranes that are impossible to probe during use. Furthermore, the conditions inside the steel housing that contains the membranes are relatively harsh, with high pressure, sometimes high temperatures during CIP and low and high pH-values (again during CIP) making it a harsh surrounding for a spectroscopic probe/process analyzer. It was therefore decided to investigate used membranes taken out of the process right after CIP.

Measuring the cleaned and unwound membrane cartridges with infrared spectroscopy results in a large data set with many samples and even more

variables – and this information should be used for extracting relevant information. Assignment of the peaks was a necessary task in order to know which peak is investigated. But when looking into the literature the most common data analysis of membranes is univariate, i.e. measuring the height of one single peak and relating that to a calculated concentration. The driving force behind this investigation is the fact that the amount of whey produced each year has been increasing worldwide and future predictions promise an even larger increase due to the development in protein addition to foods. What makes fouling of great interest in both research and industry is because it is the largest uncontrollable factor in dairy whey processing when using membrane technologies (Berg et al., 2014, Kiefer et al., 2014). Gaining knowledge and understanding about the residual fouling will prove useful when optimizing the cleaning procedures and designing new membrane systems. Several studies has previously been applying ATR FT-IR to membrane/fouling system (Belfer et al., 1999, Rabiller-Baudry et al., 2002), but almost exclusively on membranes fouled (unrealistically) in a laboratory scale set-up (Berg et al., 2014).

1.3 Outline of the thesis

The thesis consists of a main body which is divided up into different chapters: **Chapter 2** provides an introduction to the theory behind the filtration processes in the dairy industry. **Chapter 3** gives a thorough introduction to infrared spectroscopy and the challenges with the penetration depth of the infrared beam. **Chapter 4** provides an introduction to the different data analytical methods that have been employed. **Chapter 5** describes the principles behind process analytical technology (PAT) which has been the mental framework of this thesis work. **Chapter 6** describes some unsuccessful experiments using fluorescence spectroscopy to probe residual fouling. Finally, **Chapter 7** contains a discussion of the thesis results and their future perspectives. These chapters will give an introduction to the theory that is used in the scientific papers (**Papers I & II**). The third paper is the basis of this thesis consisting of a literature review (**Paper III**).

Filtration

2.1 Membrane filtration and cleaning

Membrane separation processes have become a basic operation for process design and product development and spiral wound membrane cartridges account for the vast majority of the membrane area in use worldwide (Wagner, 2001). These processes are used in a variety of separation and concentration steps in the dairy industry but a major challenge related to these operations is membrane fouling by proteins and other biomolecules in the feed stream demanding regularly cleaning of the membranes to remove both the foulants deposited on the surface and/or into the membrane. Cleaning is a vital step in maintaining the permeability and selectivity of the membrane which in the end will lead to a plant that runs at almost optimal capacity throughout the production time and, at the same time, minimize risk of bacterial contamination - of utter important to make safe products and keep up standards (Regula et al., 2014). Fouling also results in flux decline, which increases the energy demand to maintain production capacity constant. Also to counteract this problem membranes are cleaned (hence for cost-optimization), and when cleaning becomes ineffective, the membranes must be replaced, a second important aspect of overall operating costs.

Box 2.1 – Technical terms commonly used in the dairy filtration.

Permeate is the portion of the feed that passes through the membrane

Retentate is the portion of the feed that is retained in the membrane

Transmembrane pressure (P_T) is a factor that describes the difference in pressure between the retentate and permeate side of the membrane. It is the driving force for flux. In cross-flow systems such as ultrafiltration and microfiltration it is measured as the average of the inlet and outlet pressures minus permeate back-pressure (Cheryan, 1998).

$$P_T = \frac{\text{Inlet pressure} + \text{Outlet pressure}}{2} - \text{Permeate back pressure}$$

Flux (J) is defined as the amount of fluid travelling through the membrane. The unit of flux is liters/m²/hour (LMH) taking volume, area of the membrane and time into consideration. For an ideal semipermeable membrane flux is calculated as such:

$$J = A(P_T - \pi_F)$$

where **J** is the flux, **A** is the membrane permeability coefficient, **P_T** is the transmembrane pressure, and **π_F** is the osmotic pressure of the feed solution. Flux requires a positive driving force which infers that **P_T** must always be larger than **π_F** (Cheryan, 1998). Flux is commonly used as measure of the effect of the CIP, flux should be restored after cleaning.

2.2 Protein recovery by filtration

The protein recovery from whey with filtration and in this case ultrafiltration consists of four unit operations:

- Filtration
- Evaporation
- Drying
- Bagging/Packaging

The process is initiated when feed (whey) is pumped into the process line and each following step increases the total protein content. The first step is the filtration unit, it will hold several loops and each loops several housings with several UF membrane cartridges (Figure 2.1). In the filtration unit whey is separated into permeate and retentate where retentate contains the protein fractions and other large molecule solids. Permeate contains water and all the molecules that are small enough to pass through the membrane: lactose and amino acids. Both liquid streams are transferred to large separate tanks. During filtration the solids content is increased to approximately 25%. The retentate is transferred to the evaporators where most water is removed and finally transferred to the spray drier after which the final product is bagged/packaged. The permeate contains fractions that are useful but less valuable than the protein, these fractions follow the same recipe as the retentate resulting in lactose powder (Tetra Pak, 1995).

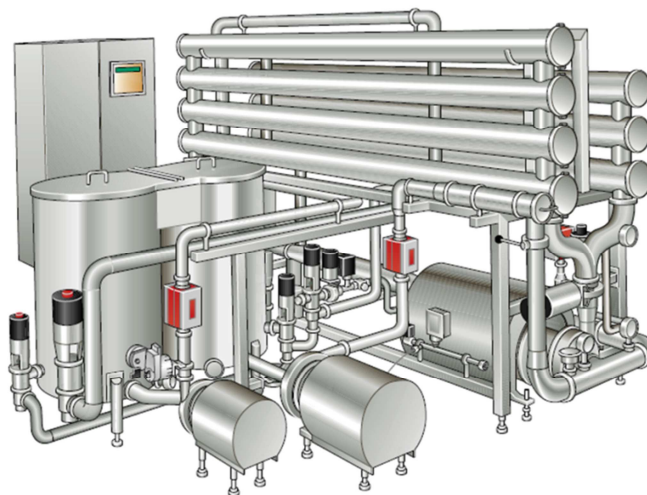


Figure 2.1 – Production module for UF processing (Tetra Pak, 1995).

Membrane cartridges in UF and MF steel housing are separated and kept in place by so-called Anti Telescoping Devices (ATD's) or sometimes Energy Saving Anti Telescoping Devices (ESA's; Figure 2.2a). A frequently encountered configuration would have three membrane units per steel housing, with several housings and *loops* per UF/MF production unit (Bylund, 2003). The ATD (or ESA) ensures that the membrane cartridge

does not partially unfold, but also functions as a separator keeping the permeate flowing throughout the process, in the right channels. The overall design (in case of three membrane cartridges per housing) creates a pressure drop on the retentate side from tube inlet (approximately 4-5 bar for UF) to tube outlet (approximately 1-2 bar), maintaining an overpressure in the cavity between the membrane surface and the inner surface of the membrane housing (personal communication, 2013; Figure 2.2b).

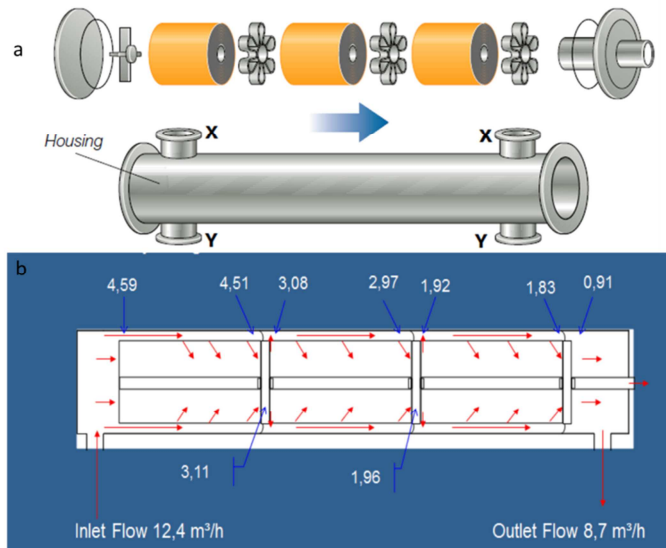


Figure 2.2 – a) the configuration of the membrane cartridges separated by ATD’s (ESA’s) in the steel housing (Tetra Pak, 1995), b) pressure drop over three membranes in one steel housing (numbers are in bar; source: personal communication (2013)).

This pressure differential can still create a deformation in the membrane cartridges that is very distinct when the membranes are deconstructed (Figure 2.3). The membranes primarily exhibit deformation in the exit section of the spiral wound membranes, and the intensity of the deformation is always more severe at exit end.

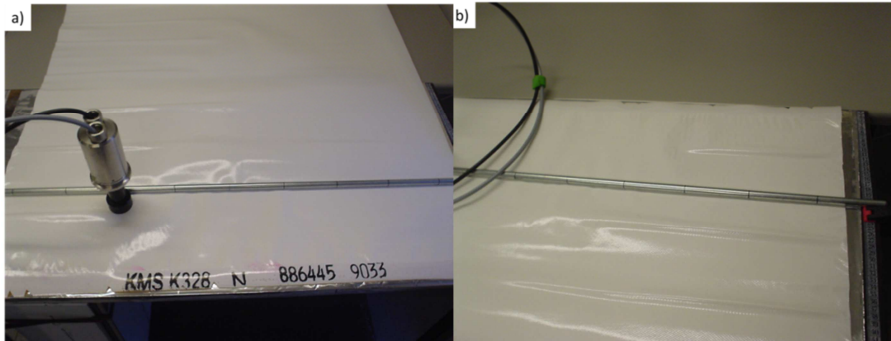


Figure 2.3 - a) Deformation of full leaf, b) detail of deformation on leaf.

The morphology of the membrane and pressure profiles in the cartridge and cartridges-plus-tube ensemble can give rise to a large variation on the membrane and residual fouling. It is assumed that this residual fouling is inversely proportional with membrane capacity, performance and/or energy demands.

2.3 Filtration membranes

Filtration membranes exist in a large variety of materials, sizes, functionalities and brands. There are four main principles within filtration: microfiltration (MF), ultrafiltration (UF), nanofiltration (NF), and reverse osmosis (RO), where the materials can be either organic (polymers) or inorganic (ceramic); see details in Table 2.1.

Table 2.1 – Overview of the most common traits for different membrane processes

	Microfiltration	Ultrafiltration	Nanofiltration	Reverse Osmosis
Thickness (μm)*	110-150	150-250	150	150
Pore size (μm)	0.2-4	0.02-0.2	<0.002	<0.002
Rejection of	Particles Bacteria	Macro molecules Proteins Polysaccharides Vira	Proteins Short chained saccharides	Proteins Salts Glucose Amino acids
Membrane material (support- & work-layer)	Polyvinylidene-fluoride (PVDF) Polypropylene (PP) Polyether-sulfone (PES) ceramic	Polyethersulfone (PES), Polysulfone (PS), Polyvinylidene-fluoride (PVDF), ceramic	Cellulose acetate (CA)	Cellulose acetate (CA)
Membrane module	Spiral wound Tubular Hollow fiber	Spiral wound Tubular Hollow fiber Plate-and-frame	Tubular Spiral wound Plate-and-frame	Tubular Spiral wound Plate-and-frame
Operating pressure (bar)	<2	1-10	5-35	15-150

*) Total thickness of the membrane including support layer and active layer.

Organic membranes are most often employed in the dairy filtration industry and are made from hydrophobic materials such as polysulfone and polyethersulfone due to their thermal, mechanical and chemical stability, low purchase prices and wide knowledge/understanding of the production principles. The disadvantage of this type of membrane is the hydrophobicity that promotes membrane fouling (Van der Bruggen, 2009). There are also different structures of the membranes and unit operations: plate and frame, tubular, hollow fiber and spiral wound. The latter is the most common in the dairy industry and the focus in this thesis. A spiral wound membrane consists of several envelopes and each envelope consists of two membrane leaves that

are glued together with the service area facing outwards. The open ends of the envelopes are glued to a perforated center tube that leads permeate away from the membrane (frequently assisted by a wider spacer net tightly wound around the center tube). The two leaves are separated internally by a permeate spacer that ensures a good flow towards the center tube. Between each envelope a second type of spacer is utilized, namely the feed (retentate) spacer that serves as a channel for the retained macromolecules (Figure 2.4). All this is rolled into a spiral and closed with an outer mesh of rigid plastic. The number of envelopes depends on the thickness of the different spacers in the membrane and the desired cartridge diameter.

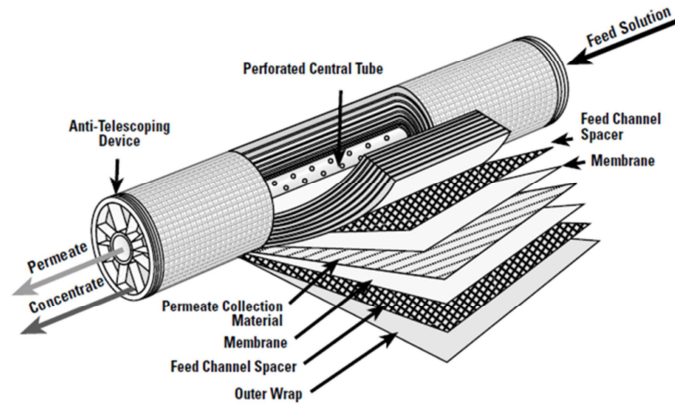


Figure 2.4 – Composition of spiral wound membrane.
(<http://civilenggseminar.blogspot.dk>, accessed 05-02-2015).

In this project ultrafiltration (PES) and microfiltration (PVDF) spiral wound membrane cartridges have been investigated. In microfiltration ideally only suspended solids, primarily fat and bacteria, are retained, while proteins pass freely (Wagner, 2001). This is the reason why microfiltration is often used prior to ultrafiltration in order to remove large particles, decreasing the propensity of the ultrafiltration membranes to foul. The characteristics of the ultrafiltration membrane is that high molecular weight component such as proteins and fat are retained (*stay in the retentate*) while the pores of the membrane cartridges are too large to retain mono- and di-saccharides, salts,

and amino acids that all exits the membrane as permeate and are discarded or go to downstream processing (Wagner, 2001).

The membranes possess an overall stability but are susceptible to change and degradation due to several parameters that are considered extreme. Temperature plays a large role during cleaning, and organic membranes often have an upper temperature limit of 55°C. All membranes are sensitive to pressure, and compaction is often used to describe the irreversible *flattening* of a membrane due to pressures resulting in decreased flux explained as a reduced volume of the membrane pores (Gekas, 1988, Wagner, 2001). Extreme pH can damage the membrane and decrease the lifetime significantly (Regula et al., 2014); especially the membranes that use polyester as support material are sensitive towards high pH with an upper limit of 11.5 (Wagner, 2001).

2.4 Sample description

A common method for detecting membrane fouling is by using IR spectroscopy. The membrane cartridges we have investigated are both ultrafiltration and microfiltration membranes and they have been used in industrial settings for variable periods of time. They are standard spiral wound units and consist of a varying number of leaves (Table 2.2). To get an overview of the full membrane area samples were collected in a specific pattern remaining statistically certain that the true picture is delivered. Measuring the full membrane cartridges would be an overwhelming task which is the reason for dissecting the membrane cartridges ensuring a spatial measuring point distribution over the full membrane (Paper I, Figure 1).

Table 2.2 – Membrane cartridge details. Sample set A: One ultrafiltration membrane cartridge made of polyethersulfone (PES). Sample set B: Three ultrafiltration membrane cartridges made of PES originating from the same steel housing. Sample set C: Two microfiltration membrane cartridges made from polyvinylidene fluoride (PVDF). Figures at the bottom show a sample from each sample sets.

Cartridge	Sample set		
	A	B1, B2, B3	Ca, Cb
Membrane type	UF	UF	MF
Dimensions			
Diameter	6.3"/160 mm	6.3"/160 mm	6.3"/160 mm
Length	38"/965 mm	38"/965 mm	38"/965 mm
Spacer thickness	31 mil/0.79 mm	80 mil/2.04 mm	46 mil/1.17 mm
No of leaves	11 x 2	7 x 2	8 x 2
App. leaf length ^{a)}	36"/920 mm	35"/900 mm	43"/1100 mm
Membrane area ^{b)}	228 ft ² /21.2 m ²	117 ft ² /10.9 m ²	171 ft ² /15.9 m ²
Material	PES	PES	PVDF
Cut off	10 kilo Dalton	10 kilo Dalton	800 kilo Dalton
Product	Sweet whey	70k whey	WPI
Loop	3	8	1 (Ca), 4 (Cb)
Tube	5	3	7 (Ca), 4 (Cb)
Age	2 years, 3 months	5 months, 3 days	1 year, 9 months
Leaves investigated	1, 4, 11	1, 2, 5	1, 2, 5
Size of coupon	70 x 100 mm	100 x 100 mm	100 x 100 mm

^{a)} Based on our observations/measurements made during cartridge dissection.

^{b)} Based on specifications of the manufacturers.



The membranes have three distinct layers; a membrane support layer that consists of polyester (PE), an active layer that is the filtering part of the membrane which consists of polyether sulfone (PES) for ultrafiltration membrane cartridges and polyvinylidene fluoride (PVDF) for microfiltration membrane cartridges, finally a residual fouling layer that consists of build-up (e.g. protein, minerals and fat) from the process (Figure 2.5).

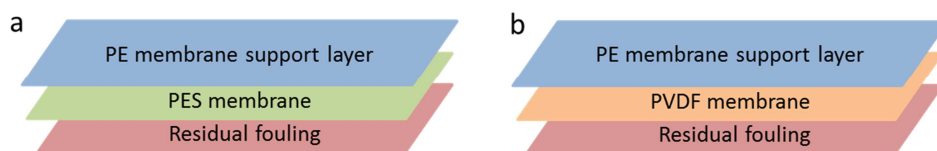


Figure 2.5 – Schematic overview of the structure of a fouled membrane, a) ultrafiltration membrane, b) microfiltration membrane. PE: polyester, PES: polyether sulfone, PVDF: polyvinylidene fluoride.

2.5 Macro components in whey and membrane fouling

The whey that is used for producing whey powder is a discarded bi-product from cheese production and it therefore holds a large variety of the chemical components found in processed milk. Whey is the remainder when fat and the majority of the protein is removed/used and leaves (ideally) only soluble milk salts, milk sugar (lactose) and the remainder of the milk proteins. The two liquids naturally resemble each other with more lactose, and less protein and fat in the whey due to them being used during cheese production (see Table 2.3).

Table 2.3 – Chemical composition of cow’s milk and cheese whey

Component	Milk		Whey	
	Range (%)	Mean (%)	Range (%)	Mean (%)
Water	85.5-89.5	87.0	89.4-93.0	90.1
Total solids	10.5-14.5	13.0	6.7-10.6	9.8
Fat	2.5-6.0	4.0	0.03-0.06	0.05
Proteins	2.9-5.0	3.4	0.65-1.5	1.3
Lactose	3.6-5.5	4.8	5.2-7.9	7.5
Minerals	0.6-0.9	0.8	0.6-0.7	0.6

2.6 Fouling

Fouling is the general term applied to the accumulation of soil or foulant on the surface or within the pores of a membrane. Fouling shortens the total hours of processing time, increases energy and cleaning costs, decreases separation efficiency and if severe it may lead to irreversible clogging of the membrane rendering them useless (Brans et al., 2004).

In this thesis I will differentiate between two types of fouling, namely reversible and irreversible. The reversible fouling can be removed by cleaning the membranes while the irreversible fouling is fixed to the membrane after cleaning has taken place, hence it is not as damaging as the irreversible clogging but it will change the condition of the membrane. The fouling consists of a build-up of protein and minor volumes of fat and minerals and can be attributed to different fouling mechanisms. A concentration polarization will occur during filtration, this means that a large number of molecules will be in close vicinity to the membrane surface (Figure 2.6, a). It arises due to the static attraction between molecules and the membrane and is not a large problem during cleaning as it is completely reversible. Four concepts have been put forward as to how the proteins are irreversibly fixated to a membrane: adsorption (b), cake layer formation (c), pore blocking (d), and depth fouling (e) (Brans et al., 2004). In adsorption the foulant adheres to the membrane primarily on the surface but also in the pores, narrowing them and reducing the flux. Cake layer formation arises when the whey molecules aggregate and form bridges and piles that cover sections of the membrane. Pore blocking occurs when a large molecule blocks a pore. This can further develop into depth fouling when the larger molecule is forced into a pore.

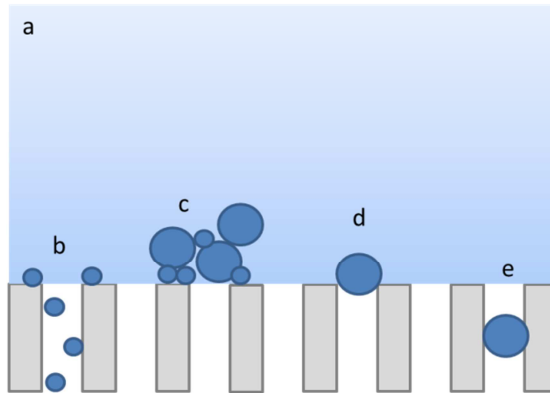


Figure 2.6 – Schematic overview of the four fouling mechanisms

This study will not distinguish between the four combined fouling interactions but rather the total residual fouling, the foulants present right after a cleaning-in-place (CIP, see below). This study investigates used membrane cartridges from full scale dairy UF and MF operations for the processing and up-concentration of sweet whey. Attenuated total reflection Fourier-transform infrared (ATR FT-IR) spectroscopy and multivariate data analysis is employed to identify and quantify – or semi-quantify in a relative sense - protein and fat residues. Based on these measurements the residual fouling load over a wide range of different membrane leaves and cartridges can be compared.

2.7 Cleaning In Place (CIP)

Cleanliness of ultrafiltration membranes is defined in three ways two of which are destructive rendering the membrane useless for further production and one that keeps the membrane intact but results in less information on the fouling. The physical-chemical cleanliness is determined by employing spectroscopic methods which detect the molecules on the membrane surface; ATR FT-IR is most often used for this purpose. These methods give information on fouling distribution but not directly on the permeability of the membrane. It is a destructive method that is not appropriate for an industrial setting. The microbiological cleanliness is detecting microorganisms on the membrane surface and is a destructive method as well, hence most commonly this cleanliness parameter is determined indirectly by analyzing the effluent

from the production. The hydraulic cleanliness is based on restoring the flux (during production or the so-called clean-water-flux) after a cleaning cycle and builds on restoring the permeability of the membrane under controlled conditions. It is the method used as standard in the industry (Regula et al., 2014) as the two others give too little day-to-day information in comparison with e.g. costs of changing membranes.

The cleaning performed at a full scale dairy filtration operation is complex and involves several consecutive steps. The cleaning that takes place is a CIP which infers that the membranes remain in their position while all cleaning agents are pumped through the system. The cleaning requires a lot of clean potable water, several types of chemicals and large volumes of these and - most importantly - a lot of time; 6-7 hours is not uncommon in downtime. The chemicals are almost always supplied by distinct/specialized businesses with no (direct) connection to the dairy, and often these companies are involved in designing CIP programs (in cooperation with the equipment/hardware vendors and dairy managers). The chemicals that the CIP encompasses are recirculated for various periods of time. During downtime no product is being produced making it an expensive, unavoidable demand. Cleaning is required approximately every 24 hours due to a rise in pressure in the membrane cartridges caused by the pores getting blocked by, mostly, protein but also fat and minerals builds up on the membrane, plus for hygienic reasons.

The elaborate cleaning procedure employed in full scale whey production can vary considerably, but is frequently as complex as the following nine-step program (Figure 2.7; Berg et al., 2014; Poster I, 2012):

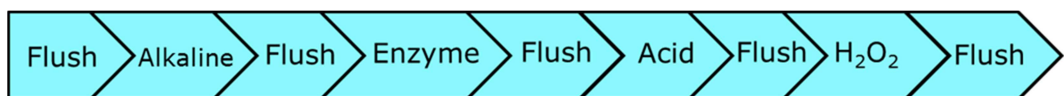


Figure 2.7 – Overview of the cleaning procedure in whey production

2.7.1 Membrane Flushing

The flushing consists only of water (either fresh/tap water, or process water cleaned on-site by reverse osmosis). Flushing has two purposes depending on the cleaning step. The first flushing is to remove any loose deposits (which will be recovered), further along in the cleaning it is also used to wash out any residual cleaning agent along with the fouling that has been released from the membranes into the waste water treatment. A proper flushing step prior to initiating the chemical cleaning can possibly reduce the cleaning time and the usage of chemicals making the cleaning cheaper and faster.

2.7.2 Alkaline treatment

When applying alkaline to the cleaning process it refers to two different chemicals: NaOH or KOH. Along with the active ingredient a composite detergent systems and pH buffering/control is added. The NaOH and KOH are highly alkaline substances that rapidly hydrolysis proteins and other organic residues and also it saponifies fats and oils especially at raised temperatures (>50°C). Hydroxide solutions of high pH (pH 11-12) are recommended for removing protein foulants and their cleaning power is often enhanced by sodium hypochlorite addition (D'Souza & Mawson, 2005).

2.7.3 Enzyme treatment

In the case where a membrane is heavily fouled with protein as is the case with whey filtration units enzymatic cleaning shows good results (D'Souza & Mawson, 2005). The main cleaning component is typically proteases, but a combination with lipases can increase the effect (Allie et al., 2003). The enzymes play a vital role when cutting specific points in the protein, this will decrease the average size enabling them to exit the membrane together with the permeate stream.

Use of enzymes offers several advantages (D'Souza & Mawson, 2005, Regula et al., 2014)

- Biodegradable and thereby posing fewer pollution problems
- Less aggressive to the membrane as they are highly substrate and reaction specific
- Rinsing volume is decreased leading to waste water reduction
- Improve cleaning efficiency
- Reduce energy costs by working at decreased temperature
- Low concentration
- Prolonging membrane cartridge lifetime

and disadvantages

- Narrow tolerance of pH and temperature for its optimum activity (beyond specific values the enzymes will denature)
- Low tolerance for surfactants and detergents
- The action of enzymes is limited to organic matter, with great specificity
- Slower cleaning rate
- Enzymatic activity can be carried over to the product
- The necessity to employ a deactivation step (extreme pH, heat shock or oxidation)

The price of the enzyme used to be a disadvantage but with the decreasing prices of the enzymes along with prolonged life of the membranes due to less harsh treatment an economical balance has been reached (Rabiller-Baudry et al., 2009).

2.7.4 Acid treatment

Acids are used to dissolve precipitates of inorganic salts or oxide films. Nitric acid or phosphoric acids are commonly used. Citric acid is gaining in popularity due to its mildness and the fact that it rinses easily and does not corrode surfaces (e.g. the stainless steel housings of the membrane cartridges; D'Souza & Mawson, 2005). The acidic treatment is also a way to deactivate the enzyme step ensuring that there is no carry over to the product (Regula et al., 2014).

2.7.5 Disinfectant/sanitizer

Disinfectants (as such officially not a part of the CIP program) are applied to a membrane filtration unit in order to prevent microbial growth. It is not sufficient for the disinfectant to be effective, it should also have limited short- and long-term effects on the membranes. It is also important that the disinfectant can reach all parts of the membrane ensuring that no bacterial growth will occur (D'Souza & Mawson, 2005). Hydrogen peroxide and hypochlorite are often used and have proven effective. Hypochlorites are membrane-swelling agents thus assisting in flushing out material that has become lodged within the pores. However this often decreases the lifetime of the membrane unit (Cheryan, 1998). Many more disinfectants have been investigated but with varying success (Bohner & Bradley, 1992).

The cleaning procedure removes the main fouling layers, regenerating the capacity of the filtration unit operation, albeit some irreversible residual fouling is left even after such a sophisticated CIP program. The cleanliness is assessed based on indirect evidence; the composition of the cleaning/final flushing water but also appearance and smell can reveal if the optimal cleanliness is achieved. More technical methods such as water flux is a common optimization strategy, as it can be evaluated from the process operators office and compares the flux from the previous cleaning to the current cleaning (Bohner & Bradley, 1992).

Each step has its own specific purpose and in some instances not all steps are necessary. Most CIP cycles are run recipe wise because real-time control is considered too complex (Lyndgaard et al., 2014) meaning that the cleaning procedures are standardized from the manufacturer of cleaning agents. Investigation of the membrane and cleaning performance in laboratory scale rarely offers any final solution (Berg et al., 2014). No risk should be taken when cleaning a filtration production as it can be rather costly to dispose a batch of bacteria contaminated whey protein. At the same cleaning costs should be considered as this is a large expense on a daily basis and an optimized cleaning procedure could potentially save a substantial amount of money. There are a lot of variables and interactions involved in membrane performance and residual fouling: the membrane age combined with the

short- and long-term product history of the membrane cartridges, the (often varying) whey feed stream composition, etc. For these reasons, a fundamental understanding of CIP and residual fouling in full-scale dairy membrane production is highly desired (Linkhorst & Lewis, 2013)

2.8 Grafting of membranes

Fouling is a big issue in the filtration industry and is one of the most important challenges faced in ultrafiltration membrane operations. A lot of thoughts and resources are spent to minimize fouling during production. Of the operating costs of a typical UF plant, 30–50% is spent on membrane replacement, 10–30% on membrane cleaning, and 20–30% on energy. Membranes that resist residual fouling, therefore, are one of the most important solutions leading to more feasible UF membrane processes (Asatekin et al., 2007). The surface of the membrane can have different interactions that increase the fouling propensity of the membrane such as van der Waals, electrical, hydration, hydrophobic or steric forces but also surface properties such as hydrophilicity, charge and surface roughness that all affect the membrane fouling (Kochkodan et al., 2014). One way to avoid the fouling (albeit not completely) is to use membranes that are modified. These modifications can be inflicted on the membrane by blending (mixing of two (or more) polymers achieving the required properties), grafting (monomers are covalently bonded to the polymer chain) or curing (physical forces are applied to ensure that an oligomer mixture coating adheres to the substrate; Figure 2.8). The most commonly used method when modifying filtration membranes is grafting.

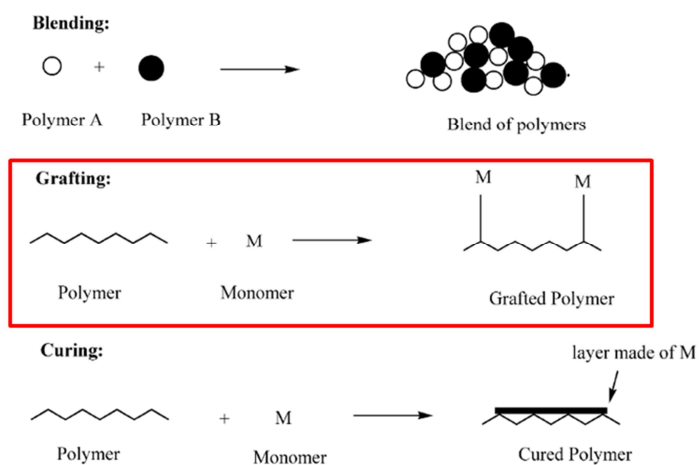


Figure 2.8 – Schematic representation of polymer modification methods (Bhattacharya & Misra, 2004).

The most used method currently is photochemical grafting where the modification happens when a chromophore on a macromolecule absorbs light (e.g. UV) and goes into an excited state which may dissociate the backbone into reactive free radicals through bond rupture. The free radicals on the backbone react with the free radicals in the monomer forming a grafted copolymer. Sometimes the release of free radicals on the backbone does not occur and sensitizers can be introduced to the process. The sensitizers extract hydrogen atoms from the backbone producing the radical sites required for grafting (Bhattacharya & Misra, 2004). The monomers that are used in modification of the membranes are selected due to their chemical reactivity. The modified polymers are very useful as they are tailored to facilitate the requirements of specific applications/separation.

From a scientist point of view working with grafted membranes and IR can be challenging due to the proprietary nature in commercially available membrane cartridges. No prior knowledge exists or is readily available on the grafting molecules that have been used to modify the membrane possibly resulting in unknown peaks in the spectrum. This again might interfere with qualitative or quantitative studies, a strong argument for the use of chemometric/multivariate analysis.

2.9 Visualization of membrane fouling

To better understand the fouling distribution and thereby the measurements performed with IR the membranes were stained. Protein staining is a simple method where a color, in this case amido black, is chemically and selectively attached to the protein. A method described by Platt and Nyström (2007) has been used for this purpose. The experiment by Platt and Nyström (2007) was performed on membranes that are fouled in a bench top scale unit and are little relatable to the large productions, but the method exhibits the strength of visualizing the residual protein fouling in the present experiment. The method was initially used to investigate if it was possible to develop a calibration curve from the coloration on the membrane and therefore experiments were tested in laboratory scale, using a dead-end filtration unit with a volume of 50 ml (Figure 2.9). The unit had the option of stirring if needed. This method could potentially be a solution for quantification of the fouling in combination with imaging equipment, e.g. the Videometer (Ropodi et al. 2015).

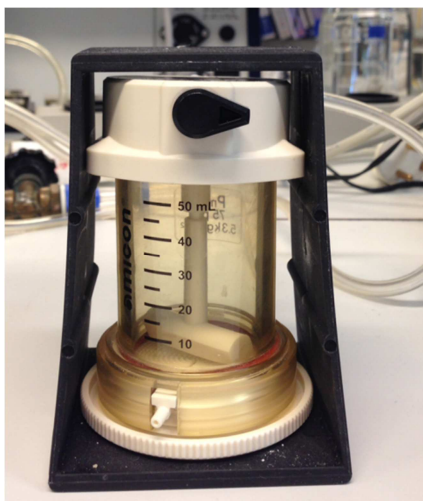


Figure 2.9 – Dead-end filtration unit for staining experiment.

The membrane pieces used for this investigation were the same type as the membrane cartridges (PES) but originally intended for plate and frame filtration. Smaller pieces were cut to fit the filtration unit (area 16 cm²) and

care was taken not to touch the membrane without wearing gloves as the residue from skin could affect the staining results. A quantitative calibration set was made with reconstituted whey with concentration dilutions ranging from 20 to 10,000, the stock solution was not a part of the experiment. They are made from a stock solution containing 1 μ l reconstituted whey in 5 ml water with a calculated protein content of 0.9% (Table 2.4). The experiments are run with stirring as the pressure in the filtration unit did not have enough force to push the water through the membrane after initial fouling. Figure 2.10 shows the fouling distribution of the eight experiments and there is a clear decrease in protein content on the membranes that correlates with the protein concentration.

Table 2.4 – Dilution and concentration of whey calibration solutions.

Dilution	Protein concentration (%)
1	0.9
20	0.045
50	0.018
100	0.009
500	0.0018
1,000	0.0009
2,500	0.00036
5,000	0.00018
10,000	0.00009

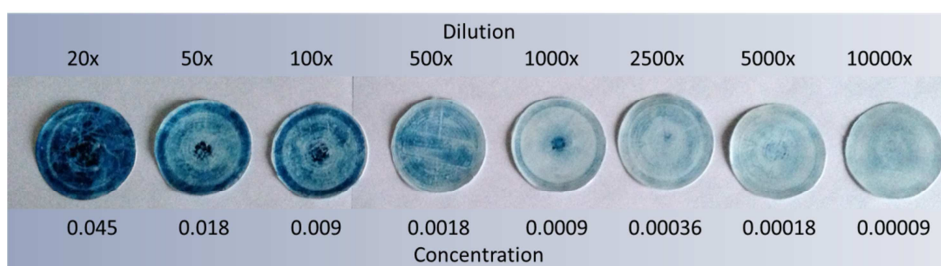


Figure 2.10 – Distribution of fouling, stained with amido black, for the eight dead-end filtration samples.

It was the intent to determine the amount of blue in each pixel on the membrane by image analysis (Videometer, Videometer Lab A/S, Denmark) and correlate the concentration to color intensity. Unfortunately the variation in the blue is too large to be used and the stirring disturbed the distribution making it difficult to determine the correct blue for the specific protein concentration. This method also has issues with regards to protein concentration as the intensity of the blue (ranging from the lightest to the darkest blue) at some point cannot get any darker while the concentration of the protein could (in principle) still increase. This problem can be compared to the non-linear response of a spectroscopic calibration curve where concentration no longer has a linear relationship with the light intensity (thus violates Lambert-Beers law). Further it was established that these experiments did not resemble the reality of membrane filtration; the real process is much more complex and the membrane and feed interactions play a significant role in fouling.

A method for determining protein concentration was not achieved but it provided a method to visualize and describe the fouling distribution on the real size production ultrafiltration membranes (Figure 2.11). To describe the distribution of the fouling a set of spatially distributed samples over a full leave were investigated. The membrane (after industrial CIP) exhibits only little fouling prior to staining and it can mostly be seen close to the center tube where some discoloration following the shape of the spacer mesh is seen (Figure 2.11a). After staining according to the method reported above it is obvious that the residual fouling is present and a decrease of fouling towards the outer edge is also very apparent (Figure 2.11b). This image also gives an explanation as to why IR measurements measured in a close vicinity to each other can exhibit large variations – the spacer and the flow creates a distinct pattern that cannot (and should not) be avoided when measuring random sample points. The inhomogeneity is a distinct part of the membrane and should be included and discussed.

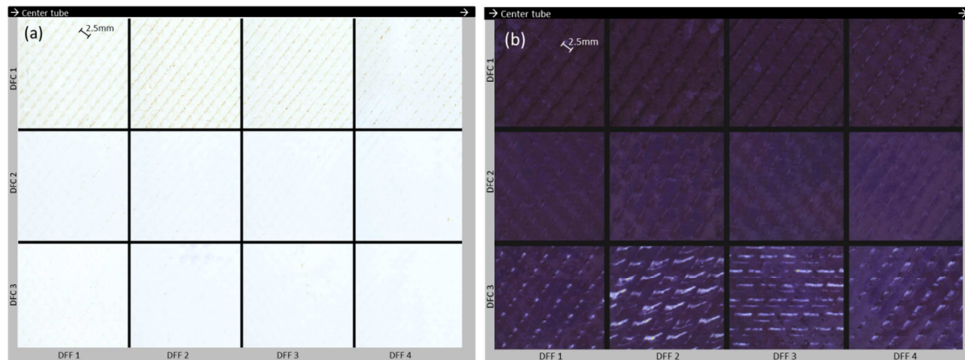


Figure 2.11 - a) Fouling of one membrane leaf, b) fouling of one membrane leaf, stained.

The binding of the deposits, the construction of the spacer, and the design of the cartridges resulted in inhomogeneous membrane surfaces and large variations within the data, as illustrated by protein staining. Despite this observed inhomogeneity the findings on the distribution of residual fouling using ATR FT-IR measurements are in good agreement with the conclusions from earlier studies based on thickness measurements (Schwinge et al., 2004, Figure 2.12), with the added benefit of a direct interpretation of the identified chemical species.

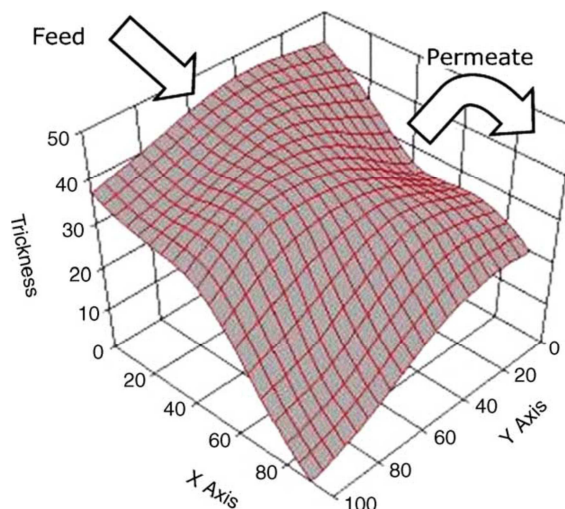


Figure 2.12 - Results from the thickness measurements performed by Schwinge et al. (2004).

Infrared Spectroscopy

Theory, Materials and Samples

The electromagnetic spectrum is the range of all types of electromagnetic radiation, reaching from low frequency long wavelength radio waves to high frequency short wavelength gamma rays. It includes the visual light we use in our houses and the microwaves we use to heat our food (Figure 3.1). This study uses infrared light to investigate membrane fouling. The infrared light is sufficiently energetic to resonate with molecular vibrations and can thus provide a fingerprint of the molecular composition. The infrared region can be further divided into three sections: near infrared (14,000-4,000 cm^{-1}), mid infrared (4,000-400 cm^{-1}) and far infrared (400-10 cm^{-1}); in this thesis all the IR-measurements are performed with mid infrared radiation and will from now on be referred to as infrared.

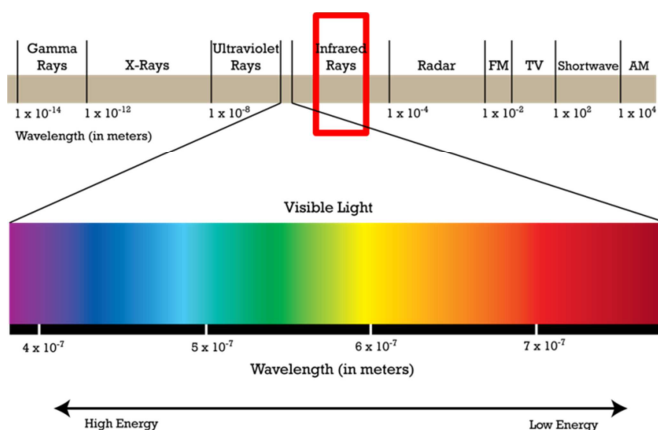


Figure 3.1 – Electromagnetic spectrum, red square indicates our working range; mid infrared. (<http://www.pion.cz>, accessed 02-02-2015).

Infrared spectroscopy can be used to study a wide range of sample types either in bulk or in microscopic amounts over a wide range of temperatures and physical states. As the photons in the infrared is of relative low energy infrared is a non-destructive method and as all molecules exhibit molecular vibrations in principle all components of a sample can be measured in one spectrum. Infrared spectroscopy is thus a multivariate analytical method that with benefit can be analyzed using complex mathematical/chemometric tools. Infrared spectroscopy is one of the most frequently employed analytical methods along with near infrared (NIR), Raman and Nuclear Magnetic Resonance (NMR) (Chalmers & Griffiths, 2002).

All molecules exhibit molecular vibrations and different molecular bonds vibrate with their own specific frequency. The bond vibrations occur as symmetrical and asymmetrical stretching vibrations that vibrate at nearly the same frequency but many other types of molecular vibrations exist. The CH₂ group in poly-methylene exhibit for example six different molecular vibrations: asymmetric stretch, symmetric stretch, scissoring, wagging, twisting and rocking. (Figure 3.2). The precise wavenumbers of absorption bands depend on inter and intra molecular effects, including bond angles and hydrogen bonding patterns.

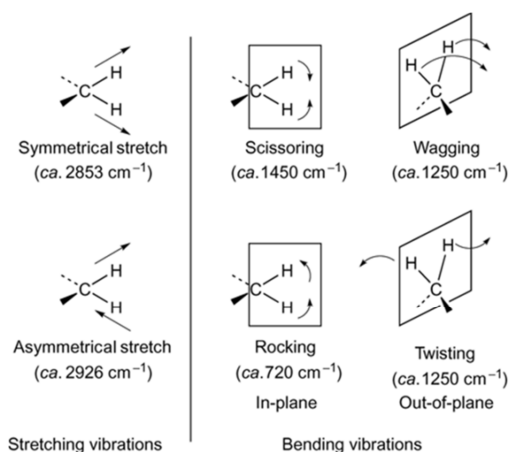


Figure 3.2 – Molecular vibrations of poly-methylene (CH₂) groups (Miller, 2001).

The number of vibrational normal modes (degrees of freedom) for non-linear molecules is $3N-6$, where N equals the number of atoms in the molecule, and the number of normal vibrations thus increases with increasing complexity of a molecule. By illuminating samples with infrared light the vibrations that naturally occur in the molecule will resonate and absorb the incoming photons. It has to be noted that not all molecules are able to absorb infrared light, but only those that have a dipole moment or an induced dipole moment during the molecular vibration. Few molecules are thus unable to interact with infrared radiation including diatomic molecules built with the same atoms such as H_2 , N_2 and O_2 (Figure 3.3a). Fortunately, all relevant biological molecules such as water, carbohydrates, proteins and fats have dipole moments and are thus detectable using infrared radiation.

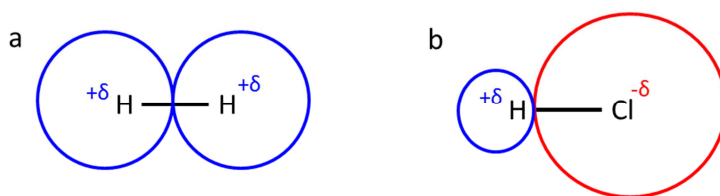


Figure 3.3 – Dipole moment, a) IR inactive, b) IR active.

In principle all atoms in a polyatomic molecule move during a normal vibration. While polyatomic molecules have many normal vibrations, assignments of infrared spectra rely on the concept of group frequencies. A group frequency is a normal vibration that is robust and primarily localized to a specific functional group for example the carbonyl stretching vibration ($C=O$) is called group frequencies. Figure 3.2 shows some relevant group frequencies for fats, other prominent examples of group frequencies are the ester carbonyl stretch of triglycerides ($C=O$) at 1745 cm^{-1} and the carbonyl stretch ($C=O$) of the peptide bonds in proteins at 1650 cm^{-1} also called the Amide I band.

3.1 Attenuated Total Reflectance

IR is traditionally difficult to measure due to the high absorbance levels and thus the very small path lengths required, but many problems were solved when Attenuated Total Reflectance (ATR) sampling units was introduced. ATR offers an alternative solution to the traditional transmission IR sampling for measurements of materials which are either too thick or too strongly absorbing to be analyzed by transmission spectroscopy or when only the surface of the material is of interest. Using the ATR sampling it is possible to obtain infrared spectra of samples that are difficult to deal with, such as solids with limited solubility, films, threads, pastes, adhesives, and powders (Figure 3.4).

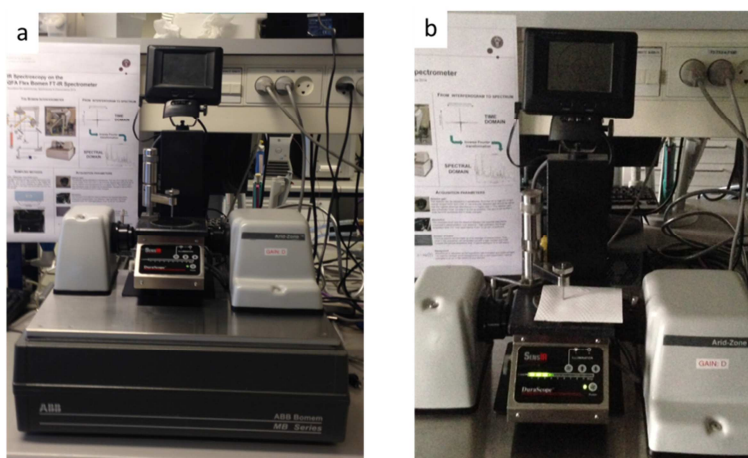


Figure 3.4 – a) ATR FT-IR spectrometer at the Department of Food, SPECC, University of Copenhagen, b) ATR FT-IR spectrometer with membrane coupon during measurement.

ATR is based on the concept of total internal (sample) reflectance. This effect can only be achieved if the internal reflection element (IRE) typically a crystal has a higher refractive index than the sample. Zinc selenide (ZnSe), AMTIR (chalcogenide glass), Diamond and Germanium are commonly used as IRE materials due to their high refractive indices: 2.4, 2.5, 2.4 and 4.0 respectively. The advantage of the diamond IRE is that it is extremely hard and largely chemically inert and thus not affected by treatment with high pressures and harsh cleaning agents. Moreover the diamond has a wide

transmission range and a relatively large refractive index of 2.4 (Fontanella et al., 1977). Should the sample have a higher refractive index than the IRE, then the principle of total internal reflectance will fail and the light is transmitted resulting in missing signal to the detector and no recorded spectrum. ATR requires good optical/physical contact between the sample and the ATR crystal and to acquire reproducible spectra pressure is often applied to bring the sample towards the IRE.

Normally a single bounce IRE crystal is used for strongly absorbing materials (and small sample volumes) and the multiple reflectance ATR is used for less strongly absorbing samples. The latter is often used for liquids or soft, easily deformable solids as they can achieve excellent contact with the ATR. This is a very important caveat for the use of the ATR sampling technique: only a few micrometers of the sample is penetrated and spectra of heterogeneous samples with layered structures or sedimentation should be analyzed with care. In order to achieve good contact between the sample and the IRE a horizontal ATR accessory is often utilized, here the top plate is the sampling surface and reproducible contact is achieved by a sample clamp or pin (Figure 3.4). This way, good quality spectra can be obtained for materials that usually present problems in conventional IR setups (Günzler & Gremlich, 2002). In this study a single bounce ATR was employed in order to obtain good optical contact between the sample and the IRE which could not be achieved with a multi-bounce unit to produce reproducible spectra.

3.2 Total internal reflection

IR spectroscopy with ATR sampling requires total internal reflection and this happens when radiation moves through a material with high refractive index n_1 and impacts the interface with a material with a lower refractive index n_2 at an angle greater than the critical angle (Chalmers & Griffiths, 2002). The critical angle is defined as the angle of incidence above which total internal reflection occurs. It is calculated by finding the value for θ_i (Eqn. 3.1) when $\theta_t = 90^\circ$ and thus $\sin\theta_t = 1$. The resulting value of θ_i is equal to the critical angle θ_c (Eqn. 3.2). The critical angle is thus defined with respect to the normal (dotted line in Figure 3.5) (Chalmers & Griffiths, 2002).

$$\sin\theta_i = \frac{n_2}{n_1} \sin\theta_t \quad (3.1)$$

$$\theta_c = \theta_i = \sin^{-1}\left(\frac{n_2}{n_1}\right) \quad (3.2)$$

A necessary and useful side effect to the total internal reflection is the appearance of an evanescent wave that is formed at the boundary between two different materials that have different wave motion properties. The evanescent wave propagates beyond the boundary surface. This implies that, even though the entire incident wave is reflected back into the ATR crystal (the dense medium) there is still some penetration into the sample (the rarer medium) arising from a standing wave established at a totally reflecting interface (Figure 3.5).

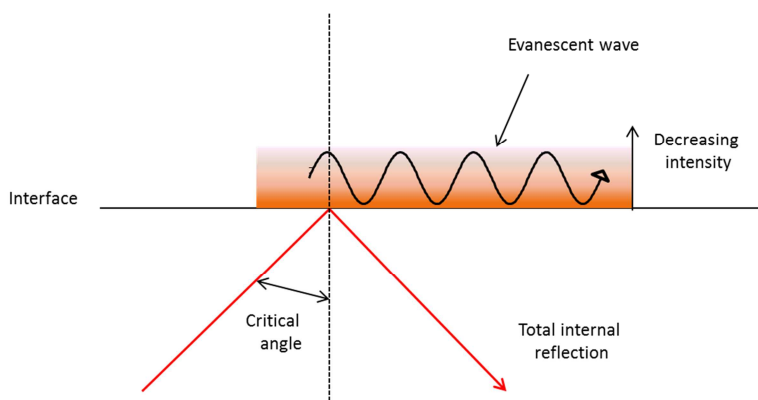


Figure 3.5 – Schematic overview of the evanescent wave.

This evanescent wave is a diffuse wave and has components in all spatial orientations. The wave exhibits exponential decay as a function of the distance from the boundary at which the wave was formed and is thus most intense within approximate one third of the wavelength from the surface of formation. Thus the evanescent wave is confined to the (close) vicinity of the surface of the sample. In theory and for the ease of the description of the evanescent wave the original propagating radiation loses no energy to the sample. This is an idealized picture as it is obvious that absorption of energy must be made in order for an IR measurement to be useful (Mirabella, 1993).

The decrease of the evanescent wave can be expressed as:

$$E = E_0 \cdot \exp -\frac{2\pi}{\lambda_1} \cdot \sqrt{(\sin^2\theta - n_{21}^2)} \cdot Z \quad (3.3)$$

Where E is the electric evanescent field, E_0 is the decrease in the electric field, Z is the distance from the surface, $\lambda_1 = \lambda/n_1$ is the wavelength of the radiation in the denser medium and n_1 is again the refractive index of the denser medium (IRE), n_{21} is the ratio between the refractive indices less dense medium (sample) and denser medium (IRE).

The properties of the evanescent field in the sample depends on the thickness of this sample and therefore two cases have to be taken into consideration: one where the sample exists in bulk where the electric field amplitude decreases to a very low value through the sample, and the second case where the sample only exists in a very thin film in such a manner that the electric field amplitude remains largely constant. For the second case where the sample is such a thin film that it has no controlling effect on the evanescent field it would be the layer behind the sample (with breaking index n_3) that would control the decay of the evanescent field. This implies that for the equations above n_{21} could potentially be replaced by $n_{31} = n_3/n_1$ or $n_{32} = n_3/n_2$. Hence the penetration depth becomes less of a problem when you have a homogenous sample in excessive amounts, when you can assure the thickness of sample is exceeding the calculated maximum penetration depth. The problem arises when the sample volume is small or if the sample is inhomogeneous. We have proven inhomogeneity in our samples and we theoretically have two refractive indices; one that belongs to the membrane material and one that belongs to the fouling that consists mainly of different proteins, but also minor quantities of fat (plus minerals which will be spectroscopically inactive in the IR range) and it is due to the inhomogeneity that we have to consider n_3 (Figure 2.5). When working with inhomogeneous samples or as in this case with layered samples, quantification becomes a problem. The first layer is easily quantifiable providing the light penetrates through the layer. Quantification of the second layer becomes more problematic because the volume of light hitting the sample is unknown as

some is absorbed in the previous layer. The complexity increases when the previous layer has a varying thickness making the possible illuminated volume the limiting factor for the quantification.

Whey proteins are expected to be deposited on the membrane as residual fouling after the final production and cleaning cycle. Table 3.1 shows the composition of the whey proteins. The main fraction is β -lactoglobulin (55-65%).

Table 3.1 – Overview of protein distribution in whey (Marshall & Daufin, 1995).

Protein	% of whey proteins	Molecular weight (kDa)
β-lactoglobulin	55-65	18.4
α-lactalbumin	15-25	14.2
Immunoglobulins	10-15	80-900
Bovine serum albumin (BSA)	5-6	66.3
Proteose – peptone	10-20	4-80
Minor proteins	< 0.5	30-100

When measuring used membranes we thus have a minimum of two layers: the membrane itself and the residual fouling. Due to the ATR penetration depth the final IR spectra is influenced by both sample layers. The penetration depth in our experiment will not only vary with the wavelength and the refractive index of our IRE, but also with the material (sample) that is in contact with the IRE. This means that we have a rather unpredictable n_2 which affects what could be perceived as n_3 , the membrane material. Fluctuations in the n_2 can have an influence on the critical angle of incidence and thereby effect the total internal reflection. However, this is more a theoretical speculation as the refractive index of our samples never increases to the level of the diamond in the IRE with a refractive index of 2.4. The refractive index of PES is 1.62 (Kuriki et al., 2004) which might be changed due to proprietary modifications (grafting) of the membrane material done by the supplier. The refractive index of the protein mixture that originates from the whey is difficult to determine for the specific environment in relation to the membrane, but β -lactoglobulin, which is the main constituent, has a refractive index of 1.46 (Bauer et al., 1999). These values will never surpass the value of the IRE and thereby break one of the conditions of the total

internal reflection. It therefore does not make sense to use a different n_2 or n_3 as the refractive indices are relatively close. Figure 3.6 shows the expected penetration depth for PES and β -lactoglobulin in the working range for the data analysis for my research; the largest difference is found at the lower wavenumbers, about $0.8\mu\text{m}$.

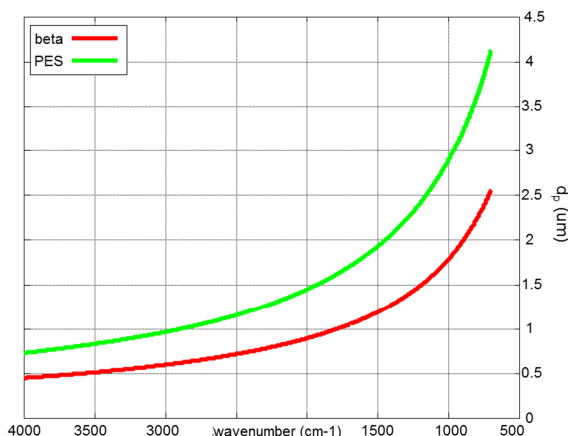


Figure 3.6 – Penetration depth for PES (green) and β -lactoglobulin (red).

Previous studies have shown that there is a heterogeneous spatial distribution of fouling on a membrane leaf, hence the thickness of the fouling layer varies resulting in varying influence from the membrane material on the spectra (Schwinge et al 2004). These changes can obviously affect the coherence with Lambert-Beers law, resulting in the intensity of the peak no longer correlating with the concentration of fouling and these features are relevant to investigate.

3.3 Lambert-Beers law

Lambert-Beers law relates the attenuation of light to the properties (concentrations) of the material through which the light is traveling. In IR spectroscopy the amount of absorbed electromagnetic radiation is determined by the interaction with the molecular vibrations in the sample. The ratio of the radiation intensity prior to and after passing through the sample at a certain wavelength is the heart of the quantitative IR measurement. The

Lambert-Beers law describes the relationship of the spectroscopic information with sample concentration.

$$A = -\log_{10} \left(\frac{I}{I_0} \right) = \varepsilon \cdot l \cdot c \quad (3.4)$$

Where A is the absorbance, I and I₀ are the transmitted and the incident radiation respectively, ε is the absorption coefficient that is material and wavelength dependent, l is the (effective) path length and c is the concentration of the attenuating species in the sample (the parameter that is most often of interest) (Günzler & Gremlich, 2002).

There are some sources of errors that can influence the concentration calculation. Some can be attributed only to the spectrometer such as detector non-linearity when high absorbance is reached as this can cause deformed spectra, drift resulting from insufficient temperature equilibration, beam divergence in the sample compartment. Some can be attributed to the chemical and physical phenomena including scatter from particulates, interferences, molecular interactions, changes in refractive index at high concentrations, shifts in chemical equilibrium as a function of concentration, stray light and changes in sample size/path length. When using Lambert-Beers law for mixture analysis it is required that the absorbing species behave independently of each other and that the absorption occurs in a uniform medium (Harris, 2007), that is that the absorption of individual species are additive.

To make use of Lambert-Beers law in a chemistry environment a calibration curve is traditionally prepared over the range of concentration that are expected for the unknown sample and keeping the absorbance level within the linear response of the instrument (in classical spectroscopy A < 0.5). Unfortunately this classic approach is not possible for a large variety of real life samples e.g. because the sample material is from a source where pure samples are impossible to retrieve or as in this case where the samples originate from a production environment where the end-product is very different from the original feed stream. The residual fouling that is the subject of this thesis work is attached to the membrane and as a consequence the IR spectra contain evidence of both residual fouling and membrane

materials. Removing the residual fouling from the membrane without unfolding and possibly degrading the proteins or losing any other molecular component is difficult/impossible and is not within the scope of this thesis. Whey cannot be used as a reference material as the composition of the residual fouling is expected to be different due to the nature of the filtration unit operation (including the CIP) where fouling fragment are selectively removed. Nevertheless, it is assumed that Lambert-Beers law can be used as a relative, quantitative comparator of residual membrane fouling provided that samples are measured on the same instrument under the same conditions.

3.4 Spectral resolution

Spectral resolution is defined by the type of instrument used and can typically be downgraded (selected) if maximum resolution is not required for the given purpose. The spectral resolution is typically optimized according to the maximum time that a spectral measurement must take and the natural linewidths of the finer spectral details in the sample spectrum. In condensed phase it is rare to find natural FWHM less than 6 cm^{-1} which will then be the maximum obtainable resolution. For this thesis work it was decided to use the best possible spectral resolution i.e. 4 cm^{-1} .

3.5 Interpretation of IR spectrum

The IR region was measured between 4000 cm^{-1} and 700 cm^{-1} . The IR spectra contain many absorption bands arising from various functional groups present in water, lipids, proteins and polysaccharides which makes IR spectroscopy a valuable method for food analysis.

In this study work, the ATR IR spectra of the used membranes contain several peaks (Figure 3.7) that originates from various sources. Firstly the spectra include bands originating from the membrane material polyethersulfone (PES) of the ultrafiltration cartridge and this material can be grafted by the manufacturer with different species. Secondly, the spectra contain information about the fouling which consists of several protein types plus fat and minerals. Correct assignment of the most significant peaks is crucial for the interpretation of the results.

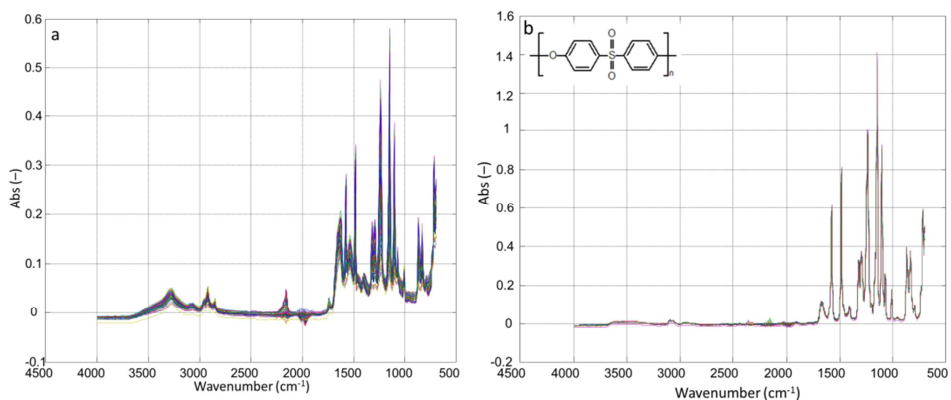


Figure 3.7 – a) IR spectra of residual fouling and membrane material system, b) spectra of virgin membrane, inset: molecular structure of PES.

At wavenumbers with values greater than 1500 cm^{-1} it is generally possible to assign each absorption band to a specific functional group i.e. we observe group frequencies (Figure 3.8).

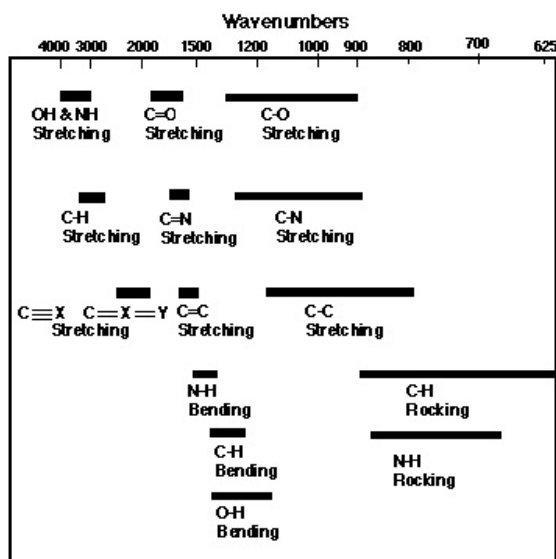


Figure 3.8 - overview of the fundamental vibrations in IR spectroscopy (Modified from <http://www.wag.caltech.edu>).

The IR spectra we have obtained from the used membrane samples contains proteins from the residual fouling even after cleaning which is evidenced by the two signals at 1650 and 1550 cm^{-1} that originates from amide I and II vibrations of proteins or peptides (Chalmers & Griffith, 2002). More ranges could be investigated as there are potentially nine normal modes of peptides: A, B, and I-VII in order of decreasing frequency (increasing wavenumber). The amide bands I (80% C=O stretch, near 1650 cm^{-1}), amide II (60% N-H bend and 40% C-N stretch, near 1550 cm^{-1}), and amide III (40% C-N stretch, 30% N-H bend, near 1300 cm^{-1}) are generally employed to study protein structure (Dong et al., 1990). For mapping the fouling on membrane leaves it is mostly the amide II absorption band that has been investigated (Delaunay et al., 2008, Bégoïn et al., 2006) as there is little or no interference from the membrane peaks in that particular range of IR. In contrast the amide I absorption band is interfering with the water bending absorption band (adsorbed moisture) and in addition we have found possible evidence for an unknown molecule that could be used for grafting the membrane.

The spectra also contain evidence of fat molecules, but very small concentrations. This makes good sense as microfiltration membrane cartridges usually are employed prior to ultrafiltration and upconcentration of the whey (TetraPak, 1995). The fat signals from the membrane residual fouling appear as the ester carbonyl stretching band at 1740 cm^{-1} and further evidenced by C-H stretching bands around 2929 and 2960 cm^{-1} . IR is also one of the most used analytical/spectroscopic methods to identify polymers (Carragher, 2010). In this case it was particularly interesting to obtain an overview of polyethersulfone (PES) (inset Figure 3.8b) that the spiral wound ultrafiltration membrane cartridges are made of. The most significant peaks for this specific polymer are the asymmetric stretch of the aromatic ether group (Ar-O-Ar) appearing at 1241 cm^{-1} and the absorption bands due to the asymmetric (1323 cm^{-1}) and symmetric (1159 cm^{-1}) stretches of the sulfone group (O-S-O) that are clearly identified (Nair et al., 2001). The absorption band at 1241 cm^{-1} is important when performing data analysis in the classical sense (height measurement) as this peak is often used as a reference peak to calculate protein concentration versus the membrane material.

For the absorption bands at wavenumbers below 1500 cm^{-1} the assignment of peaks becomes difficult (few group frequencies) due to more sensitivity inter- and intra-molecular interactions and this region is commonly referred to as the fingerprint region. An IR spectrum can have hundred or more absorption bands in this region, but assigning them is difficult if not impossible and only the most intense bands such as esters, ethers and alcohols may be of importance. The fingerprint region is mostly assigned by using a spectral library as reference to find the most similar molecule (Günzler & Gremlich, 2002). In Table 3.2 the most important peaks from the IR spectrum of fouled ultrafiltration membranes are listed.

Table 3.2 – Assignment of significant peaks in the IR spectrum of the fouled spectra.

Wavenumber (cm^{-1})	Assignment	Chemical compound
825-875	NH bend out of plane	Amide
1550	C-N stretch, N-H bend	Amide II
1640	C=O stretch, amide	Amide I
1745	C=O stretch, ester	Fat
2700-3000	C-H stretch, CH_2 , CH_3	Methyl, methylene
3300-3500	N-H stretch	Amide
1100	Aromatic ring	PES
1150	SO_2	PES
1240	C-O ether	PES
1300	SO_2	PES
1325	SO_2	PES
1475	C=C ring	PES
1575	C=C ring	PES

3.6 The IR instrument

There are primarily two different main principles within commercial infrared spectroscopy instrumentation: dispersive infrared spectrometers and Fourier transform infrared spectrometers (FT-IR).

3.6.1 The dispersive IR spectrometer

The dispersive infrared spectrometer consists of three main components: a light source, a monochromator and a detector. In a dual-beam instrument the

light source is divided into two parallel beams of equal intensity using mirrors (beam splitters). The sample and the reference are placed in each of the beams. After passing through the sample/reference the light passes through the monochromator that consists of a beam splitter (beam chopper) that passes the two beams to a diffraction grating. The grating spreads/diffracts the frequencies (wavelengths) of the radiation before they reach a thermocouple detector. The detector senses the differences between the intensities of the sample and the reference, ruled by the chopper. This means that the background of e.g. atmospheric gasses like carbon dioxide and water vapor are subtracted from the final spectra (Pavia et al., 2009). The dispersive infrared spectrometer records spectra as a function of the wavenumber of infrared radiation by rotating the diffraction grating selecting through a slit only one wavenumber at a time and record its intensity on the detector. It is thus operating in the frequency-domain or the wavenumber-domain (Figure 3.9).

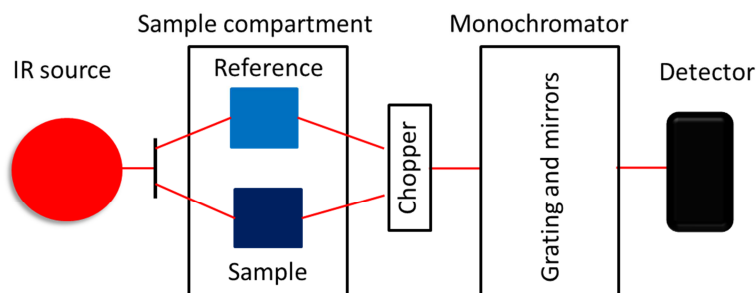


Figure 3.9 – Overview of the dispersive infrared spectrometer.

3.6.2 The FT-IR spectrometer

The Fourier transform spectrometer in contrast works in the time-domain, as the interferogram is essentially a plot of intensity versus time or optical path difference (see later), but it is much more interesting to investigate the frequency-domain spectrum. Therefore a mathematical operation known as Fourier transform (FT) is used to separate the individual absorption frequencies from the interferogram producing a spectrum that closely resembles the spectra from the dispersive spectrometer. The mechanics in the FT-IR spectrometer (Figure 3.10) consists of a light source that passes light

through a beam-splitter which is positioned at a 45° angle to the incoming radiation. The beam-splitter separates the light in two beams one that is undeflected (continuing in a straight line) and one that is oriented in a 90° angle. The latter goes to a stationary mirror and is returned to the beam-splitter. The undeflected beam goes to a moving mirror (it is the maximum displacement of the moving mirror that defines the achievable spectral resolution). The motion of the moving mirror causes the path length of the two beams to vary. Finally, the beam is returned to beam-splitter and the two beams recombine and due to path length differences both constructive and destructive interferences occur. The beam that is passed through the sample contains all wavelengths and they are simultaneously absorbed by the sample which creates an interferogram. The interferogram contains information about the energy that was transmitted to the detector at a given optical path difference. Such interferograms cannot be easily interpreted, but are instead treated with a fast Fourier transform by a computer converting the time-domain to the frequency domain and thus resulting in the classical absorbance spectra that we can recognize and investigate quantitatively and qualitatively. The FT-IR normally operates in a single-beam mode and therefore a background spectrum has to be recorded prior to measuring the sample. This means e.g. that all atmospherically gasses, carbon dioxide and water vapor have been subtracted from the sample before data is collected at the detector. The main advantages of the FT-IR instrument is the throughput advantage as all wavenumber are measured simultaneously and no slits are required to select the individual wavenumbers and the fact that the moving mirror distance can be measured very precisely and thus make it possible to obtain a very accurate wavenumber calibration (see box below).

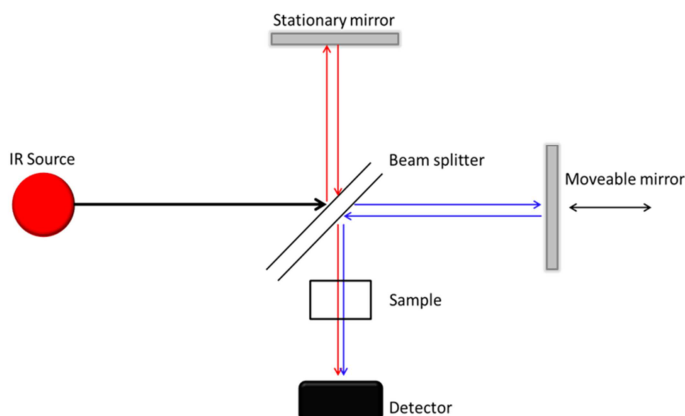


Figure 3.10 – Overview of the Fourier transform infrared spectrometer.

Box 3.1 – Description of Fourier transform.

Advantages of the FT-IR spectrometer

There are a number of specific advantages in using the Fourier transform spectrometer; the multiplex advantage (also called Fellgett advantage) that improves the signal-to-noise ratio in proportion to \sqrt{N} where N is the number of sampling scans (Günzler & Gremlich, 2002). The method is called multiplex because the FT-IR system measures all wavenumbers simultaneously. It is much faster than the dispersive infrared spectrometer because the dispersive instrument measures one wavelength after the other, while one scanning time in an FT spectrometer is decreased to the time needed to move the mirror over a distance that is proportional to the resolution (Wartewig, 2003).

The second advantage is the throughput advantage (Jacquinot advantage) which gives the FT-IR-spectrum a better resolution due to the larger volume of light being emitted from the circular collimated beam, while in a dispersive spectrometer the light is limited by the slit-width for the wavenumber selection (Günzler & Gremlich, 2002, Wartewig, 2003). A third advantage of FT-spectrometers is the so-called Connes advantage which defines the stability of the spectra that arises from the fact that the frequency scale of the FT-instrument can be accurately measured by a He-Ne laser which provides an internal reference for every interferogram. This results in

an accurate frequency calibration of the spectra. Moreover there are two more advantages of the FT-IR spectrometer namely the constant resolution throughout the entire wavenumber region and finally the interferometer include no discontinuities related to gratings and filters.

Both spectrometer setups have the same limitations with regard to the sampling as it is basically limited to two types of sample materials: liquids that can be contained in cuvette with a path length of less than 1 mm or solids that can be turned into a fine powder and diluted with for example KBr to create a KBr+sample-tablet for transmission experiments. Most other sample types require the use of an attenuated total reflectance (ATR) sampling unit. It should be mentioned that it is of course possible to measure IR spectra using diffuse reflectance, which for example is an absolute necessity for large intractable samples such as paintings and sculptures, but due to the low energetic IR sources it is a very poor sampling option.

Data analysis

Methods

It was previously mentioned in the spectroscopy chapter (Chapter 3) that typically one single peak arising from the fouling material is investigated when extracting information on membrane fouling in a univariate fashion. A common method is height determination of specific peaks followed by calculating the ratio of the fouling peak of interest with a reference peak; these peaks can e.g. be the protein peak at 1540 cm^{-1} and a peak arising from the membrane material at 1240 cm^{-1} (Eqn. 4.1; Bégoïn et al., 2006).

$$\text{Height ratio} = \frac{H^{amide\ II}}{H^{1240\text{cm}^{-1}}} \quad (4.1)$$

This method is further developed by Delaunay et al. (2008) where a baseline is subtracted from the ratio in Equation 4.1 and equating corrected ratio to a model parameter that depends on the type of membrane (α) multiplied with the protein concentration (expressed in $\mu\text{g}\cdot\text{cm}^{-2}$ [P]; Eqn. 4.2).

$$\frac{H^{amide\ II}}{H^{1240\text{cm}^{-1}}} - H^{baseline} = \alpha \cdot [P] \quad (4.2)$$

Equation 4.2 can only be realistically solved in laboratory scale experiments where protein concentration is predetermined, and the parameter α can be estimated based on training, as the protein residual fouling for industrial scale membranes is unknown due to many months/years of use under varying conditions and multitude of CIP cycles.

Equations 4.1 and 4.2 do not give feasible solutions to solving the fouling distribution problem. The IR spectrum has evidence for the same chemical compound in several regions and e.g. protein is not only found in one peak

but in several peaks over the full spectrum. This feature is obviously not taken into consideration when employing univariate peak-height strategies. These equations do not take underlying features into consideration which could potentially be important when investigating a complex arrangement such as the membrane-fouling-system.

In literature a second method for mathematically extracting the milk component contribution from the membranes is described (Rabiller-Baudry et al., 2002). The method is called *double difference method* and is calculated as follows:

Difference spectrum 1 = recorded spectrum – water spectrum

Difference spectrum 2 = difference spectrum 1 (fouled membrane) – difference spectrum 1 (virgin membrane)

The first difference spectrum calculation is performed on both virgin membrane and fouled membrane. This method is said to aid in enhancing the phenomena that are interesting for the fouling process while removing the remaining *background effects*, making the protein fouling stand out and the follow-up univariate data analysis easier. This could aid in giving a pure spectrum of the fouling perhaps eliminating some underlying features that originates from the membrane which could possibly interfere with the height measurement. This method requires some computation and by removing features regarding the membrane information about this cannot be recovered.

By applying multivariate/chemometric tools we expect to extract more information because we perform data analysis on a wider range of the spectrum, that way enhancing the important features and eliminating the insignificant features by decomposition of the spectra.

4.1 Principal component analysis (PCA)

The most commonly used multivariate technique is principal component analysis (PCA). The method can be used for a large variety of purposes: data reduction, modelling, outlier detection, variable selection, unsupervised classification, etc. The data matrix is decomposed into a bilinear model as shown in Equation 4.3

$$\mathbf{X} = \mathbf{TP}^T + \mathbf{E} \quad (4.3)$$

Where \mathbf{X} is the data matrix, \mathbf{T} is the score matrix (describes the column space or samples) and \mathbf{P} is the loading matrix (describes the loading space or variables) that captures the main variation in the data, and \mathbf{E} is the error that contains any un-modelled variation. It is sometimes useful to apply a pre-processing to the spectra prior to data analysis. This could be mean centering (subtraction of the mean from each variable) or auto scaling (subtraction of the mean from each variable and divide with the standard variation in each variable) that handles different data-ranges in the same measurement. We are interested in modelling as much of the variation as possible which is achieved by decomposing the data into linear combinations called principal components (PCs). The PCs are found from consecutive orthogonal vector outer-products based on the largest variation in the data. This infers that the first principal component describes the largest variation in the data. The second PC explains the second largest variation in the data while at the same time being orthogonal to the first PC, and so forth. Each PC is thus the product of a score vector (\mathbf{t}) and a loading vector (\mathbf{p} ; Eqn. 4.4).

$$X = t_1p_1 + t_2p_2 + \dots + t_ip_i + E \quad (4.4)$$

The number of PCs defines the number of sources of variation observed in the data, hence the number of independent features. In spectral data it is common to observe co-variation which decreases the number of PCs to a considerable lower set than the original number of variable. This is very useful as we often have thousands of variables and reducing the data to a three of four coordinate systems simplifies and increases the interpretability.

In PCA there is an orthogonality constraint imposed between the principal components which simplifies the result as it forces them to be completely uncorrelated. Each PC describes a pattern in the data inferring that if two components co-vary they cannot be resolved and the loadings will not display pure information (e.g. spectra) of the chemical components (Wold et al., 1987). PCA is thus often used as a visual or exploratory method and the results can be displayed in a score plot or a loading plot or combined in a so-called bi-plot. The score plot describes objects that have similarities by clustering the samples. This also offers the opportunity to find samples that are significantly different from the remaining samples (outliers). In the loading plot detection of significant variables for each PC is possible and can be used for variable interpretation and selection.

We have from PCA determined that the number of PCs should be two – one PC that describes the polyethersulfone (PES) and one that describes the residual fouling which mainly consists of protein (Figure 4.1a). A third principal component results in over-fitting as it models parts of the error judged by its erratic/chaotic appearance (Figure 4.1b). Two principal components is a qualified initial guess as we are investigating a two layer system. But from the literature we know that there possibly could be more features that co-vary with either of the two contributors, e.g. secondary structure in the protein fouling, presence of fat or grafting used to change the hydrophilicity of membranes.

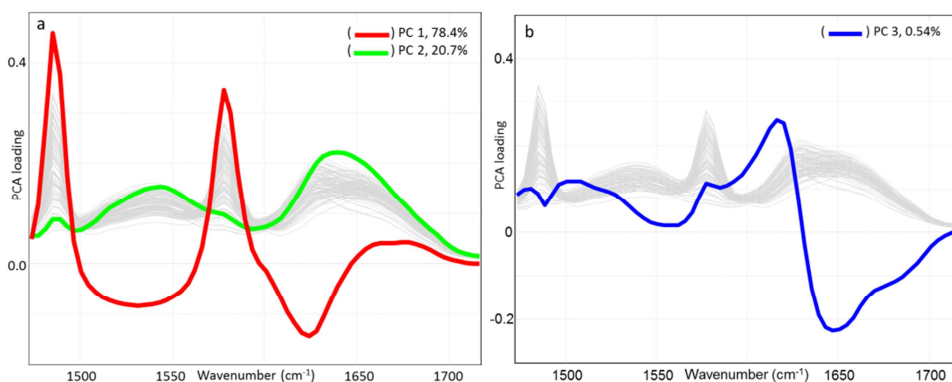


Figure 4.1 - Principal component analysis (N=100), data is mean centered, a) two component model, b) the third component in the PCA model.

This implies that another method for determining the number of components needed to describe the data is necessary.

4.2 Multivariate Curve Resolution (MCR)

MCR was originally developed to encompass evolutionary analytical data from e.g. a process or an analytical measurement (Lawton & Sylvestre, 1971). The method is meant to solve the mixture analysis problem; it builds on the bilinearity and utilizing constraints to get the best resolved model, limiting the ambiguities (Jaumot et al., 2004). Multivariate curve resolution does not contain a build-in (intrinsic) constraint on orthogonality as PCA does and is therefore (conceptually) better at resolving true chemical components, even if they co-vary. It is particularly well suited for analyzing and modelling spectroscopic measurements since the underlying analytical pattern in these measurement is already a bilinear model (Eqn. 4.5), namely Lambert-Beers law (Chapter 3.3). The Lambert-Beers law is a model of pure signal contributions, where concentrations are directly proportional to the intensity (or absorbance) of the light, hence MCR fits these measurements because it precisely mimics the structure of the analytical measurement.

The model that MCR follows is

$$\mathbf{D} = \sum_i \mathbf{c}_i \mathbf{s}_i^T + \mathbf{E} = \mathbf{C}\mathbf{S}^T + \mathbf{E} \quad (4.5)$$

Where \mathbf{C} contains the elution (or concentration) profiles of all components and \mathbf{S} the related pure spectra, \mathbf{E} is the matrix that expresses the error or the unexplained variance by the bilinear model (Juan et al., 2014).

4.2.1 MCR algorithm

The MCR algorithm has been developed in two forms: the non-iterative and the iterative.

The non-iterative MCR approach - The first and most significant approaches are Window Factor Analysis (WFA) (Malinowski, 1992), Sub-window Factor Analysis (SFA) (Manne et al., 1999) or Heuristic Evolving Latent

Projections (HELP) (Kvalheim & Liang, 1992). The non-iterative MCR methods combine information of small sections, that in the literature is referred to as subspaces, of data that are constructed based on global and local rank information to obtain pure profiles. The subspaces can be concentration windows or sections of the data matrix that have a particular property. This can e.g. be the presence or absence of certain components/information. For the methods to be applicable the data set that is investigated should have a sequential (or very ordered) concentration direction where concentration windows can be fixed reasonably well. This type of method requires an evolving system (process/reaction kinetics, chromatography, etc.) (Juan & Tauler, 2006).

The iterative MCR approach - The most commonly used approach in MCR is the iterative form because it requires less prior information about the system, due to the flexibility to deal with several kinds of data structures and chemical problems, and the ability to accommodate external information in the resolution process. The iterative methods are e.g. Iterative Target Transformation Factor Analysis (ITTFA) (Vandeginste et al., 1985) that works by optimizing the concentration profile direction under constraints, followed by the recovery of the spectral matrix in the bilinear model by a least squares step. Another method is Multivariate Curve Resolution Alternating Least Squares (MCR-ALS, Gampp et al., (1985) which works by optimization of both concentration profile (**C**) and pure spectra (**S**) in each iterative cycle (Juan & Tauler, 2006). There are five main steps in the MCR-ALS algorithm:

1. Building the data matrix **D**
2. Determine the rank of **D**
3. Find the initial estimates for the spectral or concentration profiles
4. Initiate ALS iterations to calculate spectral and concentration profiles
5. Test for convergence

After building the data matrix and the determination of the rank by e.g. employing SIMPLISMA (Windig & Guilment, 1991) the initial estimate for the spectral profile or the concentration profile is set. Next the estimates of

the two profiles are optimized with predetermined constraints applied until a convergence criterion is reached (Juan et al., 2014). Two different options exist when using a convergence criterion: a predefined number of iterations or a threshold value defining the difference in fit-improvement between consecutive iterations. Once convergence is reached a set of quality parameters that are related to the model fit can be evaluated such as variance explained and lack of fit (LOF, Eqn. 4.6).

$$\%LOF = 100 \sqrt{\frac{\sum_{i,j} e_{i,j}^2}{\sum_{i,j} d_{i,j}^2}} \quad (4.6)$$

Where $d_{i,j}$ is an element of the data matrix \mathbf{D} and $e_{i,j}$ is the related residual (Jaumot et al., 2004).

4.2.2 Rank determination and initial guess

When computing a MCR model determination of the rank of system is vital and often Evolving Factor Analysis (EFA, Keller & Massart, 1992) is employed. There are some assumptions that have to be fulfilled: the data has to have an intrinsic order, non-negativity of concentrations and that the Lambert-Beers law is valid (Keller & Massart, 1992). The fundamental idea of EFA is to follow the evolution (change) of the rank of the growing data matrix \mathbf{X} as a function of the ordered variables. This is done by PCA computed from the increasing data matrix.

The EFA can be performed in two directions forward (red, Figure 4.2) and backwards elimination of variables (black, Figure 4.2). The eigenvalues (or their logarithm) for both directions are plotted against the ordered variable in the same figure. At that point in the ordered variable sequence where an eigenvalue rises above the noise level a new substance appears, increasing the rank of the system by one. The opposite is the case with the backward EFA. Thus, an EFA graph provides information on both appearing and disappearing compounds/analytes and also the number of factors present in the system (Figure 4.2). In order to correctly associate the appearance of a compound with the disappearance it is assumed that the first to appear is also the first to disappear and so forth (Keller & Massart, 1992). When analyzing

multiset data tables with EFA it is advised that each subset should be evaluated individually (Juan et al., 2014)

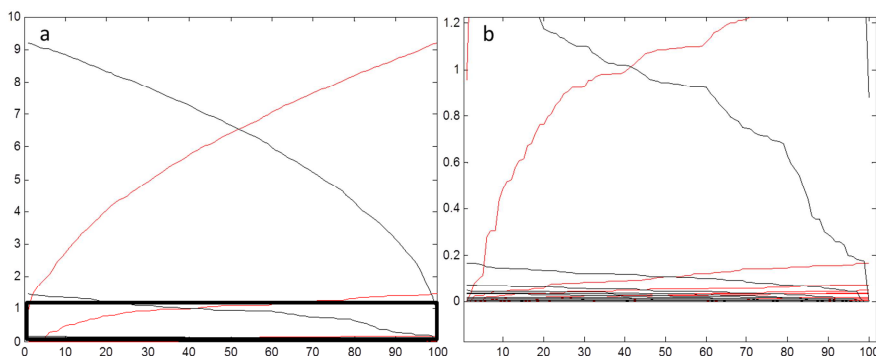


Figure 4.2 – Evolving factor analysis (EFA), a) full EFA for data in Paper II, box is presented in b, b) zoom on the lower part of the EFA. The red lines represents the forward evolving factor analysis, black lines represents the backwards evolving factor analysis.

EFA is also utilized when determining the initial estimates for MCR-ALS. The initial estimates for the spectra or concentration profile should be *sensible guesses* as it is the starting point for the optimization process and the choice might/will influence the end-model if the applied constraints (and the data) do not lead to a mathematically unique solution. A sensible initial estimate can be found if there is prior knowledge on the system, e.g. pure spectra of some of the components. MCR-ALS works on single data matrices by optimizing a set of initial estimates in an alternating least-squares fashion in iterative cycles under the action of constraints until convergence is reached. The EFA that detects the appearance and disappearance of components in the system, thus providing concentration profiles under the assumption of a sequential order of appearance/disappearance for all components. EFA is a method that was originally developed to work with data that has a certain structure such as process/reaction-like data (Keller & Massart, 1992). If structure in the data is absent then it is common to use a set of methods called *pure variable selection*, and one of the most commonly used is Simple-to-use Selfmodelling Analysis (SIMPLISMA) (Windig &

Guilment, 1991). Most of the self-modeling techniques are based on principal component analysis. The core is to select the two most dissimilar rows or columns in a matrix and use these as the initial estimates for spectra or concentration profiles. Hence, SIMPLISMA does not require any reference spectra. There is one requirement though, the presence of pure variables. The first pure variable can be found by determining the vector (projected onto a subspace) with the largest length. This implies that a variable with a relatively high intensity will be relatively pure suggesting that a variable with low intensity will have contributions from several components. The variable with the highest intensity is the first pure variable (Windig & Guilment, 1991).

4.2.3 Ambiguities

Creating a model of data is always linked with some uncertainty. In the case of MCR it is also linked to ambiguities. This is a problem because different combinations of concentration profiles and spectra can reproduce the original data with the same quality of fit. There are three different types of ambiguities: permutation, intensity and rotation.

- Permutation ambiguities represent the fact that there is no natural sorting order for the MCR components (unlike e.g. PCA). They therefore can be mixed/reordered within the spectra and concentration matrix and obtain identical results.
- Intensity ambiguities arise when dyads of profiles (concentration and spectral profile of one MCR component) have the same shape but different relative scales between the concentration profile and the spectra reproduce the original data equally well. This is the reason why concentration values (c_i) and pure response intensity (s_i^T) profiles are always in arbitrary units unless real concentration values are available/known. To avoid intensity ambiguity it is custom to normalize either the concentration profile or the spectra (in the absence of reference concentration values within the optimization).
- Rotational ambiguities are the most relevant ambiguities because dyads of concentration profiles and spectra with different shapes can reproduce

the original data with the same fit quality. Mathematically it can be expressed as Eqns. 4.5 and 4.7

$$\mathbf{D} = \mathbf{CS}^T + \mathbf{E} \quad (4.5, \text{repeated})$$

$$\mathbf{D} = (\mathbf{CT})(\mathbf{T}^{-1}\mathbf{S}^T) + \mathbf{E} \quad (4.7)$$

Where \mathbf{T} is any transformation matrix which continues to provide profiles that obeys specific sets of constraints when optimizing the MCR model. The best way of decreasing or suppressing ambiguities is to introduce constraints with uniqueness/selectivity features, or by using multi set structures. The diversity of the subsets in the multiset structure makes the possible combinations of profiles that describes the variation and fulfills the constraints smaller.

Multi sets - Multi sets (augmented matrices) are frequently used in MCR. The idea is very flexible and can be based on data matrices of different sizes and meanings (Juan et al., 2014). They can be structured as a row-wise augmented matrix (Eqn. 4.8) where data tables are appended next to each other, e.g. when using several instruments to monitor or investigate the same process. It can be structured as a column-wise augmented matrix (Eqn. 4.9) where data tables are on top of each other, e.g. different batch runs of the same process monitored or investigated. Finally the matrices can be augmented in both the row- and column-wise direction (Eqn. 4.10). The multi set matrices appear more complex but they obey the same bilinear models under Equation 4.5 and therefore MCR can be applied.

$$\begin{aligned}
[D_1 \ D_2 \ D_3 \ \cdots \ D_L] &= C[S_1^T \ S_2^T \ S_3^T \ \cdots \ S_L^T] + [E_1 \ E_2 \ E_3 \ \cdots \ E_L] \\
&= CS_{aug}^T + E_{aug} \quad (4.8)
\end{aligned}$$

$$\begin{pmatrix} D_1 \\ D_2 \\ D_3 \\ \cdots \\ D_K \end{pmatrix} = \begin{pmatrix} C_1 \\ C_2 \\ C_3 \\ \cdots \\ C_K \end{pmatrix} S^T + \begin{pmatrix} E_1 \\ E_2 \\ E_3 \\ \cdots \\ E \end{pmatrix} = C_{aug} S^T + E_{aug} \quad (4.9)$$

$$\begin{aligned}
\begin{bmatrix} D_{11} & D_{12} & D_{13} & \cdots & D_{1L} \\ D_{21} & D_{22} & D_{23} & \cdots & D_{2L} \\ D_{31} & D_{32} & D_{33} & \cdots & D_{3L} \\ \cdots & \cdots & \cdots & \cdots & \cdots \\ D_{K1} & D_{K2} & D_{K3} & \cdots & D_{KL} \end{bmatrix} \\
= \begin{pmatrix} C_1 \\ C_2 \\ C_3 \\ \cdots \\ C_K \end{pmatrix} [S_1^T \ S_2^T \ S_3^T \ \cdots \ S_L^T] + \begin{pmatrix} E_{11} & E_{12} & E_{13} & \cdots & E_{1L} \\ E_{21} & E_{22} & E_{23} & \cdots & E_{2L} \\ E_{31} & E_{32} & E_{33} & \cdots & E_{3L} \\ \cdots & \cdots & \cdots & \cdots & \cdots \\ E_{K1} & E_{K2} & E_{K3} & \cdots & E_{KL} \end{pmatrix} \\
= \\
C_{aug} S_{aug}^T + E_{aug} \quad (4.10)
\end{aligned}$$

There are some conditions that should be fulfilled when building a meaningful multiset; data tables that are analyzed together should share some kind of common information, and the data tables that have been appended should have a common mode which can be the spectral or the concentration mode where a common profile can be established.

4.2.4 MCR constraints

MCR-ALS is very flexible and often exhibits a uniqueness issue and in order to ensure that the computed model is reliable constraints are commonly applied. Constraints are not compulsory if the model can be resolved uniquely but can aid in making the model more interpretable. It can be

applied in both the row (sample) and column (variable) space. The flexibility in the application of constraints explains the versatility of the MCR algorithm which can be adapted to many scenarios through proper selection of constraints. Selecting the appropriate constraints and knowing how to apply them is the most crucial point to ensure that meaningful and reliable solutions are obtained (Juan et al., 2014, Juan & Tauler, 2006). Many different constraints exist and can be divided into natural constraints and mathematical constraints.

The natural constraints are:

- Non-negativity forces the profiles to contain (almost) only positive values. The negative values can be eliminated by simply replacing them with zeros or softer modelling can be applied such as non-negativity least squares (NNLS, Hanson & Lawson, 1974) or fast non-negativity least squares (FNNLS, Bro & De Jong, 1997). This constraint applies to all concentration profiles and many instrumental responses (absorbance spectra, chromatograms, etc.) where negative numbers are unexpected.
- Unimodality defines the presence of one single maximum per profile.
- Closure is a mass-balance constraint which is most commonly applied to profiles of reaction systems e.g. degradation of protein into amino acids (Juan et al, 2014).
- Known pure spectra/concentration profile is an equality constraint that forces the peaks to be a certain predefined shape - e.g. Gaussian or Lorentzian - or if a spectrum of a pure component exist this can be applied (Beyramysoltan et al., 2013). Equality constraints helps avoiding the rotational ambiguity that soft modelling methods can suffer from.

The constraints that are related to the mathematical conditions are:

- Selectivity relates to the zones of absence of the components in some regions in the profiles (Manne, 1995). This constraint usually applies to the concentration profiles. It can be used within a matrix or subset in a multiset structure and increases the accuracy in the definition of the profiles.

- Correspondence of species is only applied to column-wise augmented matrices and expresses the correspondence and presence/absence of components in the analyzed samples which is indicated in the algorithm by a binary code of 0 (absent) and 1 (present) (Tauler & Barcelo, 1993).
- Hard-modelling forces the concentration profiles to be fitted by a parametric physicochemical model (Juan et al., 2014). This can be applied when a peak shape can be defined by a parametric equation. This constraint implies performing model-fitting during the iterative optimization process.
- Correlation constraint means application of an internal univariate calibration model to the concentration profiles, this allows for prediction of concentration of unknown samples, hence the data set is separated into a calibration set and a test set (Juan et al., 2014).

4.3 Analysis of Variance (ANOVA)

Analysis of variance is an established procedure for isolating the sources of variability in a set of measurements. The purpose is to determine the extent to which the effect of an independent variable is a major component (Girden, 1992). It is used in comparative studies in order to analyze the differences between group means and to determine if these are equal or not. ANOVA is useful in comparing three or more means to test if there is a statistical significant difference between them. The statistical significance of the experiment is determined by a ratio of two variances. This ratio is independent of several possible alterations to the experimental observations: adding a constant or multiplying a constant to all observations does not alter significance. The statistical significance of the ANOVA results are thus independent of constant bias and scaling errors.

ANOVA is built on the principle of hypothesis testing, e.g. the null hypothesis H_0 , where a test result is statistically significant if it is deemed unlikely to occur by chance. A statistically significant result is achieved when the probability is lower than a predetermined threshold value which justifies the rejection of the null hypothesis. The null hypothesis in ANOVA is typically that all groups are random samples from the same population and

that the predefined treatment has the same effect on all samples ($H_0: \mu_1 = \mu_2 = \mu_3 = \dots = \mu_k$).

ANOVA most commonly uses a linear model that relates the response to the treatment. The model is typically linear/additive in the parameters but may be non-linear across factor levels. The linearity of the model requires some assumptions for it to be valid:

- Independence of the observations
- Normal distribution of the residuals
- Equality (homogeneity) of variance – the variance of the data in groups should be the same

This all implies that the errors are independently, identically, and normally distributed.

ANOVA is derived from a splitting of total variability into its separate parts. The total corrected sum of squares

$$SS_T = \sum_{i=1}^a \sum_{j=1}^n (y_{ij} - \bar{y}_{..})^2 \quad (4.11)$$

is used as a measure of overall variability in the data. This equation can be rewritten as

$$\sum_{i=1}^a \sum_{j=1}^n (y_{ij} - \bar{y}_{..})^2 = n \sum_{i=1}^a (\bar{y}_{i.} - \bar{y}_{..})^2 + \sum_{i=1}^a \sum_{j=1}^n (y_{ij} - \bar{y}_{i.})^2 \quad (4.12)$$

which states that the total variability in the data as measured by the total corrected sum of squares, can be split into a sum of squares of differences between the treatment averages and the grand average plus a sum of squares of differences of observations within treatments from the treatment average. Equation 4.12 can be shortened to

$$SS_T = SS_{Treatment} + SS_E \quad (4.13)$$

When calculating the sum of squares the matching degrees of freedom is an important concept defined as the number of values the final calculation of a statistics is free to vary. SS_T has $N-1$ ($N = a \times n$) degrees of freedom when there are a levels of the factor and hence a treatment which infers that $SS_{\text{Treatment}}$ has $a-1$ degrees of freedom. Finally within any treatments there are n replicates providing $n-1$ degrees of freedom to estimate the experimental error (Montgomery, 2005).

Calculating if the treatments are different from each other (rejecting H_0) is based on an F-test (also known as Fisher's F-test). The F-test compares two (or more) variances σ_1^2 and σ_2^2 that has been estimated by s_1^2 and s_2^2 . The F-value is calculated by computing a ratio between the two variances: dividing the largest variance with the smallest variance (Massart et al., 1997). The result is compared to a table with critical F-values where the degrees of freedom and significance level determines the critical F-value. If the critical F-value is larger than the calculated F-value the null hypothesis is accepted concluding that no effect of the treatment is observed/identified.

Two kinds of errors may be committed when testing hypotheses (Montgomery, 2005). If the null hypothesis is rejected when it is true a type I error has occurred (the α error) hence detecting an effect that is not present. If the null hypothesis is not rejected when false a type II error has been made (the β error) hence failing to detect an effect that is present. To minimize the risk of these errors a significance level is defined during hypothesis testing and is commonly set to 0.05.

4.4 Non-linear regression

In order to move away from the univariate methods when measuring fouling on ultrafiltration membrane cartridges non-linear regression was used to extract information from the spectral measurements.

There are two approaches to non-linear regression: an empirical approach and a mechanistic approach (Massart et al., 1997). The empirical approach tries to model as well as possible the form of the response by means of a simple function. The choice of the functional form is suggested by the data. It is used

when no prior information is known about the functional form of data. The simplest approach is to fit a polynomial function of a certain degree. The basis of this approach is the fact that any well-behaved mathematical function can be approximated by a higher-degree polynomial. The mechanistic approach on the other hand requires more understanding of the process that is studied and the appropriate functional form can be selected beforehand or can be derived from underlying physic-chemical phenomena or from theoretical considerations. The experimental data is then modelled with this function. The primary goal for this approach is to estimate the function coefficients by fitting the model (and compare those e.g. for different experimental conditions, rather than the data as such).

A combined mechanical/empirical approach has been used in this thesis in order to develop a new method for determining the relative concentration of residual fouling on the ultrafiltration membranes. Curve fitting is often used to fit spectroscopic and chromatographic data and the shape of the peak indicates which model should be used. The only prior knowledge about the amide peaks in the IR-spectrum is the approximate peak shape. They exhibited both Gaussian and Lorentzian characteristics and at times a mixture which complicated the use of non-linear regression. To extract the most correct information from the data curve fitting was performed on the peaks of interest: amide I (1600-1700 cm^{-1}), amide II (1500-1550 cm^{-1}), and fat (1700-1740 cm^{-1}). The simplest mathematical function including noise is:

$$y = \beta_1 \exp\left(-\frac{x-\beta_2}{\beta_3}\right)^2 + \varepsilon \quad (4.14)$$

where estimations of the parameters of the model hold the information on peak characteristics such as peak height/area (β_1), the position of the top inside the wavenumber interval (β_2) and the peak width (β_3). Several attempts were made using the area under the curve following the idea that it would give a better estimation of the relative fouling concentration. Unfortunately that was not the case and eventually the parameter that described height was used for concentration determination and mapping (Poster II) which was merely a replicate of the original univariate measurement. The reason for the limited success with non-linear regression can be partly found in Paper II: it

is hard (maybe even impossible) to define the correct number of absorbing species under e.g. the amide II band. The end solution will thus be very dependent on the mechanistic model (one band, two bands, etc.) and the right/appropriate decision on model complexity can vary considerably within one system (e.g. one UF cartridge) and even stronger between different systems.

Process Analytical Technology

Process analytical technology (PAT) is a regulatory framework defined by the Food and Drug Administration (FDA) as *a mechanism to design, analyze and control pharmaceutical manufacturing processes through the measurement of critical process parameters (CPP) which affects the critical quality attributes (CQA)*. It is no longer only important for the pharmaceutical industry but is also an important field for monitoring, optimizing and controlling processes in the food industry along with the pharmaceutical industry (<http://www.fda.gov>, accessed 04-02-2015).

The PAT framework was developed and is promoted in order to support innovation and efficiency in pharmaceutical development, manufacturing, and quality assurance. It is founded on process understanding to facilitate innovation and risk-based regulatory decisions by industry and the FDA. The framework has two main components: 1) a set of scientific principles and tools to support innovation and 2) a strategy for regulatory implementation that will accommodate innovation. A desired goal for the PAT framework is to design and develop well understood processes that will consistently ensure a predefined quality at the end of the manufacturing process (FDA).

The FDA provides four types of tools for generation and application of process understanding.

- Multivariate tool for design, data acquisition and analysis that represent a class of analysis methods
- Process analyzers are metrics that describe the state of the system and can be both univariate and multivariate
- Process control tools include techniques for monitoring and actively manipulating the process to maintain a desired state
- Continuous improvement and knowledge management tools stresses the importance of integrated data collection and analysis procedures throughout the life-cycle of a product

The goal of PAT is to enhance understanding and control of the manufacturing process and also understanding that quality cannot be tested into the products; it should be built-in hence it should be there by design which should be done by implementing Quality by Design (QbD, Figure 5.1, Rathore & Winkle, 2009). QbD is a systematic approach to pharmaceutical development. It promotes designing and developing formulations and manufacturing processes to ensure predefined product quality. Some of the QbD elements include:

- Defining a target product quality profile
- Designing product and manufacturing processes
- Identifying critical attributes, process parameters and sources of variability
- Controlling manufacturing processes to produce a consistent quality over time

Quality is built into pharmaceutical products through understanding of the intended therapeutic objectives, the chemical, physical, and biopharmaceutic characteristic of the drug, the design of the manufacturing process using principles of engineering, material science and quality assurance to ensure acceptable and reproducible product quality.

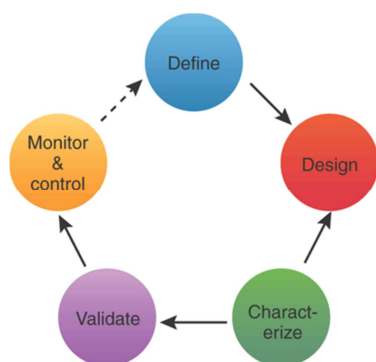


Figure 5.1 – Schematic overview of Quality by Design (QbD) (Rathore & Winkle, 2009).

Before introducing the full package of spectroscopic probes in all flows, tanks and bioreactors it is of uttermost importance to know your process and product, and determine what influences the final quality of the product. A process is considered well understood when the ability to predict the outcome to a high degree is present. This ability originates from three definitions; 1) all critical sources of variability are identified and explained; 2) variability is managed by the process, and 3) product quality attributes can be accurately and reliably predicted over the design space established for materials used, process parameters, manufacturing and environmental conditions.

In my opinion there are three main stages in implementing PAT in a production: Initiation, basic monitoring and full inline control including advanced monitoring with real time release as the absolute goal. The initiation requires several practical aspects to be dealt with such as e.g. the infrastructure of the data path - it is the greatest hurdle to overcome but also very important. Automated data acquisition systems, data bases, networks and synchronization must be in place. Many pharmaceutical and food industries collect vast amounts of data and store them but often the data has never been actively used in process control because earlier regulatory environments required re-validation if using historical data (Eriksson et al., 2006). When the infrastructure is prepared the data acquisition can be initiated. First and foremost getting to know the process well is of great importance. This can be done in many ways but small scale (pilot production

or laboratory scale) can be preferred due to less administrative work with *Good Manufacturing Practice* (GMP). Sampling from the process will give understanding of the different unit operations and how they affect the final quality of the product. Measurements are done off-line in the laboratory by using spectroscopy, chromatography or other established methods along with known chemical/physical methods, to relate *old* quality control data to the *new* spectroscopic data. An illustrative example of the initiation of a PAT project is given by Lyndgaard et al. (2014) where a UV-VIS process analyzer has proven successful due to its ability to monitor tryptophan that is a strong UV chromophore in whey protein in the ppm range and has the ability to measure in-line with speeds of less than a second. It is of great interest to be able to follow the cleanliness state of the membrane system and move from the recipe driven cleaning to data driven cleaning. Unfortunately it is impossible to monitor the membranes when they are part of the process due to the nature of the spiral wound membrane and therefore another method is needed. Lyndgaard et al. (2014) describes the use of UV-VIS in the whey purification production. The UV-VIS probe was not implemented in-line initially but samples were extracted from different positions in the process and at different important time points during cleaning and were measured off-line. As previously described in Chapter 2 there are several steps in a CIP-cycle and after each cleaning step a flushing is initiated to remove released fouling debris and excessive chemicals. The flushing should return the chemical environment in the process to pure water or as close as possible, and to monitor this UV-VIS was employed. Figure 5.2 shows the evolution of the tryptophan during cleaning and especially the enzyme step is crucial for releasing proteins from the membrane. The tryptophan content increases during recirculation for the duration of enzymatic cleaning (Figure 5.2b). From the plots in Figure 5.2c it is obvious that the cleaning can be shortened as both the enzymatic step and the hydrogen peroxide step has reached water purity levels after a few minutes leaving the remaining flushing time redundant and a waste of water and time.

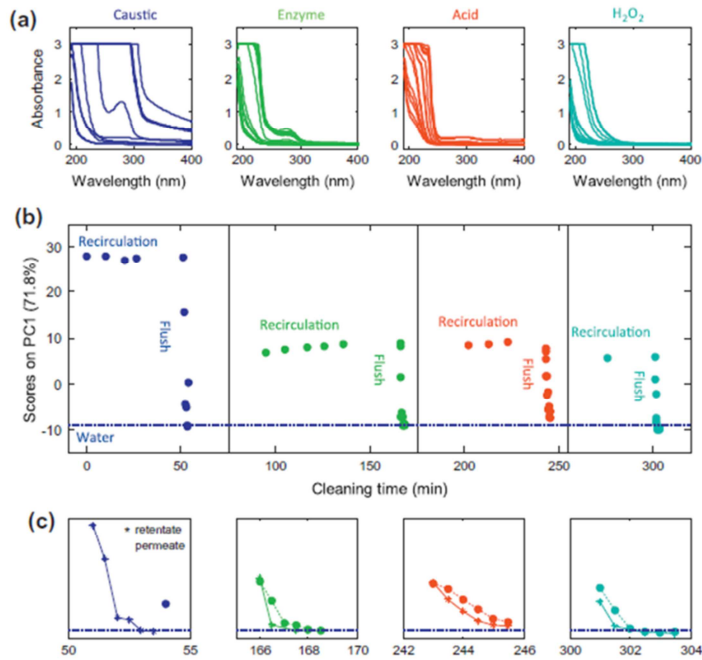


Figure 5.2 – Figure from Lyndgaard et al. (2014), a) UV absorbance spectra from different cleaning steps, b) PCA score plot of a water sample and samples collected during cleaning procedure, c) Zoom-in on PC1 scores vs time during flushing.

It is important to determine the most optimal process parameters in an efficient way. This means that the knowledge space should be determined which is done by using Design of Experiments (DoE, Eriksson et al., 2008) as processes often are multi-factorial and the traditional one-factor-at-the approaches will not suffice. Determining the knowledge space with DoE determines which process parameters are significant and at which range they produce products within quality specifications (Figure 5.3). Second, the design space is determined. It is a multi-dimensional region that encompasses the various combinations of product design, manufacturing process design and operating process parameters plus raw material variations (Somma & Signore, 2008). Where the product meets quality specifications is defined by a model. The design space is the minimum quality target for each batch. Finally the control strategy/normal operation space is determined. It is where the knowledge is gathered and refined into a control strategy for the process to deliver consistent results; it addresses process operating parameters and

raw material quality to maintain the process within the design space (Somma & Signore, 2008). Within the control strategy space all products are within specifications (and quality criteria are met) and it is the overall target for each batch.

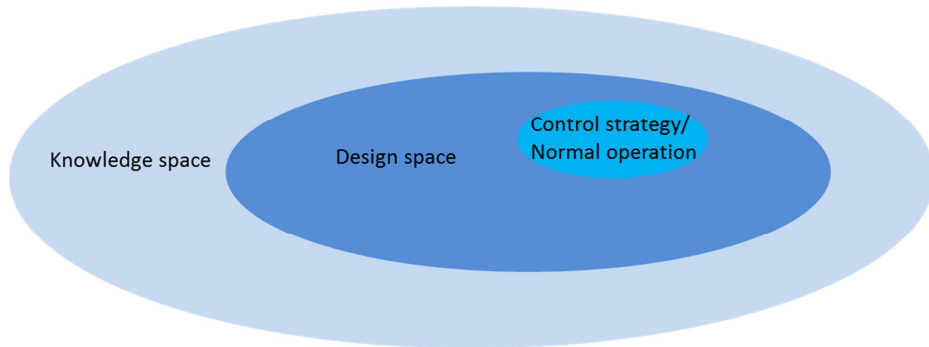


Figure 5.3 – An overview of the knowledge space, the design space and the control strategy/normal operation.

At this stage the most appropriate process analyzer (Box 5.1) for data acquisition should be determined. The process analyzers can be traditional univariate pH, temperature and pressure gauges that most commonly already are implemented in the process, but also more sophisticated multivariate process analyzers/probes can be implemented that give information on biological, chemical, and physical attributes. Experiments conducted with process analyzers during product and process development can serve as building blocks of information that increases in complexity throughout the life of a product.

Box 5.1 - Process analyzers

There are several in-line (frequently called real-time) process analyzers available and only the purpose of the measurement can determine which is the correct one to implement in the process (Chalmers, 2000). Design and construction of process analyzers and their interfaces are critical to ensure that collected data is relevant and representative of process and product characteristics. Robust design, reliability, and ease of operation are important aspects. The implementation of process analyzers in production equipment should only be initiated after risk analysis to ensure that the process and product quality is not undesirably affected. Process analyzers can be the univariate gauges such as temperature, pH, and pressure but also more sophisticated process analyzers are implemented such as spectroscopic probes/process analyzers.

Process analyzers typically generate large volumes of data which requires multivariate methodologies to extract critical process knowledge (FDA). It also requires minimal sample preparation as the product is measured in the process, and have real-time or near real-time response as some processes are changing rapidly perhaps within minutes or less (Berg et al., 2013), though some processes do not require constant surveillance e.g. a fermentation process will not need measurements every five seconds as the process is slow and takes sometimes up to days. But first and foremost the spectroscopic process analyzers should be applicable to the process; it must be suitable for measuring the content and the molecule/compound of interest (Berg et al., 2013).

There are three stages at which the process analyzers can be implemented which depend on the level of PAT implementation in the process:

- At-line: The sample is removed, isolated from, and analyzed in close proximity to the process stream
- On-line: The sample is diverted from the process stream, and is often returned
- In-line: The sample is not removed from the process stream,

measurements are performed in the current vessel.

The next step is to implement the knowledge from initial experiments in laboratory and pilot plant to the production. Upscaling from laboratory scale or pilot plant to production can cause problems as the conditions are never the same. E.g. the bacteria in a fermentation tank do not perform equally well maybe because aeration is different or the stirrer has different impellers. In this step basic monitoring and basic control is implemented. Statistical Process Control (SPC) is often employed in basic monitoring along with off-line multivariate analysis to ensure that the multivariate process control in the future steps is validated. The basic control consists of pattern recognition tools in the SPC regime where simple rules are applied and alarms will be raised when the process is out of specifications. Those events that are responsible for out of specification products are investigated and mapped. The process control is not necessarily a validated system and actions from operators will be required. The quality control is a feedback system and is mainly performed in the laboratory, which also builds more validity to the calibrations from the initial step. During this step a lot of information on the process and the product is gained that can be used when progressing to the final step: full inline control.

In the final step all (relevant) PAT tools are introduced along with advanced monitoring and advanced control; SPC is potentially substituted with multivariate statistical process control (MSPC) because multivariate process analyzers are implemented. This ensures the most important information is extracted and used for process control.

Implementation of feed-forward in a real-time release production, ensuring that the variations in the raw material do not affect the final product is the highest reachable achievement within PAT in my opinion (Figure 5.4). Full inline control is not achieved immediately after implementing PAT and can take several years but with persistence and determination it can be reached. Reaching this final stage does not mean that the work is over; models have to be maintained and the production should still be under quality control in order to avoid drift/unforeseen changes of the production.

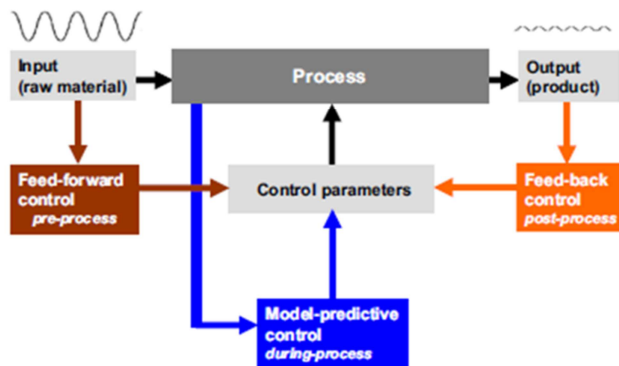


Figure 5.4 – Overview of control strategies in food manufacturing (Figure from Berg et al., 2013).

These are the definitions of PAT, does this project meet up to these standards of being a PAT project? If we take the current understanding of PAT into consideration then this project is probably not the best example, as it lacks in-line control, we are not investigating the process by real life monitoring, no feed-forward or feed-backward control of the raw material which of course would be important here (I think) due to e.g. seasonal changes in the milk, it originating from different farmers/herds and from different cheese production sites. But if one takes into consideration the fundamental form of PAT - get to know your process and from that stand point you develop your (in-line) strategies - then this project resembles the very core of PAT. One of the desired goals in the PAT framework is to reduce production cycle times by using at-, on-, and/or in-line measurements and controls (Box 5.1). This project should aid in improving the cleaning by giving a better understanding of the fouling distribution on the membranes, giving valuable input for novel membrane designs (deducted to dairy/food applications), and ultimately move from recipe driven cleaning/production to data driven cleaning/production by taking production history into account.

A second important goal in the PAT framework is the prevention of rejects, scrap and re-processing. In this project to prevent rejects and optimize the use of the raw material water from the filtration process could potentially be used for cleaning, cooling, or other purposes as a lot of water generally is

consumed at a production sight and as whey consists of 90% water it would be an advantageous usage. Unfortunately the Danish law does not permit reuse of prior contaminated water all the way into the product unless it is proved to be the same quality as drinking water (Box 5.2). This potentially means that reused water can be used for processes that are separate from the production such as flushing and cooling/heating material.

Box 5.2 - Rules regarding reuse of water in the industry (Translated from Foedevarestyrelsen.dk)

Water used in food productions must in principle be drinking water, and there must be access to sufficient quantities of drinking water in the production. Reuse of water for processing or as an ingredient, as a starting point must be of the same quality as drinking water. Water reuse for any purpose other than processing, e.g. for cleaning, as a starting point must also be of drinking water quality. If a company wants to recycle water, it must be able to account for the recycling system and demonstrate that the quality of the water cannot affect food safety. The company must carry out a risk analysis for the processes which are reused or recycled water, and must be able to document water quality with analysis of the relevant parameters.

Fluorescence Spectroscopy

An attempt was made to quantify the residual fouling on the ultrafiltration membranes using fluorescence spectroscopy (Chalmers, 2000). Fluorescence spectroscopy is a method that is commonly used when amino acids are present in a (liquid) sample as they are in residual fouling due to trapped proteins on the membrane. Initially both types of membranes (UF and MF) were measured with a Bioview (Bioview® sensor, Delta, Denmark) instrument using an interface that would ensure large measurement areas during data collection. By an increased total area of the membrane that is measured/sampled the measurement time could be decreased while also improving the statistics. For this experiment the membrane leaf was not dissected into sample coupons; instead the full membrane leaf was spread out on a table that had markings for every ten centimeters in the first direction and a metal rod that also had markings for every ten centimeters was used as a guide for sampling in the second direction (Figure 6.1).

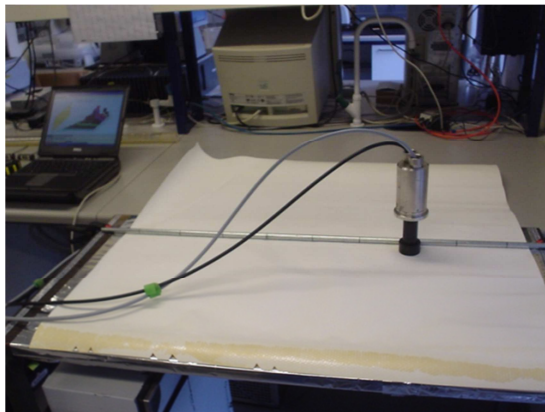


Figure 6.1 – Sampling of UF membrane leaf with Bioview.

The fluorescence data was investigated with PARAFAC (Smilde et al., 2004) in order to determine the characteristic features in the fluorescence landscape. In Figure 6.2 a selection of the samples are shown; the three first and the last three samples of a leaf, to give an impression of the changes in fouling that can be expected. Both UF membrane leaves and MF membrane leaves have been investigated, but in order to compare results with previous measurements the UF membranes were prioritized.

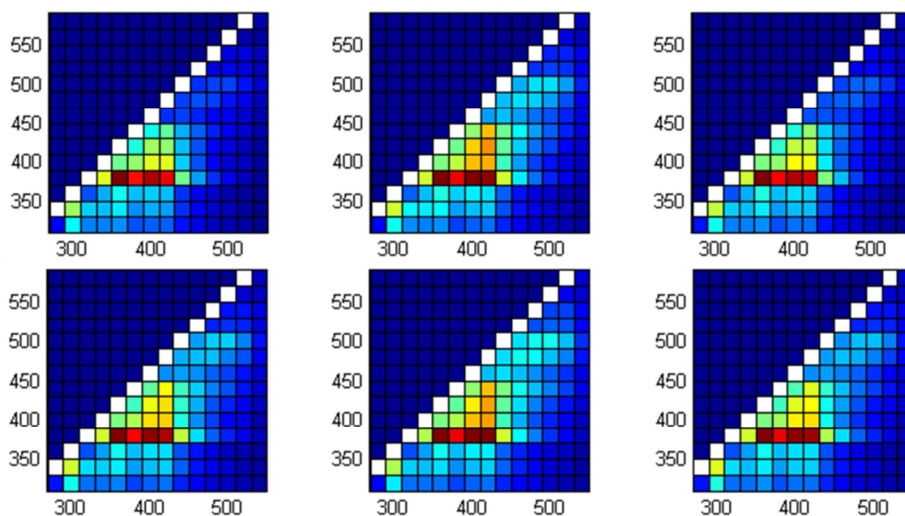


Figure 6.2 – Fluorescence landscapes of the three first samples (upper row) and the three last samples (lower row) from an ultrafiltration membrane.

PARAFAC is performed on the 90 samples that were measured on one UF leaf. The number of components in the model was determined to be five as four did not seem sufficient while five components could separate individual features without separating peaks that are supposed to be/appear to be single peaks. The five component PARAFAC model resolved five reasonably distinct features (Figure 6.3).

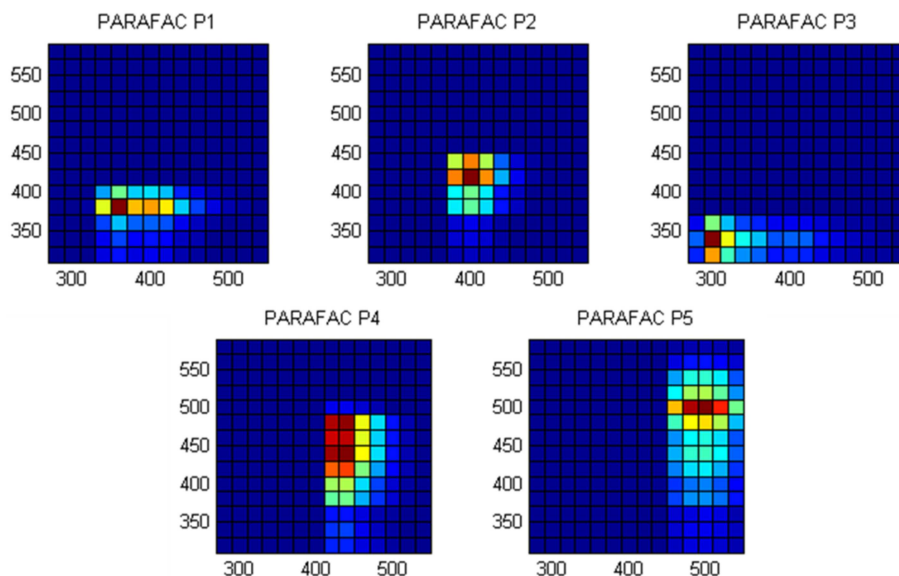


Figure 6.3 - The five PARAFAC components.

By additional fluorescence measurement of known components that could potentially be present in the residual fouling we tried to identify the different features of the model. As previously described, β -lactoglobulin is one of the main chemical components in the residual fouling and the most abundant amino acids in β -lactoglobulin are lysin and isolysin (Figure 6.4a and b). Also evidence of the polymer (PES) in the membrane should be present which we should be able to identify by measuring virgin membrane (Figure 6.4c).

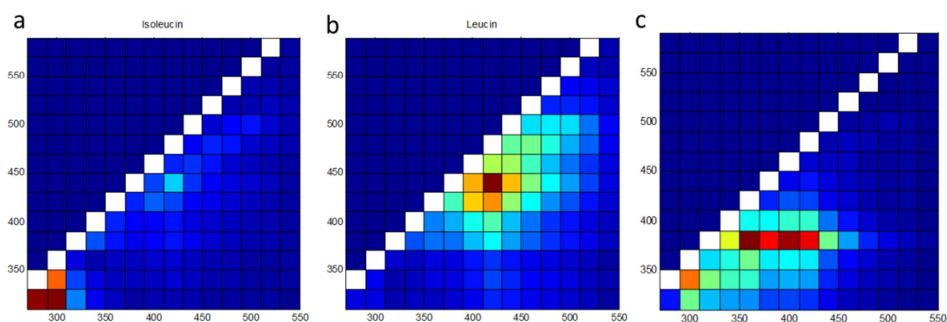


Figure 6.4 – Fluorescent landscape of a) isolysin, b) lysin and c) virgin membrane (PES).

By comparing Figure 6.3 and Figure 6.4 it is observed that the first component in the PARAFAC model fits well with the virgin membrane (PES, Figure 6.4c) as they arise in the same section of the fluorescence landscapes. The second component in the PARAFAC model can probably be attributed to the lysin present in the β -lactoglobulin from the residual fouling. The third component of the PARAFAC model could potentially be isoleucin, but the placement of the pure sample in the fluorescence landscape and the placement of the component in the fluorescent landscape in the model is slightly off and could potentially be another chemical compound of which there is no knowledge. Identifying the fourth and fifth component in the PARAFAC model has not been possible.

The fluorescence data was also investigated by using the intensity of the peak of interest as was the similar case with the IR data in order to be able to compare results. Each of the PARAFAC components were extracted for each sample and transformed into a surface plot (Figure 6.5).

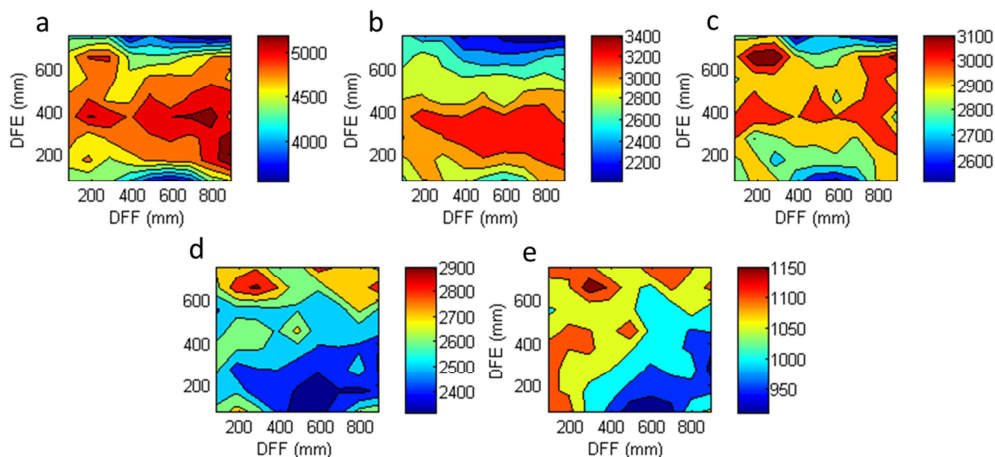


Figure 6.5 – Surface plot for the five PARAFAC components.

If the assumptions above are true then the surface plot in Figure 6.5a should correlate with the first PARAFAC component which should be PES while the second PARAFAC component should correlate with Figure 6.5b that is

assigned to lysin. We know from the IR results that PES and the fouling material exhibit opposite patterns due to *shadowing* of the membrane by the fouling, which I would expect also to be the case with fluorescence. If there were no *shadowing* from the fouling the PES component should exhibit the same intensity over the full membrane leaf, as it is a constant layer, hence in this case the penetration depth is also expected to have significant influence on the measurements.

Unfortunately the fluorescence measurements did not perform as well as expected and did certainly not reach the standard/potential the IR measurements and data analysis exhibited. This can possibly be attributed to missing information on the membranes and also insufficient knowledge about the fouling of membranes in relation to fluorescence measurements (since this has never been reported). The method would have decreased the time spend on sample preparation considerably but also on measurements as the measurement area is large which in the end would have made the statistics more reliable.

Discussion and Perspectives

Optimization of the cleaning procedure of a filtration unit is a difficult job due to it being a closed system with high pressures during processing and large variations in pH and temperature during cleaning. The spiral wound membrane cartridges that are used in whey fractionations are complicated units that cannot be dismantled, measured and reused. This means that extensive data on the distribution of fouling in a membrane cartridge has not been reported previously even though this knowledge is essential for obtaining a better understanding of the fouling process and in the future development of cleaning methods.

In order to map and get an overview of the residual fouling, concentration estimates have to be calculated. This is commonly done by univariate data analysis such as height measurement of relevant peaks. Using univariate data analysis has proven to be unsatisfying as there are several underlying features that can disturb the final picture. The underlying features play an important role when the peak for data analysis is selected, which is evident when examining the literature where the amide II peak is the most commonly used residual fouling peak. This implies that a large part of the spectrum is unused and a lot of information is potentially lost. During this project multivariate data analysis was employed to investigate the IR spectra in order to get a better understanding of the residual fouling along with a more robust data-analytical method. PCA did not capture all the relevant features of the IR spectra whereas MCR was able to find important underlying features. Unfortunately the MCR method is inherently more labile than the PCA method. Before even performing the concentration calculations of the fouling on the membranes the (practical, not mathematical) rank of the system should be determined in order to extract the correct number of factors, and this is

where the challenges with MCR started. There is a rank difference between the two most important parts of the IR spectrum of residual fouling on UF membranes suggesting that the spectrum should be divided into two parts and thus complicating the multivariate data analysis while also losing some of the convenience.

MCR did solve some of the problems when analyzing the IR spectra, but the rank deficiency cannot be solved (or handled) by MCR as it is an intrinsic problem in the data, which implies that other, alternative chemometrics methods will experience similar difficulties. The rank deficiency is also the reason why e.g. PCA could not extract more than two interpretable components. Even though the multivariate data analysis improved the understanding of the membrane and fouling system significantly compared to univariate data analysis, the modelling can potentially be improved.

The amide II band is the most commonly investigated peak as there are no underlying features that interfere with the univariate data analysis around this peak. This is the reason why it was interesting to investigate other less used peaks including the secondary structure sensitive peak: amide I. Amide I has some underlying features that potentially can lead to erroneous interpretations. With the MCR data analysis I have been able to determine the relative concentration of any peaks in the spectra leaving the method less susceptible to mistakes. This would, however, require a modelling concept that can capture different ranks/data complexities within one analysis. Multi-block methods (Roussel et al., 2014) could in principle fulfill this requirement, but they are designed to merge distinct data sources (blocks) into one analysis. In my modeling the local ranks are not known a priori, making it difficult to initiate (maybe even impossible) a multi-block strategy before all facts are known.

Nevertheless, MCR gave a satisfying, detailed insight on the membrane residual fouling patterns. The analysis determined that three factors should be included in the model in order to describe the amide and PES peaks. These three factors correspond well to the different known features of the membrane and fouling system from Paper I (Jensen et al., 2015).

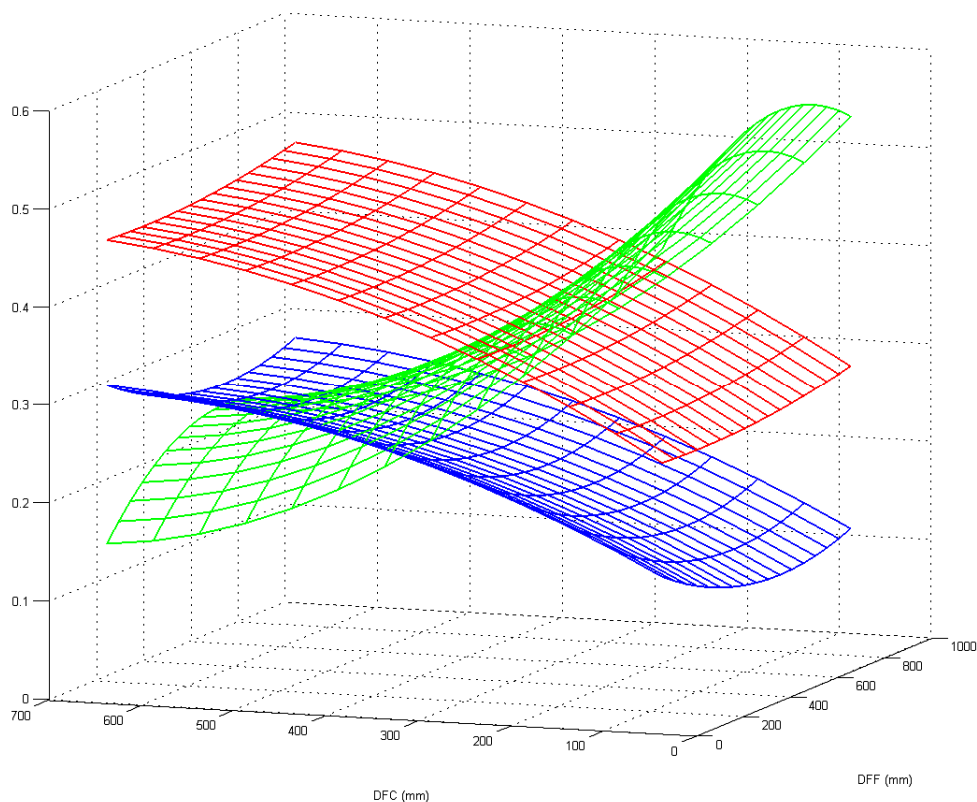


Figure 7.1 – Model of the three components under the amide I peak (Figure 8a-c in Paper II), green: describes the residual protein in the fouling, blue: describes the membrane/PES, red: describes the residual protein fouling.

The surface plots in Figure 7.1 show the difference between the three factors. Two describe the residual fouling and one describes the membrane material. It is important to keep in mind that the data has been smoothed by fitting a low-order polynomial (based on ANOVA) through the observations and is more a graphical illustration of the data than an exact representation.

The MCR data analysis extracted more information about the membrane and fouling system than was possible with univariate data analysis, but it is important and reassuring that the results from the two methods exhibit similar

results. In Figure 7.2 a direct comparison of the results from the two strategies is shown.

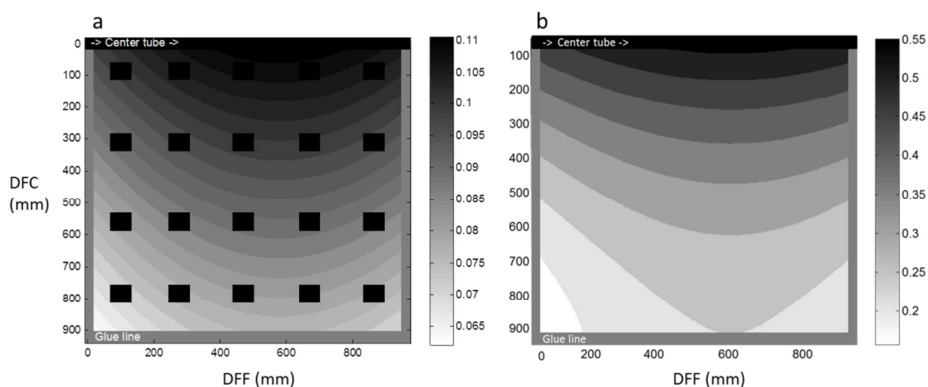


Figure 7.2 – a) Surface plot of the relative concentration for amide II estimated with univariate data analysis (height measurement), b) surface plot of the relative concentration for amide II estimated by using multivariate data analysis (MCR). The squares represent measurement points and are the same for both types of data analysis.

The results of the two data analysis methods largely exhibit the same pattern with the highest relative concentration at the center tube and a decreasing concentration outwards. Both results exhibit the *flame* pattern that we have seen several times and which has also been shown in earlier literature (Delaunay et al., 2008, Schwinge et al., 2004). This means that the two methods could potentially be interchanged. The MCR method does provide more insight about the underlying features and the data analysis is no longer limited to only analyzing the amide II peak.

In Figure 2.2 it is shown how the pressure develops in a steel housing unit in an industrial scale ultrafiltration process. This potentially would cause some systematic changes in the membranes and over the different leaves; this was not the case (not observed) in my analysis. Generally there are a lot of differences between the cartridges and the leaves, but none of them are systematic with regards to the pressure and can mostly be ascribed to random effects that I have not been able to control during (stratified) sample collection or to monitor/describe. This provides two views on the reality of

fouling (i) the fouling that could be described according to the pressure in the system/steel housings, (ii) the fouling seen in real size production membranes. Theoretically, it was expected to see more systematic fouling when investigating three membranes that have been used throughout their lifetime in the same steel housing (Sample set B, Table 2.2). This assumption is derived from the fact that the pressure drop from inlet (4.59 bar) to outlet (0.91 bar) is quite significant.

In this study work it was chosen to perform analysis on real size production membranes, which is unfortunately not very common in research on membrane fouling where almost all experiments are performed on model systems (laboratory scale). These model systems can vary largely, but flat-bed and dead-end filtration is generally used. These systems do not necessarily represent the full-scale processes happening in the membrane during filtration and cleaning. Many researches have tried to foul a membrane in laboratory scale in order to predict how the fouling builds up in real size membrane cartridges, but it is important to keep in mind that the flow behaves very differently in laboratory scale equipment such as flat-bed and dead-end filtration compared to the spiral wound membranes. Making the fouling experiments smaller certainly makes sense and it is more practical, but I think that researchers should strive to perform experiments in pilot plants where (one or more) spiral wound membranes can be investigated. Furthermore, there is a theory that has arisen at my industrial collaboration partner, namely that the full-scale membrane does not function optimally before it has been used for approximately three weeks. This indicates that the fouling to a certain extend has a positive influence on the filtration process. If this theory can be validated, the small scale experiments would have to run for longer periods to simulate the process more realistically, and this aspect is largely absent in research papers.

With the residual fouling being a large problem in the dairy industry, who really owns the responsibility for having membranes that are optimized, ensuring that the processes running in different dairies (and other food industries) run as efficient and economical as possible? The membranes that are used in the dairy industry are often developed for the water-purification

industry where less material/fouling is present and the user has less concern regarding the fouling buildup/cleaning of the membranes. At the dairy general fouling and cleaning is a large aspect that deserves a lot of attention. The water usage in CIP of membrane systems is high, and hence lots of money is spent on water, and having the water treated at a waste water plant after use is 5-6 times more expensive than the purchase of the drinking water. The dairies take their responsibility seriously and are making great efforts to decrease their water-intake which also decreases the volume that is sent to waste water treatment. Lately a lot of knowledge of in-line control of the CIP is being collected. A note should be made that the filtration units should be routinely cleaned approximately every 24 h for both hygienic (to keep bacterial contamination at a minimum ensuring a safe product) and capacity issues (reversible or easily-removable fouling layers). The final step that needs to be optimized is the membranes towards reduced irreversible (and also reversible) fouling, but the dairies cannot be held sole responsible for this part. Developing more new membrane types that works specifically in the dairy/food production is important and should be done more by the membrane production industry. Much research at university level is required on developing new types of grafting, but testing the membranes will necessarily be in laboratory scale hence the fouling is not the true picture.

Optimization of the process and the membranes would benefit the dairies, but a change in the Danish legislation would benefit all Danish production facilities. Currently a lot attention is given to the CO₂ footprint of processes: the greenhouse effect of producing goods/foods should be lowered and that our water reserves should be saved (“H₂O footprint”). An increase in the reuse of water in many Danish production facilities would decrease the CO₂ footprint and use less water resulting in a more green future and healthy environments, certainly a step in the right direction. Changing the laws would require more control at production level to ensure that the reused water reaches the highest standards.

Membrane cleaning requires a lot of time, many chemicals, energy and water. It is estimated that the annual cost for a CIP cleaning system is 380-504DKK (51-68 €) per square meter (Berg, 2014). Filtration plants usually have large

areas of filtration membranes and a Danish company employs 200,000 m² of membrane (Berg, 2014) which totals the cleaning costs at 1,360,000 – 1,810,000 € per year. This implies that an optimization of the process even by a few percent would result in large savings and a better environmental footprint.

In order to improve and optimize the cleaning of spiral wound membranes used in the dairy industry a potentially large step can be taken by leaving the recipe based cleaning methods and move towards more measurement driven methods. It is important to keep in mind that the recipes used are usually *over-cleaning* in order to prevent total pore blocking, but also to prevent microbial contamination. The experiments performed by Lyndgaard et al. (2014) shows that in-line measurements of the cleaning water with UV-spectroscopy is a step towards measurement driven cleaning. Further research within the field of membrane technology should also be more representative, hence more research should be done on real size membranes as these are the only true alternative when investigating the effects of flow and pressure on the residual fouling inside the complex structure that a spiral wound membrane is.

Jannie Krog Jensen
Frederiksberg, 2015

References

- Z. Allie, E.P. Jacobs, A. Maartens, P. Swart, Enzymatic cleaning of ultrafiltration membranes fouled by abattoir affluent, *Journal of Membrane Science* 218 (2003) 107-116
- A. Asatekin, S. Kangb, M. Elimelech, A. M. Mayesc, Anti-fouling ultrafiltration membranes containing polyacrylonitrile-graft-poly(ethylene oxide) comb copolymer additives, *Journal of Membrane Science* 298 (2007) 136-146
- R. Bauer, C. Rischel, S. Hansen, L. Øgandal, Heat-induced gelation of whey protein at high pH studied by combined UV spectroscopy and refractive index measurement after size exclusion chromatography and by *in-situ* light scattering, *International Journal of Food and Technology* 34 (1999) 557-563
- L. Bégoïn, M. Rabiller-Baudry, B. Chaufer, M. Hautbois, T. Doneva, Ageing of PES industrial spiral-wound membranes in acid whey ultrafiltration, *Desalination* 192 (2006) 25-39
- S. Belfer, J. Gilron, O. Kedem, Characterization of commercial RO and UF modified and fouled membranes by means of ATR/FTIR, *Desalination* 124 (1999) 175-180
- F.v.d. Berg, C.B. Lyndgaard, K.M. Sørensen, S.B. Engelsen, Process Analytical Technology in the food industry, *Trends in Food Science & Technology* 31 (2013) 27-35

T. Berg, Fouling and cleaning of membrane systems in the dairy industry – Towards optimization of micro- and ultrafiltration processes, PhD Thesis, Department of Food Science, University of Copenhagen (2014)

T.H.A. Berg, J.C. Knudsen, R. Ipsen, F.W.J. van den Berg, H.H. Holst, A. Tolkach, Investigation of consecutive fouling and cleaning cycles of ultrafiltration membranes used for whey processing, *International Journal of Food Engineering* 10 (2015) 367-381

S. Beyramysoltan, R. Rajkó, H. Abdollahi, Investigation of the equality constraint effect on the reduction of the rotational ambiguity in three-component system using a novel grid search method, *Analytica Chimica Acta* 791 (2013) 25-35

A. Bhattacharya, B.N. Misra, Grafting: a versatile means to modify polymers Techniques, factors and applications, *Progress in Polymer Science* 29 (2004) 767-814

H.F. Bohner, R.L. Bradley Jr, Effective cleaning and sanitizing of polysulphone ultrafiltration membrane systems, *Journal of Dairy Science* 75 (1992) 718-724

G. Brans, C.G.P.H. Schroen, R.G.M. van der Sman, R.M. Boom, Membrane fractionation of milk: state of the art and challenges, *Journal of Membrane Science* 96 (2004), 1-58

R. Bro, S. De Jong, A fast non-negativity-constrained least squares algorithm, *Journal of Chemometrics* 11 (1997) 393-401

B. Van der Bruggen, Chemical modification of polyethersulfone nanofiltration membranes: A review, *Journal of Applied Polymer Science* 114 (2009) 630-642

G. Bylund, Dairy processing handbook, Tetra Pak Processing Systems AB (2003)

C.E. Carraher, Jr., Introduction to Polymer Chemistry, CRC Press, Second Edition, USA (2010)

J.M. Chalmers, Spectroscopy in Process Analysis, Volume 1, CRC Press, USA (2000)

J.M. Chalmers, P.R. Griffiths, Handbook of Vibrational spectroscopy, Sampling Techniques, Volume 2, John Wiley & sons (2002)

M. Cheryan, Ultrafiltration and Microfiltration Handbook, Technomic Publishing Co., Inc., Lancaster (1998)

D. Delaunay, M. Rabiller-Baudry, J.M. Gozávez-Zafrilla, B. Balannec, M. Frappart, L. Paugam, Mapping of protein fouling by FTIR-ATR as experimental tool to study membrane fouling and fluid velocity profile in various geometries and validation by CFD simulation, *Chemical Engineering and Processing* 47 (2008) 1106-1117

A. Dong, P. Huang, W.S. Caughey, Protein Secondary Structures in Water from Second-Derivative Amide I Infrared Spectra, *Biochemistry* 29 (1990) 3303-3308

N.M. D'Souza, A.J. Mawson, Membrane Cleaning in the Dairy Industry: A Review. *Critical Reviews in Food Science and Nutrition* 45 (2005) 125-134

L. Eriksson, E. Johansson, N. Kettaneh-Wold, J. Trygg, C. Wikström, S. Wold, Multi- and Megavariate Data Analysis Part I Basic Principles and Applications, second edition, Umetrics, Sweden (2006)

L. Eriksson, E., Johansson, N. Kettaneh-Wold, C. Wikström, S. Wold, Design of Experiments Principles and Applications, 3rd edition, Umetrics (2008)

J. Fontanella, R.L. Johnston, J.H. Colwell, C. Andeen, Temperature and pressure variation of the refractive index of diamond, *Applied Optics* 16 (1977) 2949-2951

H. Gampp, M. Maeder, C.J. Meyer, A.D. Zuberbühler, Evolving Factor Analysis of Spectrophotometric Titrations: Forget About the Law of Mass Action?, *CHIMIA International Journal for Chemistry*, 39 (1985) 315-317

V. Gekas, Terminology for pressure-driven membrane operations, *Desalination* 68 (1988) 77-92

E.R. Girden, ANOVA, Sage Publication, Inc., USA (1992)

H. Günzler, H. Gremlich, IR Spectroscopy: An introduction, Wiley-Vch verlag GmbH&Co, Weinheim (2002)

R.J. Hanson, C.L. Lawson, Solving least squares problems, Prentice –Hall, Englewood Cliffs, USA (1974)

D.C. Harris, Quantitative Chemical analysis, 7th edition, W.H. Freeman and Company, Ed. Jessica Fiorillo, USA (2007)

J. Jaumot, R. Gargallo, R. Tauler, Noise propagation and error estimations in multivariate curve resolution alternating least squares using resampling methods, *Journal of Chemometrics* 18 (2004) 327-340

J.K. Jensen, N. Ottosen, S.B. Engelsen, F. van den Berg, Investigation of UF and MF Membrane Residual Fouling in Full-Scale Dairy Production Using FT-IR to Quantify Protein and Fat, *International Journal of Food Engineering* 11 (2015) 1-15

A. de Juan, R. Tauler, Multivariate Curve Resolution (MCR) from 2000: Progress in Concepts and Applications, *Critical Reviews in Analytical Chemistry* 36 (2006) 163-176

A. de Juan, J. Jaumot, R. Tauler, Multivariate Curve Resolution (MCR). Solving the mixture analysis problem, *Analytical Methods* 6 (2014) 4964-4976

H.R. Keller, D.L. Massart, Evolving factor analysis, *Chemometrics and Intelligent Laboratory Systems* 12 (1992) 209-224

J. Kiefer, N.H. Rasul, P.K. Ghosh, E. von Lieres, Surface and bulk porosity mapping of polymer membranes using infrared spectroscopy, *Journal of Membrane Science* 452 (2014) 152-156

K. Kimura, Y. Hane, Y. Watanabe, G. amy, N. Ohkuma, Irreversible membrane fouling during ultrafiltration of surface water, *Water Research* 38 (2004) 3431-3441

V. Kochkodan, D. J. Johnson, N. Hilal, Polymeric membranes: Surface modification for minimizing (bio)colloidal fouling, *Advances in Colloid and Interface Science* 206 (2014), 116-140

K. Kuriki, O. Shapira, S.D. Hart, G. Benoit, Y. Kuriki, J.F. Viens, M. Beyindir, J.D. Joannopoulos, Y. Fink, Hollow multilayer photonic bandgap fibers for NIR applications, *Optics Express* 12 (2004) 1510-1517

O.M. Kvalheim, Y.Z. Liang, Heuristic evolving latent projections: resolving two-way multicomponent data. 1. Selectivity, latent-projective graph, datascopes, local rank, and unique resolution, *Analytical Chemistry* 64 (1992) 936-946

W.H. Lawton, E.A. Sylvestre, Self-Modeling Curve Resolution, *Technometrics* 13 (1971) 617-633

J. Linkhorst, W.J.T. Lewis, Workshop on membrane fouling and monitoring: a summary, *Desalination and Water Treatment* 51 (2013) 6401-6406

C.B. Lyndgaard, M.A. Rasmussen, S.B. Engelsen, D. Thaysen, F.W.J. van den Berg, Moving from recipe-driven to measurement-based cleaning procedures: Monitoring the Cleaning-In-Place process of whey filtration units by ultraviolet spectroscopy and Chemometrics, *Journal of Food Engineering* 126 (2014) 82–88

E.R. Malinowski, Window Factor Analysis: Theoretical derivation and application to flow injection analysis data, *Journal of Chemometrics* 6 (1992) 29-40

R. Manne, On the Resolution Problem in Hyphenated Chromatography, *Chemometrics and Intelligent Laboratory Systems* 27 (1995) 89-94

R. Manne, H. Shen, Y. Liang, Subwindow factor analysis, *Chemometrics and Intelligent Laboratory Systems* 1-2 (1999) 171-176

A.D. Marshall, G. Daufin, Physico-Chemical aspects of membrane fouling by dairy fluids, in IDF (Ed.), *Fouling and Cleaning in Pressure Driven Membrane Processes* (1995) 8-29

T. Maruyama, S. Katoh, M. Nakajima, H. Nabetani, T.P. Abbott, A. Shono, K. Satoh, FT-IR analysis of BSA fouled on ultrafiltration and microfiltration membranes, *Journal of Membrane Science* 192 (2001) 201-207

D.L. Massart, B.G.M. Vandeginste, L.M.C. Buydens, S. de Jong, P.J. Lewi, J. Smeyers-Verbeke, *Handbook of Chemometrics and Qualimetrics Part A*, Elsevier (1997)

C.E. Miller, Chemical principles of Near-infrared technology. In P. Williams and K. Norris (Eds), *Near-infrared technology, in the agricultural and food industries*, St. Paul: St. Paul: American Association of Cereal Chemists (2001)

F.M. Mirabella, *Internal Reflection Spectroscopy Theory and Applications*, Editor: Marcel Dekker: New York (1993)

D.C. Montgomery, Design and Analysis of Experiments, 6th edition, Wiley and Sons, Inc., USA (2006)

P.K. Nair, J. Cardoso, O. Gomez Daza, M.T.S. Nair, Polyethersulfone foils as stable transparent substrates for conductive copper sulfide thin film coatings, *Thin Solid Films* 401 (2001) 243-250

D.L. Pavia, G.M. Lampmann, G.S. Kriz, J.R. Vyvyan, Introduction to Spectroscopy, fourth edition, Brooks/Cole, USA (2009)

S. Platt, M. Nyström, Amido black staining of ultrafiltration membranes fouled with BSA, *Desalination* 214 (2007) 177-192

M. Rabiller-Baubry, M. Le Maux, B. Chaufer, L. Bégoïn, Characterisation of cleaned and fouled membrane by ATR-FTIR and EDX analysis coupled with SEM: application to UF of skimmed milk with PES membrane, *Desalination* 146 (2002) 123-128

M. Rabiller-Baudry, L. Paugam, D. Delaunay, Membrane Cleaning: a Key for Sustainable production in Dairy Industry. In: Handbook of Membrane Research: Properties, Performance and Applications. Nova Science Pub Incorporated, New York, USA (2009) 219-256

F. Ran, X. Niu, H. Song, C. Cheng, W. Zhao, S. Nie, L. Wang, A. Yang, S. Sun, C. Zhao, Toward a highly hemocompatible membrane for blood purification via a physical blend of miscible comb-like amphiphilic copolymers, *Biomaterials Science* 2 (2014) 538-547

A.S. Rathore, H. Winkle, Quality by design for biopharmaceuticals, *Nature Biotechnology* 27 (2009) 26-34

C. Regula, E. Carretier, Y. Wyart, G. Ge'san-Guiziou, A. Vincent, D. Boudot, P. Moulin, Chemical cleaning/disinfection and ageing of organic UF membranes: A review, *Water Research* 56 (2014) 325-365

A.I. Ropodi D.E. Pavlidis, F. Mohareb, E.Z. Panagou, G.-J.E. Nychas, Multispectral image analysis approach to detect adulteration of beef and pork in raw meats, *Food Research International* 67 (2015) 12-18

S. Roussel, S. Preys, F. Chauchard, J. Lallemand, Multivariate Data Analysis (Chemometrics) in Process Analytical Technology for the food industry. Eds C.P. O'Donnell, C. Fagan, P.J. Cullen (2014)

J. Schwinge, P.R. Neal, D.E. Wiley, D.F. Fletcher, A.G. Fane, Spiral wound modules and spacers Review and analysis, *Journal of Membrane Science* 242 (2004) 129-153

A. Smilde, R. Bro, P. Geladi, Multi-way Analysis, Applications in the Chemical Sciences, 1. Edition, John Wiley & Sons, UK (2004)

R. Somma, A.A. Signore, Embracing Quality by Design, Applying QbD concepts can help CMOs create value, *Contract Pharma for Pharmaceutical & Biopharmaceutical Contract Services and Outsourcing*, (2008)

R. Tauler, D. Barcelo, Multivariate Curve Resolution Applied to Liquid-Chromatography Diode-Array Detection, *TrAC-Trends in Analytical Chemistry* 12 (1993) 319-327

TetraPak, Dairy processing handbook, Tetra Pak Lund, Sweden (1995)

G. Tragårdh, Membrane Cleaning, *Desalination* 71 (1989) 325-335

B.G.M. Vandeginste, W. Derks, G. Kateman, Multicomponent self-modelling curve resolution in high-performance liquid chromatography by iterative target transformation analysis, *Analytica Chimica Acta* 173 (1985) 253-264

J. Wagner, Membrane Filtration Handbook, Practical Tips and Hints, Second edition, second revision, Osmonics, Netherlands (2001)

S. Wartewig, IR and Raman spectroscopy: Fundamental Processing, Wiley-VCH Verlag GmbH&Co, Weinheim, Germany (2003)

W. Windig, J. Guilment, Interactive Self-Modelling Mixture Analysis, *Analytical Chemistry* 63 (1991) 1425-1432

S. Wold, K. Esbensen, P. Geladi, Principal Component Analysis, *Chemometrics and Intelligent Laboratory Systems* 2 (1987) 37-52

Paper I

J.K. Jensen, N. Ottosen, S.B. Engelsen, F. van den Berg

Investigation of UF and MF Membrane Residual Fouling in Full-Scale Dairy Production Using FT-IR to Quantify Protein and Fat

International Journal of Food Engineering 11 (2015) 1-15

Jannie K. Jensen*, Niels Ottosen, Søren B. Engelsen and Frans van den Berg

Investigation of UF and MF Membrane Residual Fouling in Full-Scale Dairy Production Using FT-IR to Quantify Protein and Fat

Abstract: This study investigates the distribution of residual fouling in used spiral wound ultrafiltration (UF) and microfiltration (MF) membrane cartridges. Residual fouling on four full-scale production UF membrane cartridges and two full-scale MF membrane cartridges were investigated with infrared spectroscopy inspecting fat and protein deposits. A non-homogenous distribution of residual fouling was observed with concentrations highest at the center tube decreasing away from the feed side. Analysis of variance was used to evaluate significant factors affecting the model. The observed tendencies can be explained by flow and pressure differences caused by design aspects of spirally wound membrane cartridge and the steel housing. Variations between individual sheets from the same cartridges were observed, suggesting a role from manufacturing variability in residual fouling after cleaning-in-place. This paper describes a new method for mapping fouling proposing a semi-quantifiable description. This description might guide membrane developers and users to optimize cleaning methods in the future.

Keywords: membrane filtration, residual fouling, cleaning-in-place, infrared spectroscopy

DOI 10.1515/ijfe-2014-0254

1 Introduction

The dairy filtration industry uses considerable volumes of water every day for cleaning in order to maintain the required hygienic standards and to keep the operations

***Corresponding author: Jannie K. Jensen**, Department of Food Science, Faculty of Science, University of Copenhagen, SPECC Section, Rolighedsvej 26, DK-1958 Frederiksberg C, Denmark, E-mail: janniekj@food.ku.dk

Niels Ottosen, Arla Foods Ingredients Group, R&D, Sønderupvej 26, 6920 Videbaek, Denmark, E-mail: niels.ottosen@arlafoods.com

Søren B. Engelsen, Frans van den Berg, Department of Food Science, Faculty of Science, University of Copenhagen, SPECC Section, Rolighedsvej 26, DK-1958 Frederiksberg C, Denmark, E-mail: se@food.ku.dk, fb@food.ku.dk

running at satisfactory capacities. This translates into a large loss of resources in the form of potable water and cleaning chemicals being consumed, and in production downtime while cleaning-in-place (CIP) is performed [1, 2]. After CIP this water is led back to the waste management facility which, depending on the state of the water, can again be a costly and energy demanding process. In the dairy industry a substantial effort is made to minimize the use of water, time and costs for cleaning – minimizing the so-called *water footprint*. In light of this effort our research will bring increased knowledge on the cleanliness state of the spiral wound (SW) ultrafiltration (UF) and microfiltration (MF) membrane cartridges that are routinely used in the whey processing. Sweet whey is a byproduct when making rennet types of cheeses. It has an initial total true protein (TTP) concentration around 0.5–0.7% (w/w) and a lactose concentration of 4–5% (w/w). After filtration the average TTP content of the retentate and permeate is 3.5–24% (w/w) and 0.01–0.10% (w/w), respectively, depending on the type of whey being produced. The lactose concentration also decreases during filtration to averages of 2–3% (w/w) and 4–5% (w/w) for retentate and permeate [3]. Different design factors will have an influence on the performance of the membrane cartridges; geometry of the leaves including spacer thickness, leaf size and number of leaves, plus cross-flow, flux and pressure loss all have a bigger or smaller effect on the flow and flux behavior over and through the membrane [4]. The transmembrane pressure (TMP) also has a large influence on the fouling propensity of the membrane. TMP is defined as the pressure difference between feed and permeate stream. The TMP is approximately 0.7 bar per element in an industrial UF unit but varies with pH and ionic strength of the feed [5], and this increases as a function of production time due to fouling. The biggest *uncontrollable* factor in dairy production using membrane technology is fouling. It consists of a buildup of protein, fat and minerals that to a large extent – but not completely – can be removed by cleaning [6, 7]. If the flux during production is kept constant the layer buildup over time results in an increase in

pressure, forcing the process to be periodically stopped due to escalating energy demands. The process thus has to be terminated and CIP initiated prior to severe flux decrease ensuring that the buildup layer does not increase to an undesirable thickness but the cleaning also has a strictly hygienic purpose. Failing to remove microorganisms from the production stream can result in microbiological contaminated product that needs to be discarded, potentially causing large economic losses. The fouling propensity and cleaning ability are therefore highly important (economical and ultimately environmental) factors.

The elaborate cleaning procedure employed in full-scale dairy UF or MF membrane CIP processes varies considerably, but is frequently as complex as the following nine-step program [7]: (1) *first flushing* to remove and recover free material and particles; (2) caustic cleaning to remove boundary layers and unfold proteins, making them ready for enzyme treatment; (3) flushing; (4) enzymatic cleaning to remove proteins attached to or integrated in the membrane; (5) flushing; (6) acid cleaning to remove minerals; (7) flushing; (8) hydrogen peroxide disinfection and (9) final flushing [8]. Each of the three cleaning stages (2, 4 and 6) encompasses composite detergent systems and pH buffering/control. This cleaning procedure removes the main fouling layers, regenerating the capacity of the filtration unit operation, albeit some irreversible *residual fouling* is left even after such a sophisticated CIP program. In this study we are more specifically targeting irreversible fouling from the perspective of the last production and CIP cycle onto the next production cycle. The complex logistics and supply chain management regimes in a modern, large-scale dairy facility make operation and optimization of CIP challenging. There are a lot of variables and interactions involved in membrane performance and residual fouling: the membrane age combined with the short- and long-term product history of the membrane cartridges, the (often varying) whey feed stream composition, etc. All these aspects have two main consequences: most CIPs are run recipe wise because real-time control is considered too complex [2], and laboratory scale investigations in membrane performance and cleaning are of limited use [7]. For these reasons, a fundamental understanding of CIP and residual fouling in full-scale dairy membrane production is highly desired [9].

The residual fouling consists of a buildup of protein (the major *culprit* in dairy UF and MF), fat and minerals and can be attributed to different fouling mechanisms. A concentration polarization will occur during filtration, this means that a large number of molecules will be in

close vicinity of the membrane surface. It arises due to the static attraction between molecules and membrane and is not a large problem in cleaning as it is completely reversible. Four concepts have been put forward as to how the proteins are more irreversibly fixated to a membrane: adsorption, pore blocking, cake layer formation and depth fouling [6]. In adsorption the foulant adheres to the membrane primarily on the surface but also in the pores, narrowing them and reducing the flux. Cake layer formation arises when the whey molecules aggregate and form bridges and piles that cover sections of the membrane. Pore blocking occurs when a large molecule blocks a pore. This can further develop into depth fouling when the larger molecule is forced into a pore. Membrane cartridges in SW-UF and SW-MF steel housing are separated and kept in place by so-called ATDs (Anti-Telescoping Devices) or sometimes Energy-Saving Anti-Telescoping Devices (ESAs). A frequently encountered configuration would have three membrane units per steel housing, with several housings and *loops* per UF/MF production unit [10]. The ATD (or ESA) ensures that the membrane cartridge does not partially unfold, but also functions as a separator keeping the permeate flowing throughout the process, in the right channels. The overall design (in case of three membrane cartridges per housing) creates a pressure drop on the retentate side from tube inlet (approximately 4–5 bar) to tube outlet (approximately 1–2 bar), maintaining an overpressure in the cavity between the membrane surface and the inner surface of the membrane housing. This pressure differential can still create a deformation in the membrane cartridges that is very distinct when the membranes are deconstructed. The morphology of the membrane and pressure profiles in the cartridge and cartridges-plus-tube ensemble can give rise to a large variation on the membrane and residual fouling. It is assumed that this residual fouling is inversely proportional with membrane capacity, performance and/or energy demands.

This study will not distinguish between the four combined fouling interactions but rather the total residual fouling: the foulants present right after a CIP cleaning. The study investigates used membrane cartridges from full-scale dairy UF and MF operations for the processing and up-concentration of sweet whey. Attenuated total reflection Fourier transform infrared (ATR-FT-IR) spectroscopy and multivariate data analysis are employed to identify and quantify – or semi-quantify in a relative sense – protein and fat residues. Based on these measurements the residual fouling load over a wide range of different membrane leaves and cartridges can be compared. The binding of the deposits, the

construction of the spacer and the design of the cartridges resulted in inhomogeneous membrane surfaces and large variations within the data, as illustrated by protein staining. Despite this observed inhomogeneity the findings on the distribution of residue fouling using ATR-FT-IR measurements are in good agreement with the conclusions from earlier studies based on thickness measurements [4], with the added benefit of a direct interpretation of the identified chemical species. The species that are expected to be present in the fouling layer are fat, proteins, lactose and minerals. The proteins are the largest problem in fouling as they can be retained on the membrane. Whey holds a relatively small fraction of protein – approximately 0.9–1.3% – encompassing numerous protein types (Table 1, [11]). β -Lactoglobulin forms the highest content in whey and has tendency to attach to hydrophobic molecules/surfaces [12] which to a large extent involves UF membranes.

Table 1 Protein composition of whey

Protein	% of whey proteins	Molecular weight (kDa)
β -Lactoglobulin	55–65	18.4
α -Lactalbumin	15–25	14.2
Immunoglobulins	10–15	80–900
Bovine serum albumin (BSA)	5–6	66.3
Proteose – peptone	10–20	4–80
Minor proteins	<0.5	30–100

Table 2 Membrane cartridge details

Cartridge	A	B1, B2, B3	Ca, Cb
Membrane type	UF	UF	MF
Dimensions			
Diameter	6.3"/160 mm	6.3"/160 mm	6.3"/160 mm
Length	38"/965 mm	38"/965 mm	38"/965 mm
Spacer thickness	31 mil/0.79 mm	80 mil/2.04 mm	46 mil/1.17 mm
No. of leaves	11 × 2	7 × 2	8 × 2
App. leaf length ^a	36"/920 mm	35"/900 mm	43"/1,100 mm
Membrane area ^b	228 ft ² /21.2 m ²	117 ft ² /10.9 m ²	171 ft ² /15.9 m ²
Material	PES	PES	PVDF
Cut-off	10 kDa	10 kDa	800 kDa
Product	Sweet whey	70 k whey	WPI
Loop	3	8	1 (Ca), 4 (Cb)
Tube	5	3	7 (Ca), 4 (Cb)
Age	2 years, 3 months	5 months, 3 days	1 year, 9 months
Leaves investigated	1, 4, 11	1, 2, 5	1, 2, 5
Size of coupon	70 × 100 mm	100 × 100 mm	100 × 100 mm

Notes: ^aBased on our observations/measurements made during cartridge dissection.

^bBased on specifications of the manufacturers.

2 Materials and methods

Six different membrane cartridges with a distinct history of use in a Danish Whey protein concentrate (WPC)/whey protein isolate (WPI) production were included in this investigation. All cartridges were operated with ESA-type ATDs. All membrane cartridges were cleaned according to CIP standards inside their industrial location/role prior to dismantling from their respective filtration unit operations/steel housings, and kept in cold storage (approximately 5°C) before shipment and deconstruction.

Cartridge A – One UF membrane cartridge, which will be referred to as A throughout the paper, is a KMS HFK 131 Food and Dairy UF element, model 6338 HFK-131; details can be found in Table 2. This membrane cartridge has been used to concentrate sweet whey (from approximately 3% to 25% dry matter, viewed from a full unit operation perspective) and was placed in the third loop of a nine-loop plant, as the third/last membrane cartridge in a three-cartridge long housing. It was in use for 2 years and 3 months. An obvious deformation of the membrane leaves, noted by visual inspection, was present in this cartridge starting approximately halfway down the length of the unit and increasing in severity toward the exit side. Although it is generally hard to describe a deformation in a spiral configuration – the *groves* and *curls* observed when unrolling the membrane were on a much wider scale than, e.g. the spacer mesh dimensions.

Cartridges B – Three UF membrane cartridges, which will be referred to as B1, B2 and B3 throughout the paper, are KMS HFK 328 Food and Dairy UF elements, model

6338 HFK-328; details are given in Table 2. These membrane cartridges have been used to produce so-called WPC70 and were placed in the same housing during production only separated by ESAs, in the first, second and third places looking from the feed side. The membranes were placed in the eighth loop of a nine-loop plant; all three cartridges had been positioned in the same tube and had been in use for 5 months and 3 days of production plus cleaning.

Cartridges C— Two MF membrane cartridges, which will be referred to as Ca and Cb throughout the paper, are Synder Filtration FR-3B-6338 elements. The membrane material is polyvinylidene fluoride (PVDF) with a separation range/cut-off of 800 kDa. These membrane cartridges have been used to remove fat from WPC concentrate. Cartridge Ca was placed in loop 1 and cartridge Cb was placed in loop 7 of an eight-loop plant. They have both been in use for 1 year and 9 months; further specifications are given in Table 2.

2.1 Membrane sampling

The six membrane cartridges used in this investigation, despite originating from different suppliers, have only small differences with regard to their physical construction. The main differences are therefore expected to be associated with the position in the process and the fact that they come from three different production systems with different histories. In order to get representative pictures of residual fouling over the entire membrane surface area they were sampled in the spatial fashion

shown in Figure 1. The membrane cartridges are standard SW UF and MF membranes. Each membrane leaf thus consists of an inner and an outer membrane layer that is glued together on the outskirts creating a small inactive area with regard to filtration (Figure 1). Each leaf is separated by a retentate spacer and the two layers in a leaf are separated by a second, much finer, permeate spacer.

Cartridge A – This UF membrane cartridge consisted of 11 leaves. Three leaves were sampled, but as it is an SW construct there is no natural choice for a first leaf, and a starting point was thus randomly selected and used to count out leaves number 1, 4 and 11 (an argument could be made here for a more compact numeration since leaves 1 and 11 are neighbors); we prefer to maintain the order in which the selected leaves were visited when originally unwinding the spirally wounded units, for tracking purposes). The leaves were cut from the feed tube in the center (as close as was feasible) and the inactive areas (glue lines) were removed and the leaves were saved for further investigation. This separation resulted in two layers termed inside layer and outside layer for each leaf of the membrane cartridge; for this investigation only the inside layer (physically closest to the center tube when wounded) was used. Each layer was sampled at four lanes of 100 mm width that are referred to as distance from feed (DFF; Figure 1), stretching from the feed inlet to the retentate and permeate outlet. In the second direction each membrane sheet is divided into three positions that will be referred to as distance from center (DFC), using coupons 70 mm wide, giving a total of 12 coupons of size 70×100 mm. The first DFC is

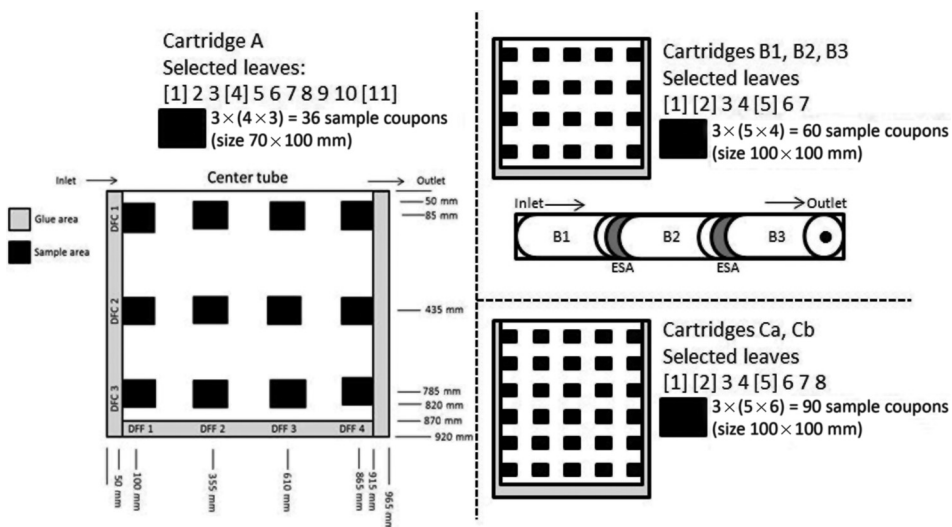


Figure 1 Sampling scheme for the different membrane cartridges

Table 3 Membrane sampling details (see Figure 1)

Cartridge		A		B1		B2		B3		Ca		Cb	
Leaf no.	No. coupons	1	12	1	20	1	20	1	20	1	30	1	30
		4	12	2	20	2	20	2	20	2	30	2	30
		11	12	5	19	5	20	5	20	5	30	5	30
ATR-FT-IR replicates		3		5		5		5		5		5	
Total spectra		108		295		300		300		450		450	

closest to the center tube and the fourth DFC is closest to the outer glue line. Table 3 describes number of leaves, coupons, repetitions and total number of samples.

Cartridges B – The cartridges from this set all have the same seven leaves configuration. As in the dissection of the A cartridge a random starting point was selected to count out leaves number 1, 2 and 5. The leaves were cut from the feed tube in the center and the inactive areas were removed. This separation resulted in two layers termed inside layer and outside layer for each leaf on the membrane cartridge, where inside layers were processed further. The layers were sampled at five DFF lanes of 100 mm width (Figure 1), stretching from the feed inlet to the retentate and permeate outlet. In the second direction each membrane sheet is divided into four DFC positions, giving a total of 20 coupons of size 100 × 100 mm, see Table 3.

Cartridges C – The MF membrane cartridge consisted of eight leaves. As in the dissection of the A and B cartridges a random starting point was selected to count leaves number 1, 2 and 7. The leaves were cut from the feed tube in the center and the inactive areas were removed. This separation resulted again in two layers – the inside layer was used. The layers were sampled at five DFF lanes of 100 mm width. In the second direction each membrane sheet is divided into six DFC positions, using coupons 100 mm wide, giving a total of 30 coupons of size 100 × 100 mm; details are given in Table 3.

All coupons were air dried for 1 h on a table top (approximately 25°C) and were stored in containers in a refrigerator during further experimental work. The coupons were assumed to be the working unit and differences between coupons, not differences within, were the object of present investigation. Great care was taken not to damage the wetted surface layer, clearly visible on the retentate side of UF membranes, while collecting and handling the coupons. Some modest scratches were introduced by the sample preparation, but they have been avoided in analysis. After drying the coupons no obvious removal of residual fouling during the

careful handling was observed. The residual fouling protein load is thus a sum of the CIP-persistent surface and internal fouling.

2.2 Spectroscopic analysis

IR spectroscopy can be used for identifying and quantifying molecules based on their vibrational modes. It is in particular the functional groups that are detectable with IR. To assist in identification, unused polyethersulfone (PES) membrane (virgin material, cleaned 24 h by soaking in water to remove glycerol used for cartridge storage) and used PES membrane coupons were measured and compared. Also used PVDF membrane coupons were measured, though without the assistance of virgin material. This will give rise to peaks that are specific to both the membrane PES/PVDF material and to the residual fouling deposit. The instrument used was a FT-IR spectrometer (ABB Bomen Model 100, detector: DTGS Model SMH307AT) operated with a resolution of 8 cm⁻¹, averaging 32 scans over the spectral range 4,000–700 cm⁻¹, interfaced with a triple-bounce attenuated total reflectance diamond probe (ATR; Durascope, SensIR Technologies). Background spectra (empty interface) were measured with 32 scans at resolution 8 cm⁻¹. It is important to consider the penetration depth and effective sampling area/volume of an ATR-FT-IR instrumental setup. Our initial investigation used a multi-bounce ZnSe ATR crystal (length 70 mm), but the contact between the membrane samples and the interface was not sufficient and could not be improved to such a degree that acceptable and reproducible spectra were obtained. For this reason a triple-bounce ATR diamond probe, applying a high and repeatable pressure, was selected (maintaining the same quantitative resistance/applied pressure settings on the ATR interface; arbitrary unit, level 3). The price to pay is a very small effective sampling area (approx. 1.5 mm² with a penetration depth of 2 μm at 1,000 cm⁻¹), reducing representativeness of the sampling procedure. To reduce this statistical error each

coupon was measured in multiple random positions; see Table 3.

2.3 Imaging and membrane staining

In order to visualize the residual protein content on the membrane, staining was used on one-quarter pieces of all coupons from membrane cartridge A. The coloration of the membrane aids in obtaining knowledge of the distribution of the remaining protein content after CIP. The fouling patterns in the membranes are enhanced as the proteins acquire a dark blue/black color with intensity proportional to the concentration of the protein-residue on the membrane. The procedure followed is a two-step method: staining by a solution of 0.1% (v/v) Amido black, 45% (v/v) methanol, 10% (v/v) acetic acid and 44.9% (v/v) reversed osmosis (RO) water, and de-staining with a solution of 25% (v/v) methanol, 10% (v/v) acetic acid and 65% (v/v) RO water. Step 1 lasted for 3 min where a coupon piece was completely immersed in the solution. This was followed by de-staining four times for 15 min with the solution changed after every time period [13]. After staining the quarter coupons were dried in a fume cabinet for 12 h at room temperature and stored in a refrigerator in a closed container. It was also investigated whether an unused (virgin) membrane would obtain any coloration as this would interfere with the interpretation of the results; this was not the case.

Imaging analysis was used to evaluate normal appearance and the intensity of the color for the stained protein residuals on the membrane, respectively. The Videometer Lab (Videometer A/S, Denmark) measures at 18 different wavelengths covering the visual range and near-IR using diffused light to avoid shadows. An RGB image can be determined from these measurements and was used for visual evaluation. A sample holder was developed to ensure that the same area was used for each sample and that the coupon remained flat inside the equipment.

2.4 Data analysis

Since the ATR-FT-IR spectra provide a fingerprint of the membrane with a large variety of peaks, some arising from the membrane material some due to fouling, it is important to ensure that the peaks being investigated and quantified are the correct ones. This is especially important since membrane manufacturers almost always use tailored version of the PES, PVDF, etc. basis, and minor modifying agent inside the membrane material – without

exception proprietary knowledge of the manufacturer – might interfere with the known signal of, e.g. the protein amide I band. The raw spectra of the membranes from cartridge A were first investigated by computing the correlation between a known material peak and the peaks of interest, where an opposite correlation is expected between the membrane material and the investigated fouling peak. The peaks of interest are specific regions of the spectra that are known to be influenced by the residual fouling constituents; the fat band (carbonyl C=O stretching in triglycerides) near $1,745\text{ cm}^{-1}$, the free fatty acid band (carbonyl stretching in free fatty acids) near $1,720\text{ cm}^{-1}$, the amide I band (carbonyl C=O stretching in amides) near $1,650\text{ cm}^{-1}$ and the amide II band (N-H bend and C-N stretch) near $1,550\text{ cm}^{-1}$. The material peak for the PES UF membranes is chosen to be the one centered at $1,240\text{ cm}^{-1}$, which arises from the asymmetric stretch of the aromatic ether in the polyethersulfone. This is the most commonly used PES membrane band in the literature [14].

Baseline removal in ATR-FT-IR spectra was performed by an in-house routine that requires specification of polynomial order of the baseline and the number of variables/support points in the spectrum that are used to estimate the baseline [15]. All spectra were baseline processed with the same settings (polynomial 2, percentage support points maintained 50). Following the removal of the baseline from the spectra peak information is collected. Peak height is measured as the maximum intensity for each of the fat, amide I and amide II peaks, and these values will be used for further investigation.

Analysis of variance (ANOVA) was performed on the median value of the replicated height measurements within one coupon (Table 3) [16]. The median value was selected because of the large variation in the residual fouling arising from the inhomogeneity of the membrane surface and influence of the cartridge spacers. Decreasing the number of factors in ANOVA to only significant factors allows us to build a model and create a response surface plot from the extracted data to visually compare leaves within each cartridge and also to compare leaves between cartridges since a map of the residual fouling has been created of estimated peak heights providing a semi-quantitative value for residual fouling. These maps can be employed in a qualitative comparison of different experimental conditions. Tukey's honestly significance difference (HSD) test is used to investigate the quantitative differences between measurement series in each category (UF and MF) and investigate the leaves for each cartridge deciding if the cartridges/leaves have significant differences [16].

The data analysis has been performed using Matlab (Mathworks, version R2014a; in-house routines), and JMP (SAS institute, version 10.0.0) has been used in statistical modeling (ANOVA).

3 Results and discussion

Figure 2 shows a representative depiction of the unstained and protein-stained UF membrane service side for cartridge A. From this figure the earlier noted inhomogeneity within a coupon piece and spatial differences between coupons over the membrane sheet are evident. In the first rows we observe that the membrane retains (surface) residual fouling in a specific pattern corresponding with the shape and placement of the spacer located between leaves. The protein fouling occurs over the entire membrane surface and

creates a covering layer as is clear from Figure 2(b) (after staining). Besides the covering layer of protein on the entire leaf there is a buildup in the corners of the spacer in the flow direction, and this pattern is more pronounced near the center tube (see Figure 1, cartridge A, DFC 1, top lane in the subplot grid). The pattern is visible as a brownish deposit that has the same structure as the retentate spacer (Figure 2(a)); this brownish color can be a product of a calcium complex. This feature can also be seen in the staining results (Figure 2(b)), where the membranes have a higher intensity of blue in the corners where the retentate spacer is in contact with the membrane leaf. In the last row (cartridge A DFC 3; Figure 2(b)) some evidence is present for the deformation of the membrane. It appears that the spacer is *rubbing* against the membrane, making the membrane look cleaner in small areas. This can also be seen in the ATR-FT-IR measurements by a large variability between samples; it is overcome by repetitive measurements and using the median value when carrying out data analysis. Overall a horizontal and vertical color gradient, translating into reduced residual protein loads in both directions, is observed in Figure 2(b).

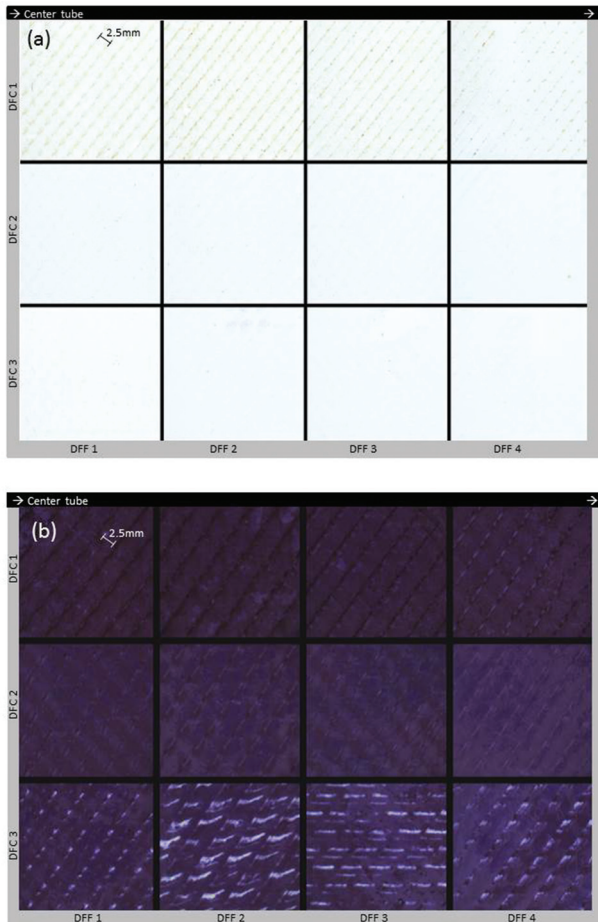


Figure 2 Representative example of (a) unstained and (b) protein-stained coupons, of leaf 1 for UF membrane cartridge A (see Figure 1 for spatial arrangement). Note that the two images sample the same coupons, but not with the same orientation or exact position within a sample coupon

3.1 ATR-FT-IR

Since there are a large number of peaks in the ATR-FT-IR spectrum of membrane material with fouling, it is important to verify the correct peaks to perform data analysis on (Figure 3). The differences and similarities are evident when inspecting the measurements. The intense and characteristic peaks in the virgin membrane spectra are a result of the sulfone- and ring-structure vibrations in the PES. The significant bands that can be assigned to the material in the membrane are the S=O stretch around $1,135\text{--}1,165\text{ cm}^{-1}$, resulting from the sulfone in the polymer. The aromatic structures in the PES also give rise to some significant absorbance bands around $800\text{--}860\text{ cm}^{-1}$ (out of plane bend, *para*-substitution), $1,240\text{ cm}^{-1}$ that corresponds to the asymmetric stretch of the aromatic ether and furthermore two peaks around $1,500$ and $1,600\text{ cm}^{-1}$ that are both assigned to the aromatic carbon-carbon stretching [17]. These peaks are also present in the used membranes, but at significantly lower intensities. This is due to the *shadowing* from the fouling by protein, fat and buildup of minerals [18] and is a direct consequence of the limited penetration depth of the ATR measurements. The peaks that can be assigned exclusively to the fouling from the whey product are some bands that are absent in the spectra for PES: an emergent broad fat peak in the range $1,720\text{--}1,760\text{ cm}^{-1}$, an amide I

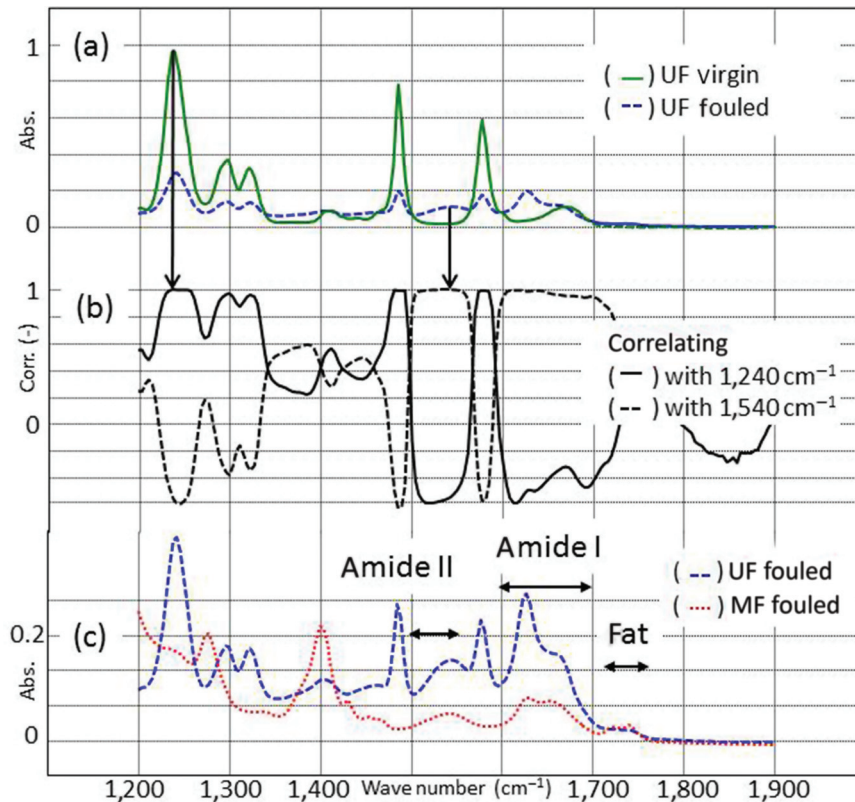


Figure 3 (a) ATR-FT-IR spectra of virgin and fouled PES UF membrane, (b) correlation plot between all spectral variables with a selected wavenumber for amide II ($1,540\text{ cm}^{-1}$) and a selective wavenumber for PES material ($1,240\text{ cm}^{-1}$) using all 108 spectra from cartridge A and (c) PES UF and PVD FMF membrane ATR-FT-IR spectra with residual fouling and indication of amide I ($1,645\text{--}1,670\text{ cm}^{-1}$), amide II ($1,500\text{--}1,550\text{ cm}^{-1}$) and fat absorbance band positions ($1,720\text{--}1,760\text{ cm}^{-1}$)

peak at $1,645\text{--}1,670\text{ cm}^{-1}$ and an amide II peak in the range $1,500\text{--}1,550\text{ cm}^{-1}$ (Figure 3(a)). In Figure 3(b) we have correlated a material peak from the PESUF membrane material that arises from the asymmetrical stretch in the aromatic ether (centered at wavenumber $1,240\text{ cm}^{-1}$) and the peak that is assumed to be amide II (centered at wavenumber $1,540\text{ cm}^{-1}$) with all wavenumbers/variables in the data set from cartridge A (108 spectra, see Table 3). The profiles for the membrane material peak and the amide II peak shows that there is an opposite correlation between the two, which indicates that there is little similarity between the two sources of variance, as anticipated. Figure 3 furthermore shows that the amide I and – to a lesser extend – the fat peaks are influenced by the membrane material and might prove difficult to model. From this information it was concluded that the amide II peak is the most suitable (and robust) peak to quantify protein residuals and will be investigated further. Measurements of the specific MF PVDF membrane materials of cartridges C in virgin state are not available to us and the correlation profiles can thus not be used here. It was chosen to investigate the MF membranes under the same circumstances as

the UF membranes based on visual inspection of similarity as illustrated in Figure 3(c). We will also model fat with regards to the MF membranes employing the free fatty acid band centered at $1,720\text{ cm}^{-1}$ as this operation is often the first step prior to up-concentrating the protein from the whey by UF (though for this particular investigation the membranes were used to remove fat from WPC). The stronger amide I band will not be used in this investigation since there is an interfering peak arising from the membrane material, making it difficult to distinguish membrane polymer from fouling peak (Figure 3(a) and (c)) and since there is a strongly overlapping band from H–O–H water bending at $1,640\text{ cm}^{-1}$.

3.2 ANOVA

Cartridge A –ANOVA is performed on the median value of the height of the amide II peak for the replicates measured on one coupon; the amide II residual fouling pattern described by the raw data (median peak heights per

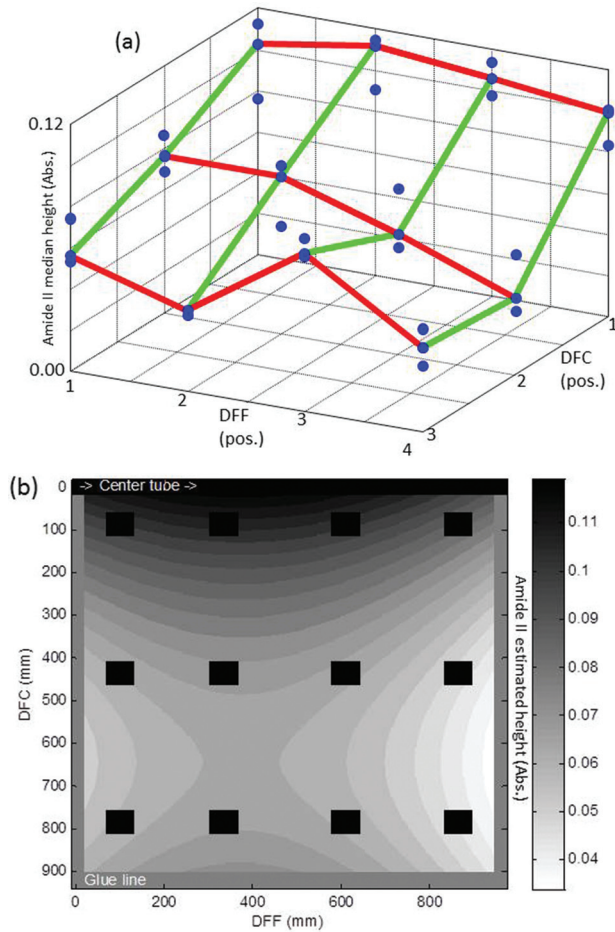


Figure 4 (a) Three-dimensional plot of data from the three leaves of cartridge A (connecting grid based on median), (b) surface response plot of the ANOVA model from cartridge A (only significant ANOVA model parameters maintained; black squares symbolize measurement coupons)

coupon for the three leaves sampled) is shown in Figure 4 (a), the ANOVA results are summarized in Table 4. The median of replicates was selected as representative statistic because of the earlier described inhomogeneity in the sample material and the minimal service area of the ATR-FT-IR interface. Cartridge A was the initial cartridge investigated and from it the data analysis methods have been developed. The leaf-to-leaf variation is evaluated and according to Tukey's HSD the three leaves in cartridge A are statistically the same resulting in one common ANOVA model. The effects of DFF (a continuous variable), DFC (a continuous variable), leaf (a nominal/discrete variable), quadratic terms and interactions are investigated and significant factors are included in the final surface response model (Table 4). When studying the analysis results a clear non-linear relationship is observed for both DFF and DFC, suggesting two quadratic

Table 4 ANOVA summary amide II for cartridge A

Cartridge A		
<i>N</i>	36	
Tukey's HSD	Leaf	
	1	A
	4	A
	11	A
ANOVA factors, <i>p</i> -values		
DFF	0.036	
DFC	<0.001	
Leaf	–	
DFF × DFC	–	
DFF × leaf	–	
DFC × leaf	–	
DFF ²	0.029	
DFC ²	0.002	
ANOVA model diagnostics		
<i>R</i> ²	0.687	
Adj. <i>R</i> ²	0.647	
RMSE (abs.)	0.015	
Intercept (abs.)	0.105	

terms are to be included in the model. The correlation coefficient for the final model is 0.687 (adjusted $R^2 = 0.647$), which indicates that the model fit and the model prediction are adequate and 69% of the initial variation is described, 65% correctly predicted. Unfortunately, the number of sample coupons and repetitions is too small to overcome the large variation that is introduced with the inhomogeneity of the residual fouling and other cartridges were thus measured with more sample coupons and repetitions (Table 3).

The amide II residual fouling pattern described by the raw data (median peak heights per coupon) is shown in Figure 4(a); the ANOVA surface response model based on the estimated parameters deemed significant (Table 4) is shown in Figure 4(b). By visually inspecting the two subplots it is evident that the model resembles the raw data to a large extent. The highest concentration of fouling arises at the center (permeate) tube with a decreasing trend outward. The leaves exhibit an increase of fouling on the outer edge of the membrane, which can be seen in both plots.

Cartridges B – The three cartridges B1, B2 and B3 were placed in the same stainless steel housing during production and it is therefore of great interest whether these cartridges behave similarly concerning residual fouling, if residual fouling is dominated by production/assembly of individual cartridges or if, e.g. the flow and pressure influences the cartridges differently. The number of degrees of freedom during ANOVA modeling is not

sufficient to include both cartridge and leaves in the same investigation and therefore the data is evaluated by a two-step procedure. First the leaf-to-leaf variation within each cartridge is investigated. A model containing the effects leaf, DFF, DFC, interactions and quadratic terms are initially inspected and the results show that there are statistically significant differences between some single leaves in the cartridges. All data from leaves that are significantly different have been removed as we want to show a representative picture of the fouling in this UF unit tube (Table 5). Removing a full leaf as an outlier instead of simply removing single measurements as outliers is done here because removing individual sample coupons would influence the pattern of residual fouling by possibly forcing our expectations. The leaves can differentiate from each other by intensity, fouling pattern and sample variability and are evaluated according to the ANOVA and by investigating the raw data.

Cartridge B1—Results from the Tukey's HSD test for cartridge B1 (Table 5, Figure 5(a)) show that the leaf factor has an influence on the model, where one leaf in the cartridge is significantly different from the rest. Inspection of the raw data demonstrates a difference in intensity between leaf 1 and leaves 2 and 5. Leaf 1 is removed from further investigation as a representative overview is the main purpose. When studying the analysis results for the reduced model a clear non-linear

relationship for the DFF was observed, suggesting a quadratic term to be maintained in the model. The correlation coefficient for the original model is 0.780 (adj. $R^2 = 0.759$) while the correlation coefficient for the reduced model drops to 0.693 (adj. $R^2 = 0.667$). It is assumed that the difference between the model fit and adjusted model (*prediction*) correlation coefficient is adequate and indicate that the model is reliable in describing 69% of the initial variation in the data, especially taking into consideration the large variations and inhomogeneity described previously.

Cartridge B2—Results from the Tukey's HSD (Table 5, Figure 5(b)) show that all three leaves are significantly different from each other and inspection of the raw data revealed that leaf one has a significantly lower intensity than the remaining two leaves indicating that the leaf/cartridge might have had some problems before being installed in production (or, alternatively, that this one leaf is more efficiently cleaned during CIP and thus likely also better performing during production – an unlikely scenario that nevertheless cannot be excluded to 100%). Since leaves 2 and 5 are also significantly different (separate analysis, not shown) it was chosen to maintain only leaf 5 based on manual comparison of the mean response compared to the other B cartridges. When studying the analysis results no quadratic term was significant, only the main effects; DFF and DFC are included in the model.

Table 5 ANOVA summary amide II for cartridges B

	Cartridge B									
	B1				B2				B3	
	Original		Reduced		Original		Reduced		Original	
<i>N</i>	59		39		60		20		60	
Tukey's HSD	1	B			1	C			1	A
	2	A	2	A	2	B			2	A
	5	A	5	A	5	A	5	A	5	A
ANOVA factors, <i>p</i> -values										
DFF	<0.001		0.006		0.004		0.003		<0.001	
DFC	<0.001		<0.001		<0.001		<0.001		<0.001	
Leaf	<0.001		–		<0.001		–		–	
DFF × DFC	–		–		–		–		–	
DFF × leaf	–		–		0.017		–		–	
DFC × leaf	–		–		–		–		–	
DFF ²	0.002		0.014		–		–		<0.001	
DFC ²	–		–		0.045		–		–	
ANOVA model diagnostics										
R^2	0.780		0.693		0.930		0.660		0.714	
Adj. R^2	0.759		0.667		0.920		0.620		0.698	
RMSE (abs.)	0.007		0.007		0.008		0.009		0.009	
Intercept (abs.)	0.101		0.107		0.085		0.107		0.113	

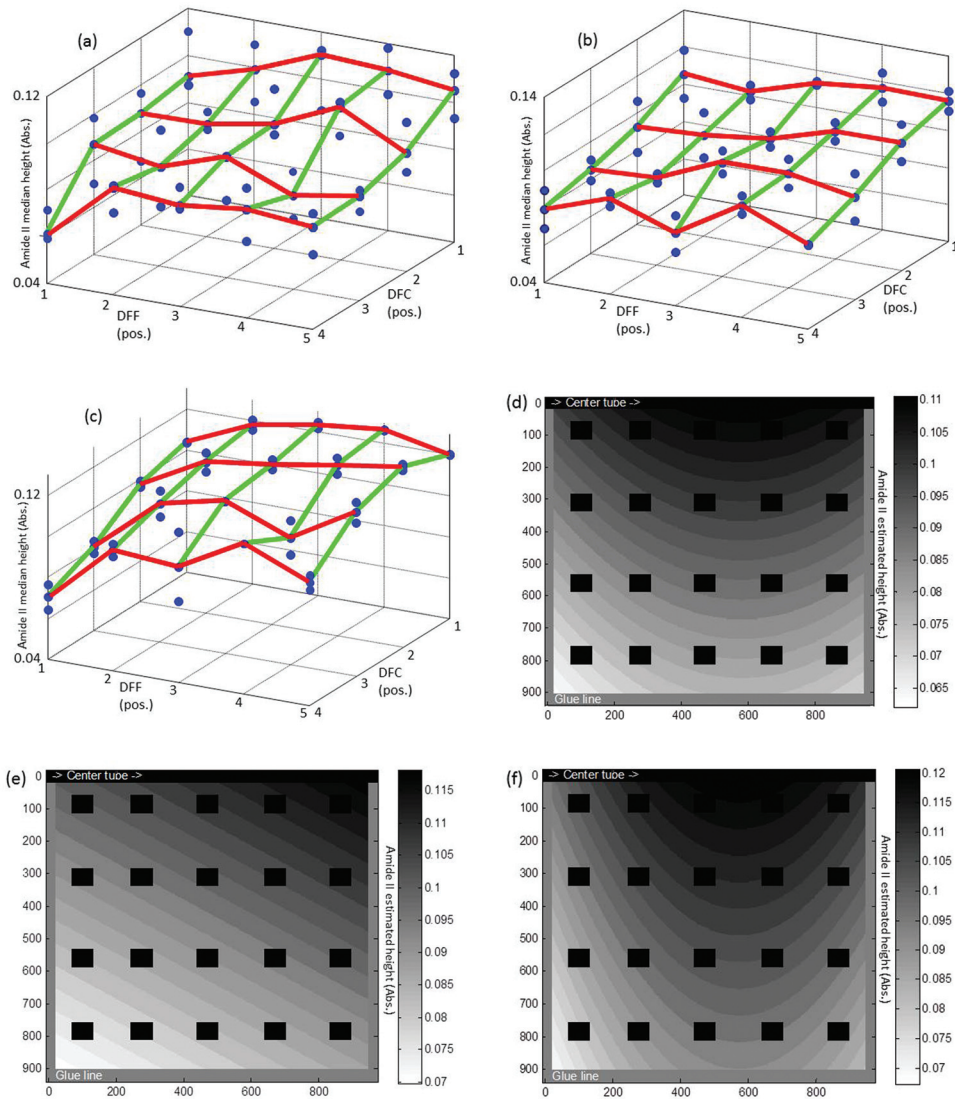


Figure 5 Three-dimensional plots of data from three leaves for cartridge B1 (a), B2 (b) and B3 (c); surface response plots of the ANOVA models for cartridge B1 reduced (d), B2 reduced (e) and B3 original (f)

The correlation coefficient for the original model is 0.930 (adj. $R^2 = 0.920$) and the reduced model has a correlation coefficient of 0.660 (adj. $R^2 = 0.620$) which indicates that a considerable amount of the explained variation is due to the differences in the leaves. Still, the prediction is acceptable and describes 66% of the initial variation in the data.

Cartridge B3—Results from the Tukey’s HSD (Table 5, Figure 5(c)) show that all three leaves are statistically the same and hence they have no influence on the model and are not included in the final model. When studying the data and analysis results a clear non-linear relationship for DFF was observed, suggesting a quadratic term to be introduced to the model. The correlation coefficient for the model is 0.714 (adj. $R^2 = 0.698$) which indicated that

the model is adequate with regard to model fit and model prediction and is reliable describing 71% of the initial variation.

The three-dimensional plots of the raw data of the three B cartridges are shown in Figure 5(a)–(c). They exhibit some clear differences in the overall shape of the pattern of the residual fouling, where cartridges B1 and B2 show a similar profile curved in two directions and cartridge B3 has a less curved and overall smooth structure. Common for all is that the intensity of the fouling increases at the outer edge of the membrane leaf. The surface plots (Figure 5(d)–(f)) that are derived from the ANOVA on the median values of the raw data exhibit clear similarities. The highest intensity, hence the largest amount of residual fouling, is found closest to the

center tube and also closer to the outlet than the inlet. Cartridges B1 and B3 show a characteristic *flame* pattern evolving from the center tube outward. Cartridge B1 shows a wider *flame* that reaches almost from inlet to outlet. The *flame* on cartridge B3 is narrower and the highest intensities are found closer to the outlet. Cartridge B2 appears different from the other two cartridges by not showing the *flame* pattern, but the overall intensity distribution is similar with the highest intensity of residual fouling at the center tube and close to the outlet. The pattern evolves in a linear fashion decreasing in residual fouling intensity from the outlet and diagonally outward. There are more details in the three-dimensional plots showing measurement results, but these details are partly due to the inhomogeneity of the residual fouling, still manifest despite using an averaging over five individual ATR-FT-IR recordings. The surface plots based on significance testing is thus a more trustworthy alternative to the three dimensional plots. The surface plots enhance the interpretability of the fouling distribution and give a good overview of the residual fouling in the cartridges though some details are lost. These minor details are of less importance for the aim of investigating the overall development of fouling between cartridges.

The second step of the investigation of cartridges B1, B2 and B3 focuses on the differences/similarities between them by estimating a global ANOVA model. The leaves that are included in the investigation are leaves 2 and 5 from cartridge B1 (39 samples/coupons in total), leaf 5 from cartridge B2 (20 samples) and all three leaves from cartridge B3 (60 samples). According to Tukey's HSD all three cartridges are significantly different, which implies that there is a dependency on the position inside the steel housing. The effects of the DFF, DFC, quadratic terms and interactions are also inspected and the main effects are statistically significant (DFF $p < 0.001$, DFC $p < 0.001$), a clear non-linear relationship for DFF was observed ($p < 0.001$) and the interaction between the two main effects is also statistically significant ($p = 0.048$). Finally, the interaction between the cartridge and DFF is significant to the model ($p = 0.001$). The correlation coefficient is 0.764 (adj. $R^2 = 0.747$), which indicates that the model is adequate with regard to model fit and model prediction and the model is reliable describing 76% of the initial variation in the data.

The data analysis in the previous paragraphs has been developed for UF membranes, and it is of interest to investigate if this can be transferred to other types of filtration membranes. We have measured MF membranes under the same circumstances as the UF membranes and

the fouling components should resemble the components from the UF membranes. The spectra for the membrane material exhibits differences due to different polymers used (see Figure 3); a direct semi-quantitative comparison within the MF systems is thus possible but a similarity check with the UF results should be done qualitatively. For the MF membranes we investigate the amide II and fat bands as MF is commonly implemented to remove fat prior to UF of whey.

Cartridge Ca, amide II– Results from the Tukey's HSD test show that the leaves have some similarities, leaves 1 and 5 are statistically the same and leaves 2 and 5 are statistically the same (Table 6). We assume the leaf pattern does not affect the model and all leaves are included for further investigation. When studying the analysis results a clear non-linear relationship for DFC was observed (results not shown), suggesting a quadratic term to be introduced to the model. DFF, which is one of the main effects in the analysis, surprisingly proves to have no influence on the final model. The correlation coefficient for the model is 0.894 (adj. $R^2 = 0.892$) which indicates that the model fit and the model prediction is good and 89% of the initial variation is described.

Cartridge Cb, amide II– Results from the Tukey's HSD test show that leaves 2 and 5 are statistically the same while leaf 1 is different (Table 6). Inspecting the raw data reveals that the overall shape of the residual fouling on leaf 1 had a decreased intensity. When studying the analysis results a clear non-linear relationship for DFC is observed, suggesting a quadratic term to be included in the model. The correlation coefficient for the model is 0.916 (adj. $R^2 = 0.911$), which indicates that the model fit and the model prediction is good and 92% of the initial variation is described.

Cartridge Ca, fat – Results from the Tukey's HSD test shows that the leaves are statistically the same (Table 6), a different finding when compared to the amide II ANOVA of this same set of measurements. When studying the analysis results a clear non-linear relationship for DFC and DFF was observed (results not shown), suggesting a quadratic term to be introduced to the model. Also the interaction term between the main factor DFF and DFC has an influence on the model indicating a correlation between the two factors. The correlation coefficient for the model is 0.612 (adj. $R^2 = 0.589$) which indicates that the model fit and the model prediction is good and 61% of the initial variation is described.

Cartridge Cb, fat – Results from the Tukey's HSD test shows that the three leaves are statistically similar (Table 6). When studying the analysis results a clear non-linear relationship for DFC and DFF was observed (results

Table 6 ANOVA summary amide II and fat for cartridges C

	Cartridge C							
	Amide II				Fat			
	Ca		Cb		Ca		Cb	
<i>N</i>		90		90		90		90
Tukey's HSD	1	A	1	B	1	A	1	A
	2	B	2	A	2	A	2	A
	5	AB	5	A	5	A	5	A
ANOVA factors, <i>p</i> -value								
DFF		–		0.014		<0.001		<0.001
DFC		<0.001		<0.001		<0.001		0.001
Leaf		0.028		<0.001		–		–
DFF ²		–		–		0.004		0.005
DFF × DFC		–		–		0.009		0.005
DFC ²		<0.001		<0.001		<0.001		<0.001
DFF × leaf		–		–		–		–
DFC × leaf		–		0.003		–		–
ANOVA model diagnostics								
<i>R</i> ²		0.902		0.927		0.612		0.548
Adj. <i>R</i> ²		0.898		0.921		0.589		0.521
RMSE (abs.)		0.006		0.005		0.014		0.018
Intercept (abs.)		0.036		0.030		0.003		–0.000(5)

not shown), suggesting a quadratic term to be introduced to the model. Also the interaction term between the main factor DFF and DFC has an influence on the model indication a correlation between the two factors. The correlation coefficient for the model is 0.548 (adj. $R^2 = 0.521$), which indicates that the model fit and the model prediction is good and 55% of the initial variation is described.

The ANOVA surface plots of the four investigations for cartridges C are shown in Figure 6. The surface plots of the residual fouling on the leaves have a similar composition as the previous surface plots with regard to the amide II band: the highest intensity of residual fouling is closer to the center tube and it evolves toward the outer edges with a decrease in intensity. The amide II surface plots are globally similar, though cartridge Cb has a characteristic *flame* shape with different orientation at the outer edge of the membrane resulting in the development over the membrane having a slight curvature. These results are a good reminder that when interpreting surface plots it is important to keep in mind the measurement uncertainty, probabilities associated with relatively small measurement sets and the main-versus-minor tendencies in the profiles. The surface plots for fat show the same profile for both Ca and Cb though the later has a slightly higher intensity of residual fat on the leaves. The surfaces for fat show the same crude tendencies compared to all amide II profiles (cartridge(s) A, B and C),

but also some characteristic indication of residual fouling after CIP not observed for protein.

The most likely reason for the increase in residual fouling closer to the center tube is that the permeate flux in an SW membrane element during production (as well as water flux during CIP) is highest closer to the center tube. At this site permeate has the shortest distance to travel inside the permeate spacer positioned between the backsides of the two membrane sheets that create the “membrane envelopes” in an SW module. Due to this, the force pulling foulants toward the membrane will be higher in this area compared to the force from the cross-flow trying to carry foulants away. This buildup of fouling is a phenomenon that is often seen in industry when inspecting membrane cartridges that were difficult to clean properly or had been exposed to water with “fouling agents.” In a similar way, the permeate flux will be higher at the inlet of each membrane cartridge due to the TMP, defined as the pressure difference between the feed and permeate stream – the driving force in the filtration unit, being the highest at this point. The naturally created pressure drop in the retentate flow direction by the cross-flow is the reason. This implies that the larger the cross-flow, the more pronounced is the difference in TMP and flux is in the DFC direction. In housings with several elements installed in a serial configuration a similar trend in TMP is present in the flow direction going from

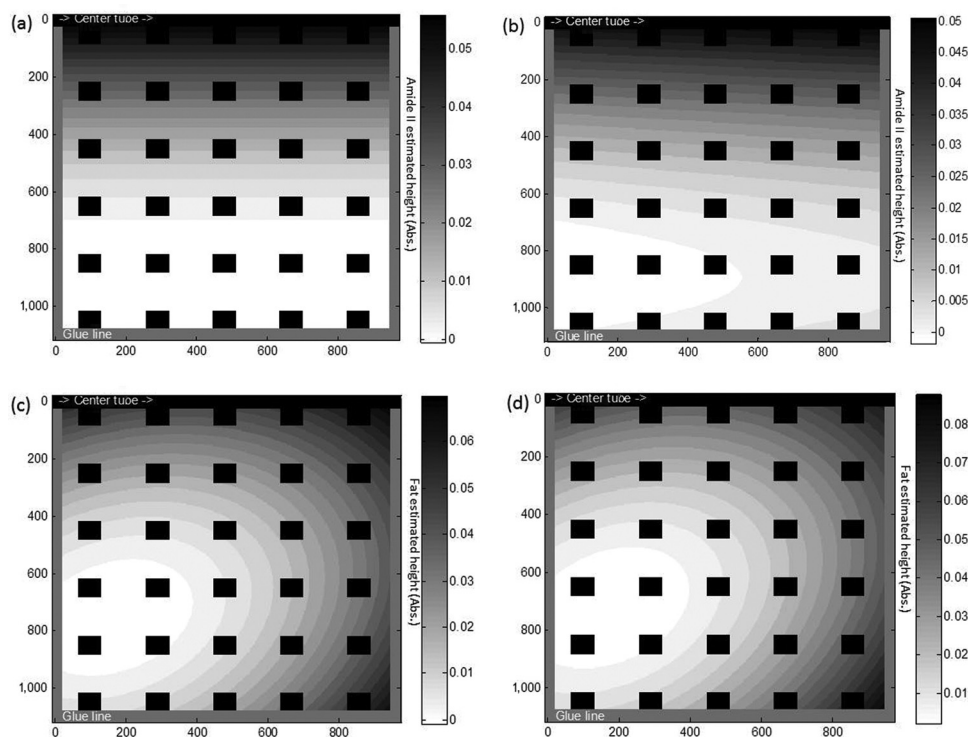


Figure 6 Surface response plots of the adjusted ANOVA models (only significant ANOVA model parameters maintained) for cartridge Ca amide II (a), Cb amide II (b), Ca fat (c) and Cb fat (d)

the first membrane cartridge to second membrane cartridge and so forth.

4 Conclusions

An extensive investigation on the residual fouling of UF and MF membranes in full-scale dairy processing has been presented. Successful measurement and data analytical methods have been developed to describe the residual fouling on membranes. ATR-FT-IR has demonstrated to be an appropriate analytical technique for measuring the different molecular components originating from the residual fouling compared to the staining method that was also presented.

Cartridge A – The staining for proteins and visual inspection aided in describing and understanding the spatial distribution of residual fouling on the membrane and helped identify the inhomogeneity that can cause large variation in the measurement results. The observations were in agreement with the (sparsely available) references on full-scale production investigations, providing confidence in our method of analyses. The staining method proved useful as a visualization tool but as a quantitative method it will not be adequate. The blue

color has limitations with regard to protein concentration since the intensity of the blue (hence, the range from the lightest to the darkest blue) at some point cannot get any darker/intense (“saturation”). The staining provides furthermore no information on the chemical structure of the residual fouling present on the membranes and large volumes of harmful chemicals are required. From this we concluded that ATR-FT-IR is a more suitable method as it is a fast and non-destructive method that provides chemical selectivity on the residual fouling.

Cartridges B – Tukey’s HSD showed that the three cartridges are significantly different, which indicates that there is no repeatability between the cartridges concerning residual fouling, even though they are positioned in the same steel housing and have experienced the exact same production and CIP cycles over the 5-month period of use. One of the leaves removed as an outlier from cartridge B2 showed significantly lower intensity compared to the remaining leaves. These statistically significant differences between leaves will most likely not occur spontaneously inside a closed production and CIP system; all leaves within one cartridge are expected to experience the same flows. This indicates that the leaf has been less (or more) exposed to the environment in the cartridge during whey processing (and cleaning). The

large variability between the leaves within one cartridge and between the cartridges is suspected not only to be a result from the use at the dairy but also caused by the manufacturing and assembly of the membrane cartridges.

Cartridges C – The investigation showed that both protein and fat show a characteristic residual fouling pattern over the leaves. The conclusion is that ATR-FT-IR is a strong (albeit labor intensive) method for semi-quantitative evaluation of the complex process of membrane filtration at an industrial scale.

The DFF and DFC directions as main and/or quadratic effects have a significant influence on the findings in all the ANOVA calculations performed on amide II and fat bands. There is a clear, non-homogeneous distribution on the membrane sheets with the concentration of residual fouling the highest at the center tube and decreases toward the glued edge along the DFC direction. These shared tendencies can likely be explained by spatial flow and pressure differences caused by the design aspects of spirally wounded modules and steel housings. The permeate flux can be credited the higher fouling concentration closer to the center tube as the flux is higher here since permeate has the shortest distance to travel. Similarly there is an increase in fouling at the feed inlet of the membrane cartridge due to TMP being at the highest at this point.

Despite the clear common trends as evidenced by, e.g. Figures 5 and 6, a large leaf-to-leaf variation is observed from, e.g. Tables 5 and 6, and a cartridge-to-cartridge variation from Table 5. A systematic *nearest-neighbor* pattern for the leaves inside one cartridge was not observed. These differences in cleaning (and probably capacity performance) can most likely be attributed to manufacturing and assembly variations in the complex structure of spirally wound membrane units.

References

- Walton M. Cleaning in place: dairy, food and beverage operations. Chapter 1. In: Tamime A, editor. Principles of cleaning-in-place (CIP), 3rd ed. Oxford: Blackwell Publishing, 2008:1–9.
- Lyndgaard CB, Rasmussen MA, Engelsen SB, Thaysen D, van den Berg FW. Moving from recipe-driven to measurement-based cleaning procedures: monitoring the cleaning-in-place process of whey filtration units by ultraviolet spectroscopy and chemometrics. *J Food Eng* 2014;126:82–8.
- Ottosen N. WPC – choosing the right UF membrane. *European Dairy Magazine* 2004;10–12.
- Schwinge J, Neal PR, Wiley DE, Fletcher DF, Fane AG. Spiral wound modules and spacers review and analysis. *J Membr Sci* 2004;242:129–53.
- Chan R, Chen V. The effects of electrolyte concentration and pH on protein aggregation and deposit: critical flux and constant flux membrane filtration. *J Membr Sci* 2001;185:177–92.
- Brans G, Schroën CG, van der Sman RG, Boom RM. Membrane fractionation of milk: state of the art and challenges. *J Membr Sci* 2004;243:263–72.
- Berg TH, Knudsen JC, Ipsen R, van den Berg FW, Holst HH, Tolkach A. Investigation of consecutive fouling and cleaning cycles of ultrafiltration membranes used for whey processing. *Int J Food Eng* 2014;10:367–81.
- Tragårdh G. Membrane cleaning. *Desalination* 1989;71:325–35.
- Linkhorst J, Lewis WJ. Workshop on membrane fouling and monitoring: a summary. *Desalin Water Treat* 2013;51: 6401–6.
- Bylund G. Dairy processing handbook. Lund, Sweden: Tetra Pak Processing Systems AB, 2003.
- Marshall AD, Daufin G. Physico-chemical aspects of membrane fouling by dairy fluids. In: IDF, ed.. Fouling and cleaning in pressure driven membrane processes. Budapest, HUN: Symposium on advances in membrane technology for better dairy products, 1995:8–29.
- Kontopidis G, Holt C, Sawyer L. Invited review: β -lactoglobulin: binding properties, structure, and function. *J Dairy Sci* 2004;87:785–96.
- Platt S, Nyström M. Amido black staining of ultrafiltration membranes fouled with BSA. *Desalination* 2007;214:177–92.
- Bégoïn L, Rabiller-Baudry M, Chaufer B, Hautbois M, Doneva T. Ageing of PES industrial spiral-wound membranes in acid whey ultrafiltration. *Desalination* 2006;192:25–39.
- Massart DL, Vandeginste BG, Buydens LM, De Jong S, Lewi PJ, Smeyers-Verbeke J. Handbook of chemometrics and quality metrics: part A. Amsterdam: Elsevier, 1997.
- Montgomery DC. Design and analysis of experiments, 6th edn. Hoboken, NJ: John Wiley & Sons, 2005.
- Nair PK, Cardoso J, Gomez Daza O, Nair MT. Polyethersulfone foils as stable transparent substrates for conductive copper sulfide thin film coatings. *Thin Solid Films* 2001;401:243–50.
- Zhu H, Nyström M. Cleaning results characterized by flux, streaming potential and FTIR measurements. *Colloids Surf A Physicochem Eng Asp* 1998;138:309–21.

Paper II

J.K. Jensen, J.M.A. Rubio, S.B. Engelsen, F. van den Berg

Protein Residual Fouling Identification on UF Membranes
using ATR-FT-IR and multivariate curve resolution

Submitted to Chemometrics and Intelligent Laboratory Systems

March 2015

Protein Residual Fouling identification on UF Membranes using ATR-FT-IR and multivariate curve resolution

Jannie K. Jensen^{*}, José M. A. Rubio, Søren B. Engelsen, Frans van den Berg

University of Copenhagen, Faculty of Science, Department of Food Science, SPECC section, Rolighedsvej 26, DK-1958 Frederiksberg C, Denmark

* Corresponding author: janniekj@food.ku.dk, +45 2272 4748

Abstract

Industrial ultrafiltration membranes and residual fouling, persistent after cleaning-in-place, is studied with ATR-FT-IR (Attenuated Total Reflection Fourier Transform Infrared) in combination with MCR (Multivariate Curve Resolution). MCR has rarely been used in combination with IR spectroscopy and has never previously been applied to spectra from ultrafiltration membranes. The MCR results revealed that by applying non-negativity to both loading and concentration profiles in combination with an equality constraint on the loadings, the optimal number of components was determined and the different chemical entities in the spectra were correctly identified as either fouling residuals (protein and fat) or membrane components (polyethersulfone and grafting). In conclusion the MCR results provided an easy and interpretable overview of the fouling distribution and visualized the potential pitfalls when measuring with ATR-FT-IR, namely the varying penetration depth and layered sample composition. This study presents a novel method to investigate and map the residual fouling on industrial ultrafiltration membranes that averages out insignificant features while enhancing the important/principal ones. The method can aid in optimization of cleaning procedures and in designing improved membrane systems and materials.

Keywords

MCR-ALS, ATR Infrared spectroscopy, ultrafiltration membranes, residual fouling

1 Introduction

Large volumes of water are being consumed when cleaning the filtration membranes that are utilized in ultrafiltration (UF) processing of whey in the dairy industry. UF is a complex process that is used to recover the protein fraction, e.g. in the form of whey powder, in the waste streams of cheese production. The cleaning of the enclosed membrane cartridges – so-called Cleaning-In-Place (CIP) performed approximately every 24 hours - consists of several sequential steps demanding considerable quantities of chemicals, water and energy, and last but not least production downtime (6-7 hours). The reason for this lengthy downtime is the fouling that the membranes are subjected to. It consists of a build-up of protein, fat and minerals that to a large extent – but not completely – can be removed by CIP, thus leaving behind an irreversible layer of residual fouling. The reason why fouling is of large interest in both research and industry is because it is the largest uncontrollable factor in dairy whey processing when using membrane technologies [1, 2].

Membrane fouling has been studied in numerous works and several studies have applied attenuated total reflectance Fourier transform infrared (ATR-FT-IR) spectroscopy to study membrane (residual) fouling after use (hence *post mortem*) [3, 4]. However, so far the data analysis has been limited to height measurement of the peak of interest or to applying a technique called the double difference method [5], or simply to the assignment of the peaks in the spectra followed by a qualitative evaluation [6]. This study aims at investigating residual membrane fouling by a comprehensive mapping of a used membrane by ATR-FT-IR and multivariate curve resolution (MCR).

The spirally wound cartridges used in industrial whey processing consist of two layers in envelopes separated internally and externally by spacer networks [7]. The membrane material consists in our case of polyethersulfone (PES) sheets deposited on a polyester (PE) support layer with constant thickness. In this study, the samples consist of coupons collected at different locations on the leaf/service area (Figure 1). The residual fouling found on the surface varies in thickness due to flow and transmembrane pressure (TMP) differences over the full UF membrane, but also locally due to the spacer network present in the cartridge (Figure 1, inset). A two-phase system such as the PES-plus-fouling-layer is a potential problem when measured with ATR-FT-IR as the determining factor is the penetration depth (d_p) of the infrared radiation. The penetration depth equals the distance travelled by the evanescent electromagnetic wave - estimated between 0.5-15 μm for the full mid-infrared range in a PES membrane system. The penetration depth is a function of the refractive indices of the sample and the internal reflectance element (IRE):

$$d_p(\lambda) = \frac{\lambda}{2\pi n_1 \sqrt{\sin^2 \theta - \left(\frac{n_2}{n_1}\right)^2}} \quad (1)$$

λ is a given wavelength, θ is the incident angle at the internal surface of the IRE, n_1 is the refractive index of the optically dense medium (the IRE), and n_2 is the refractive index for the optically less dense medium (the membrane sample with residual fouling layer) [8].

In this experiment the angle of incidence is the same for all measurements, and this parameter is only critical in ATR-FT-IR if the refractive index ratio between sample and IRE becomes too small. The IRE is made of diamond with a refractive index of 2.42 [9] and the sample consisting of residual fouling where β -lactoglobulin is the main constituent with a refractive index of 1.46 [10]. The ultrafiltration membrane layer consisting of PES has a refractive index of approximately 1.62

(Figure 2a) [11], which might be slightly altered due to proprietary modifications to the material conducted by the membrane supplier. Inside the IRE, the IR beam is totally reflected but an evanescent wave is emitted and it is the depth to which this evanescent wave penetrates the sample that is referred to as the penetration depth (Equation 1; Figure 2b). The evanescent wave is a non-transverse (diffuse) wave and the intensity of the evanescent field decreases with increasing distance (Z) into the medium normal to its surface. Therefore the evanescent field mainly exists in the near vicinity of the interface between the IRE and sample [12]. The penetration depth of the evanescent wave is (somewhat arbitrarily) defined in literature as the depth at which the field strength (E) decays to a value of $E_0 \times e^{-1} = E_0 \times 0.368$, where E_0 is the initial electric field amplitude. This means that it is the depth into the optically less dense medium where the amplitude of the evanescent wave has only 37% of its original value [12].

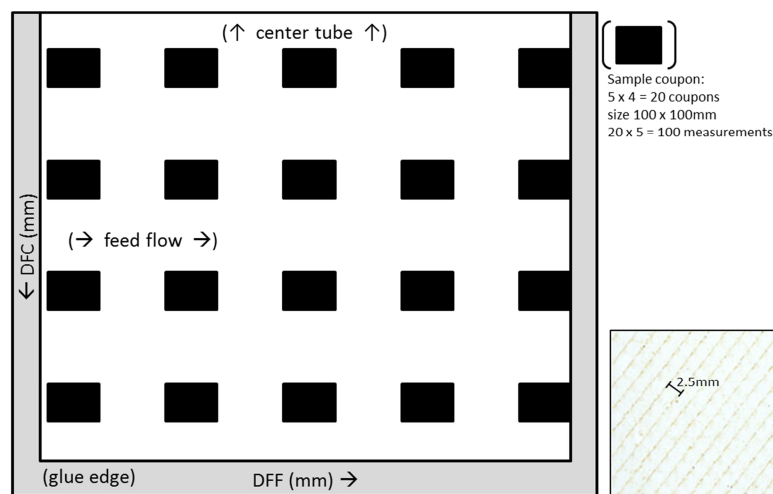


Figure 1 – Sampling scheme for the investigated ultrafiltration membrane leaves; inset: part of a UF membrane leave with clear spacer imprint.

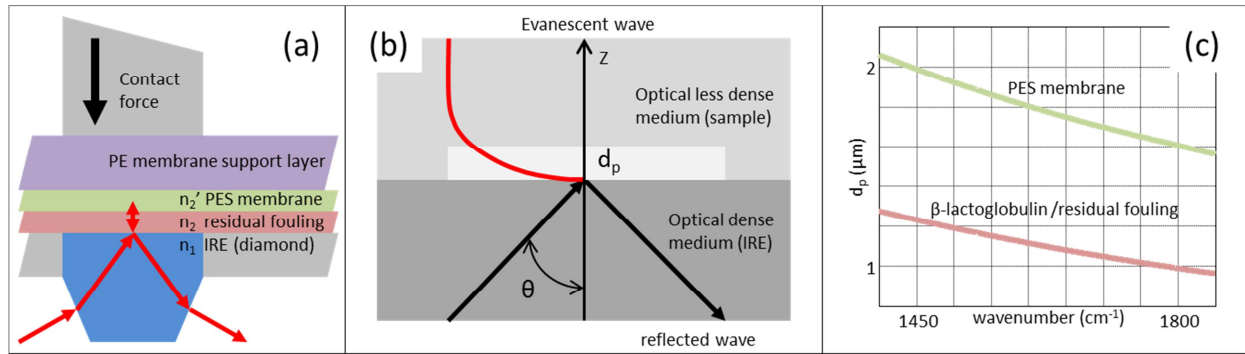


Figure 2 – (a) Illustration of the membrane interfacing with the ATR crystal: (b) schematic overview of the events during ATR/IRE measurement and penetration depth; (c) estimated penetration depth in fouling layer and membrane material.

The thickness of the fouling layer varies considerably depending on the measurement position on the UF membrane leaf due to e.g. differences in TMP encountered during the whey production. This might cause problems during data analysis as the emitted evanescent wave only reaches a few micrometers into the sample (Figure 2c) [8]. The limited path length of the evanescent wave combined with the varying thickness of the residual fouling causes an unusual pattern in the spectral data where the supposed constant part (PES sheet/leave) varies; this is caused by the varying amount of light reaching the membrane surface. This variation originates from the residual fouling *shadowing* the PES: less infrared light reaches the membrane material when the fouling layer is thick and vice versa. The intensity of the light reaching the FT-IR detector in ATR measurements is directly correlated to the concentration according to Lambert-Beer's law and when the amount of light irradiating the sample is varying it might compromise the linear relationship in Lambert-Beer's law and cause the variations observed. The nature of the ATR measurements unfortunately prevents the presented method to be used *in situ*. Attaching any object to the membranes prior to use would result in the absence of fouling in that specific area, and no useful data would thus be collected. Furthermore the environment in the steel housings surrounding the membranes is rather

harsh and would for certain wear out any measurement equipment in the process (and cleaning) stream.

Multivariate curve resolution (MCR) [13, 14] has proven to be a powerful tool for the investigation of complex chemical systems, particularly for the investigation of systems where little or no previous knowledge exists like the UF membranes in this study. These can be underlying phenomena that cannot be easily detected by e.g. principal component analysis (PCA) [15]. MCR was originally developed to encompass evolutionary analytical data from a process or an analytical measurement. It is particularly well suited for analyzing and modelling spectroscopic measurements since the underlying analytical model in these measurements is already a bilinear relationship meaning that Lambert-Beer's law holds. The Lambert-Beer law is a model of pure signal contributions, where concentrations are directly proportional to the intensity of the light. Hence, MCR fits these measurements because it precisely mimics the structure of the analytical measurement. The model that MCR follows is

$$\mathbf{D} = \sum_i c_i \mathbf{s}_i^T + \mathbf{E} = \mathbf{C}\mathbf{S}^T + \mathbf{E} \quad (2)$$

where \mathbf{C} contains the concentration values of all components and \mathbf{S} the related pure component spectra; \mathbf{E} is the matrix that expresses the error or the unexplained variance by the bilinear model.

Multivariate curve resolution with alternating least squares (MCR-ALS) works by optimizing both concentration profile and pure spectral profiles in an iterative cycle. The first step in MCR-ALS is to find a set of initial estimates followed by optimizing this estimate until a convergence criterion is reached [14]. The initial estimate can originate from several methodologies such as evolving factor

analysis [16], SIMPLISMA [17] or from previous knowledge about the system such as pure spectra. The challenges with MCR are its dependence of a good initial guess, its slow convergence and its ambiguity in the solution. The strength of MCR-ALS is its capacity to resolve the pure underlying spectra and the ease with which different constraints can be applied. These constraints might assist in modelling and also decreasing the risk of ambiguities. These are defined as rotational, permutation and intensity, and causes problems because different combinations of concentration and spectral profiles can reproduce the data with the same fit value; hence the solutions are not unique. The most commonly applied constraints are non-negativity, uni-modality, closure and equality which are all realistic constraints for chemical systems observed by vibrational spectroscopy [14]. An alternative approach to minimize the risk of ambiguities is to use multi-set data by augmenting two different series that describes the same system under different conditions, e.g. different temperatures or pH values in kinetic reaction monitoring. In our industrial investigation we do not have this level of experimental control, but we can augment our data by combining two different membrane leaves of a different age or production/fouling history. The decomposition and interpretation of IR spectra in the analysis of UF membranes is however not a trivial task. Producers of the membrane cartridges modify the PES-basis by other chemicals in order to manipulate hydrophobicity, enhance the selectivity, increase the resistance to fouling, etc. - proprietary knowledge that is not available for the data analysis, which makes it an important and relevant unknown in the investigation. Protein residual fouling is also a collective name for a number of different functional groups. Constraints in MCR, in combination with interval selection and augmentation of data sets, can be useful in the exploratory investigation of UF systems. These ideas will be used in this work to elucidate chemical rank and absorption band identification in ATR-FT-IR measurements.

2 Material and Methods

One leaf from an UF membrane cartridge with a distinct history of use in a Danish dairy industry will be described in this investigation. The full membrane cartridge was cleaned according to CIP standards inside its industrial location/role prior to dismantling from its respective filtration unit operation/steel housing. It was kept in cold storage (approximately 5°C) before shipment and deconstruction at the University of Copenhagen. The leaf that is investigated is a KMS Food and Dairy UF elements, model 6338 HFK-328. This membrane cartridge has been used to produce so-called Whey Protein Concentrate WPC70. The membrane was placed in the eighth loop of a nine loop full-scale dairy plant, and had been in use for five months and three days of production plus cleaning cycles, further specifications in Table 1.

Table 1 – Membrane cartridge details

Membrane type	UF
Dimensions	
Diameter	6.3"/160 mm
Length	38"/965 mm
Spacer thickness	80mil/2.04 mm
No of leaves	7 x 2
App. leaf length ^{a)}	35"/900 mm
Membrane area ^{b)}	117ft ² /10.9 m ²
Serves Material	PES
Support Material	PE
Cut off	10 kilo Dalton
Product	70k whey
Loop	8
Tube	3
Age	5 months, 3 days
Size of sample coupon	100 x 100 mm
Number of coupons	4 x 5 = 20
Number of spectra	20 x 5 = 100
^{a)} Based on our observations/measurements made during cartridge dissection.	
^{b)} Based on specifications of the manufacturer.	

The main differences between sample coupons are expected to be associated with the position in the chosen leaf. In order to get representative pictures of residual fouling over the entire membrane surface area the leaf was sampled in the spatial fashion shown in Figure 1. The membrane cartridge is a standard spiral wound UF membrane. Each membrane leaf thus consists of an inner and an outer membrane layer that is glued together on the outskirts (like an envelope) creating a small inactive area with regards to filtration (Figure 1). Each leaf is separated by a retentate spacer and the two layers in a leaf are separated by a second, much finer, permeate spacer. The UF membrane cartridge from which the leaves were sampled consisted of seven such leaves. The leaves were cut from the center tube (as close to as was feasible), the inactive areas (glue lines) were removed and the leaves were saved for further investigation. This separation resulted in two layers termed inside layer and outside layer for each leaf of the membrane cartridge; for this investigation only the inside layer (physically closest to the center tube when wounded) was used. Each layer was sampled at five lanes of 100 mm width that are referred to as Distance From Feed (DFF) (see Figure 1), stretching from the feed inlet to the retentate and permeate outlet. In the second direction each membrane sheet is divided into four positions that will be referred to as Distance From Center (DFC), giving a total of twenty coupons of size 100×100 mm per leaf. All coupons were air dried for one hour on a table top (approximately 25°C) and were stored in containers in a refrigerator until further experimental work. The coupons were assumed to be the working unit despite considerable variations within each coupon (as can be anticipated from the inset in Figure 1). The residual fouling protein load is a sum of the CIP-persistent surface and internal fouling and our task is to find a semi-quantitative model to describe it.

An ultrafiltration membrane that never has been in use in production was also included in this investigation and will be referred to as a virgin membrane. The virgin membrane is produced by

Alfa Laval, type GR73PE. The membrane material is polyethersulfone (PES) similar to the membrane material in the used membrane cartridges. The membranes have been treated with glycerol prior to use (for shipment and preservation) and in order to avoid spectral interference it has been washed with RO water for 24h with a regularly change of water. After washing the membrane was dried for three hours at room temperature (approximately 25°C). No further sampling is performed and the membrane is regarded our working unit.

2.1 Spectroscopic analysis

Infrared spectroscopy (IR) can be used for identifying and quantifying molecules based on their vibrational modes. Due to its selection rules it is in particular sensitive to the functional side groups. To assist in the assignments virgin PES membrane and used PES membrane coupons were measured and compared. This gave rise to peaks that are specific to both the membrane material and the residual fouling deposits. The instrument used was a Fourier-transform infrared spectrometer (ABB Bomen Model 100, detector: DTGS Model SMH307AT) operated with a resolution of 8 cm⁻¹, averaging 32 scans over the spectral range 4000-700 cm⁻¹, interfaced with a attenuated total reflectance diamond probe (ATR; Durascope, SensIR Technologies) as IRE. Background spectra (empty interface) were measured with 32 scans at 8 cm⁻¹ resolution. It is important to consider the penetration depth and effective sampling area/volume of an ATR-FT-IR instrumental interfacing (Figure 2a). Our initial investigation used a multi-bounce ZnSe ATR crystal (length 70 mm), but the contact between the membrane samples and the interface was not sufficient and could not be improved to such a degree that acceptable and reproducible spectra were obtained. For this reason a diamond ATR crystal, applying a high and repeatable pressure, was selected (maintaining the same quantitative resistance/applied pressure settings on the ATR interface; arbitrary unit, level three). The price to pay for achieving a good contact is a very small

effective sampling area (the diamond service area is approx. 1.5 mm^2 , but the effective spot size of the bounce(s)/evanescent field is much smaller). The estimated penetration depth for the clean PES material is only approx. $2 \text{ }\mu\text{m}$ at 1450 cm^{-1} which strongly reduce the representativeness of the sampling procedure (Figure 2c). To reduce this statistical error each coupon was measured at five random positions. The virgin membrane was measured at 21 random positions to keep down the statistical error and to investigate if any changes could be observed across the membrane piece.

2.2 Data analysis

Since ATR-FT-IR spectra provide a fingerprint of the samples with multiple absorbance bands, some arising from the membrane material and some due to the fouling material, it is essential to ensure that the peaks investigated and quantified are correctly identified. This is especially important and challenging since membrane manufactures use tailored versions of the polymer-basis, and minor modifying agents inside the membrane material might interfere with the fouling signals. The raw spectra were first evaluated by computing the correlation between a known material peak and the peaks of interest, where an opposite correlation is expected between the membrane material (PES in this case) and the investigated fouling peak (the amide band), see Figure 3. The peaks of interest are specific regions of the spectrum that are known to be influenced by the residual fouling constituents (Table 2): the *fat band* (carbonyl C=O stretching in triglycerides) near 1745 cm^{-1} , the free fatty acid band (carbonyl stretching in free fatty acids) near 1720 cm^{-1} , the amide I band (carbonyl C=O stretching in amides) near 1650 cm^{-1} and the amide II band (N–H bend and C–N stretch) near 1550 cm^{-1} (Figure 3b). The material peak for the PES ultrafiltration membranes is chosen to be the one centered at 1240 cm^{-1} which arises from the asymmetric stretch of the aromatic ether in the polyethersulfone (Figure 3b; Table 2). This is the most commonly used PES membrane band in literature [18].

Table 2 – The most common peaks from PES and the residual fouling found in the IR spectrum.

Wavenumber (cm ⁻¹)	Conformation	PES	Fouling
825-875	C-H out of plane bend		✓
1100	C-O stretch	✓	
1150	C-O stretch	✓	
1240	asymmetric stretch of the aromatic ether	✓	
1300	C-O stretch	✓	
1325	C-O stretch	✓	
1475	C-H bend	✓	
1650-1657	α -helix		✓
1510-1530 1612-1640 1670-1690 (weak)	β -sheet (anti-parallel)		✓
1530-1550 1626-1640	β -sheet (parallel)		✓
1655-1675 1680-1696	Turn (secondary structure β -lactoglobulin/other proteins)		✓
1640-1651	Unordered (not complying with above conformations)		✓
1745	C=O stretch		✓
2700-3000	C-H stretch	✓	✓
3300-3500	O-H stretch		✓

As Figure 3a shows there is a good opposite correlation between peaks corresponding to protein and membrane material. This gives a strong indication that the peaks are from two different sources. The area around the *fat peak* (found in the same region where a dominant PE band is observed) exhibits a weak correlation which indicates that the fat information does not correlate chemically with the remaining components. The amide I peak is separated into two parts, one affected by the residual fouling and one by the membrane material. When inspecting the correlation between 1630 cm⁻¹ and 1240 cm⁻¹ it is obvious that this section of the spectra arises from residual fouling as it has an opposite correlation with 1240 cm⁻¹ (Figure 3a). On the other hand, when inspecting the correlation between 1675 cm⁻¹ and 1240 cm⁻¹, it is clear that there is a correlation and hence that

this part of the peak most likely originates from the membrane material (Figure 3c). The correlation is possibly due to a chemical compound that has been grafted to the membrane, in order to change the hydrophobicity. PES membranes are traditionally hydrophobic, but hydrophilicity is a desired functionality of a filtration membrane, as this will make the flow in the lateral direction less obstructed. There are different compounds that can alter the hydrophobicity of the membrane. Ran et al. [19] for example have demonstrated that comb-like amphiphilic copolymers (CLACs) can make the membrane more hydrophilic. The PES membrane and the PES-CLAC grafted membrane exhibit approximately the same IR spectrum except from one peak at 1676 cm^{-1} that originates from carbonyl groups. The presence of an *unexplained* peak at exactly this position could indicate that our membrane has been grafted with CLAC, but in this study this will remain a speculation as the grafting compound is unknown to the authors and not our primary interest.

The membrane consists of two layers beside the fouling layer; the active PES layer and a much thicker support polyester (PE) layer (Figure 2a). To ensure that the penetration of the evanescent wave had not reached the support material, which could possibly affect the spectra and thereby the interpretation of the models, the support material (the back side of a used membrane) was measured under the same circumstances as the fouled membrane. The result is included in Figure 3b and shows no evidence of a PE contribution in the PES-plus-fouling ATR-FT-IR spectra.

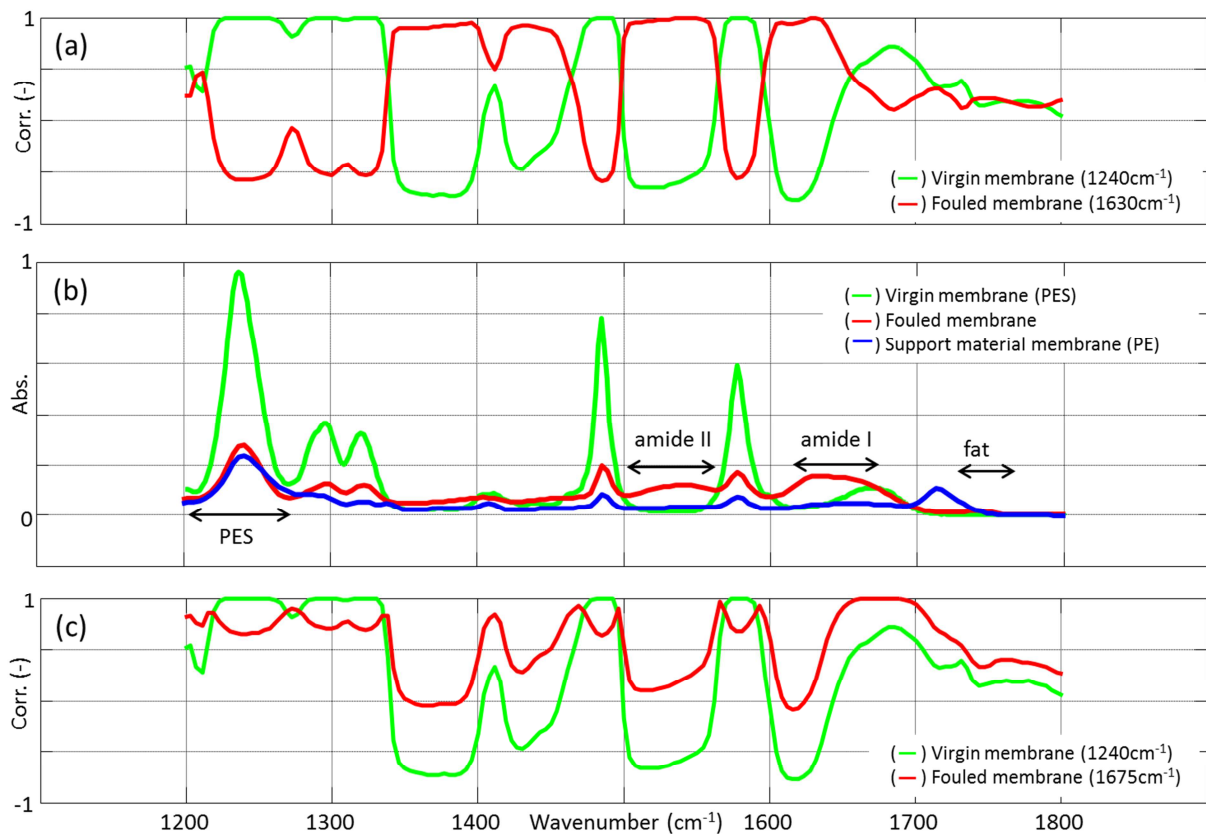


Figure 3 – Correlation ($N = 100$) over the spectral range 1200-1800 cm^{-1} with (a) absorption maximum at 1240 cm^{-1} (attributed to PES) and absorption maximum at 1630 cm^{-1} (attributed to protein-based residual fouling); (b) spectra of virgin membrane, fouled membrane and support material (PE); (c) correlation ($N = 100$) over the spectral range 1200-1800 cm^{-1} with absorption maximum at 1240 cm^{-1} (attributed to PES) and absorption maximum 1675 cm^{-1} (possibly attributed to CLAC).

As can be judged from Figure 3b, the spectra exhibit some moderate baseline artifacts, likely due to varying contact between the IRE and membrane material due to the spacer relief (see Figure 1). Although the variation is minimal compared to variation that exists in the spectral information, it was decided to remove the baseline (more accurate, offset) by subtracting the value recorded at 1800 cm^{-1} from each full spectrum, individually. This point is chosen because no spectral

information is present there. Using Figure 3b as guideline we also decided to narrow the spectral range from 1470 cm^{-1} to 1800 cm^{-1} throughout the investigation since this part of the ATR-FT-IR contains a strong signal from the PES membrane material, the most fundamental vibrations of the different protein building block and the carbonyl stretch of the fat.

Firstly the data was investigated with principal component analysis (PCA) in order to obtain the approximate number of components that are needed to describe the systematic variation. The data set is mean centered with no further preprocessing. In the main investigation multivariate curve resolution (MCR) is utilized to extract spectroscopic-meaningful information. In order to optimize the interpretation and decrease the risk of ambiguities in MCR modelling, constraints such as non-negativity (spectral/concentration profiles should not be below zero) and equality constraint (where the pure spectra of the PES is added as a loading/factor) were applied both on a *trial and error* basis but also based on previous knowledge and chemical understanding. All computations are performed in Matlab (R2014a, Mathworks Inc.) using the Matlab PLS Toolbox (version 7.5, Eigenvector Research Inc.) and in-house routines. Initializing the MCR algorithm requires a starting estimate of the model parameters and choosing an appropriate method can be crucial as differences in the initial estimates may lead to different end results, and hence to a different interpretation of the outcomes. The Matlab PLS Toolbox provides two methods for calculating the initial estimates: *distslct* which selects samples on the exterior of a data space based on a Euclidian distance and *exteriorpts* which selects points on the exterior of a normalized data space. They are both considered SIMPLISMA methods as they reduce the spectra to points in a data cloud, and by calculating the average it is possible to determine the sought after spectra that are more dissimilar being the data points that are positioned furthest away. For this investigation we have used *exteriorpts* and using the purest samples as the initialization.

3 Results and Discussion

The PCA performed on the range 1470-1710 cm^{-1} showed that two components were needed to describe the data, one component describing the contribution from the membrane material and one component describing the protein deposit from the residual fouling (Figure 4).

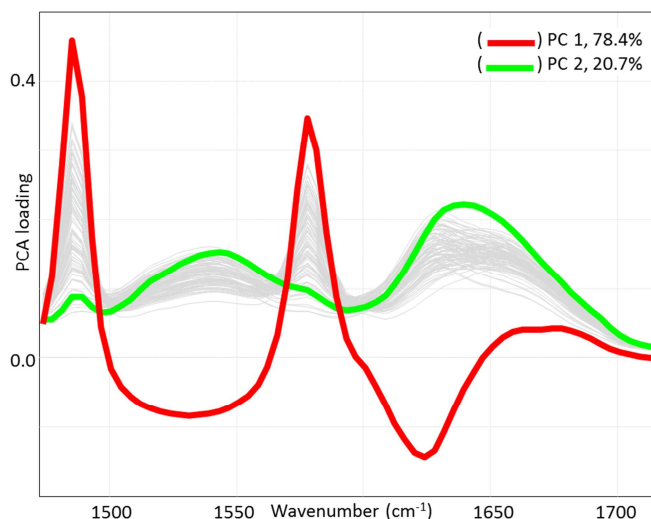


Figure 4 – Principal component analysis. Loading plot of the two first principal components (N=100). Data is mean centered.

It is well established that the amide I band (1600-1700 cm^{-1}) is sensitive to the protein secondary structure and it can thus be used to investigate the secondary structure of the protein deposit found on the UF membranes. Theoretically, it should be possible to determine α -helix, β -sheet (parallel and antiparallel), turns and unordered conformation at particular wavenumber ranges (Table 2) [20].

From the PCA calculations it is interpreted that at least two components are required to describe the system adequately. As mentioned previously the membrane samples consist of two layers of material, PES and fouling deposit consisting of mainly protein, minimal amounts of fat and minerals. From Figure 3a it was established that there is an opposite correlation between PES peaks

and the protein peaks from the residual fouling. However, the peaks from the two materials do not vary independently as the protein layer *shadows* the membrane material, thereby influencing the contribution from the PES in the spectra. Nevertheless, it can be argued that two components are suitable for the modelling: one factor to describe the membrane material, and a second to describe the fouling material. The PCA model captures the two factors in a crude, descriptive manner which is obvious from the second component in Figure 4 where next to the potential grafting material (possibly CLAC) a part of the *bi-modal* amide I band is modeled simultaneously. From simple analysis it is obvious that a different method than PCA needs to be applied to extract all relevant information from the data.

The MCR data analysis was conducted in several steps in order to ensure that the correct constraints are applied and that the correct number of factors are included in the model. Determining the number of factors that is appropriate to describe the data can be challenging in MCR. A first estimate of the number of factors can be derived from both forward and backwards evolving factor analysis [21], but our results were equivocal and a clear number of factors could not be derived. Determination of the chemical rank of the system, which corresponds to the number of factors, was instead evaluated by inspecting the spectra and by using *a priori* knowledge. For this purpose MCR models of different complexity were fitted on the spectral loadings and the concentration profiles using the data range 1470-1710 cm^{-1} . Table 3 shows how the relative amount of explained variance evolves when increasing the number of MCR factors in the model. The percentage of variation explained alone is not sufficient to evaluate which model is better and the spectral profile plots of the models have to be investigated and evaluated simultaneously (Figure 5a, b).

Table 3 – Multivariate Curve Resolution. Percent variation explained with two, three and four factor MCR models (N=100). Spectral range is 1470-1710 cm^{-1} . Non-negativity constraint is imposed on the spectral loadings and concentration profiles.

No. of components \ Component	2	3	4
1	44.7%	52.6%	63.1%
2	55.3%	8.9%	7.0%
3	-	38.5%	19.8%
4	-	-	10.2%

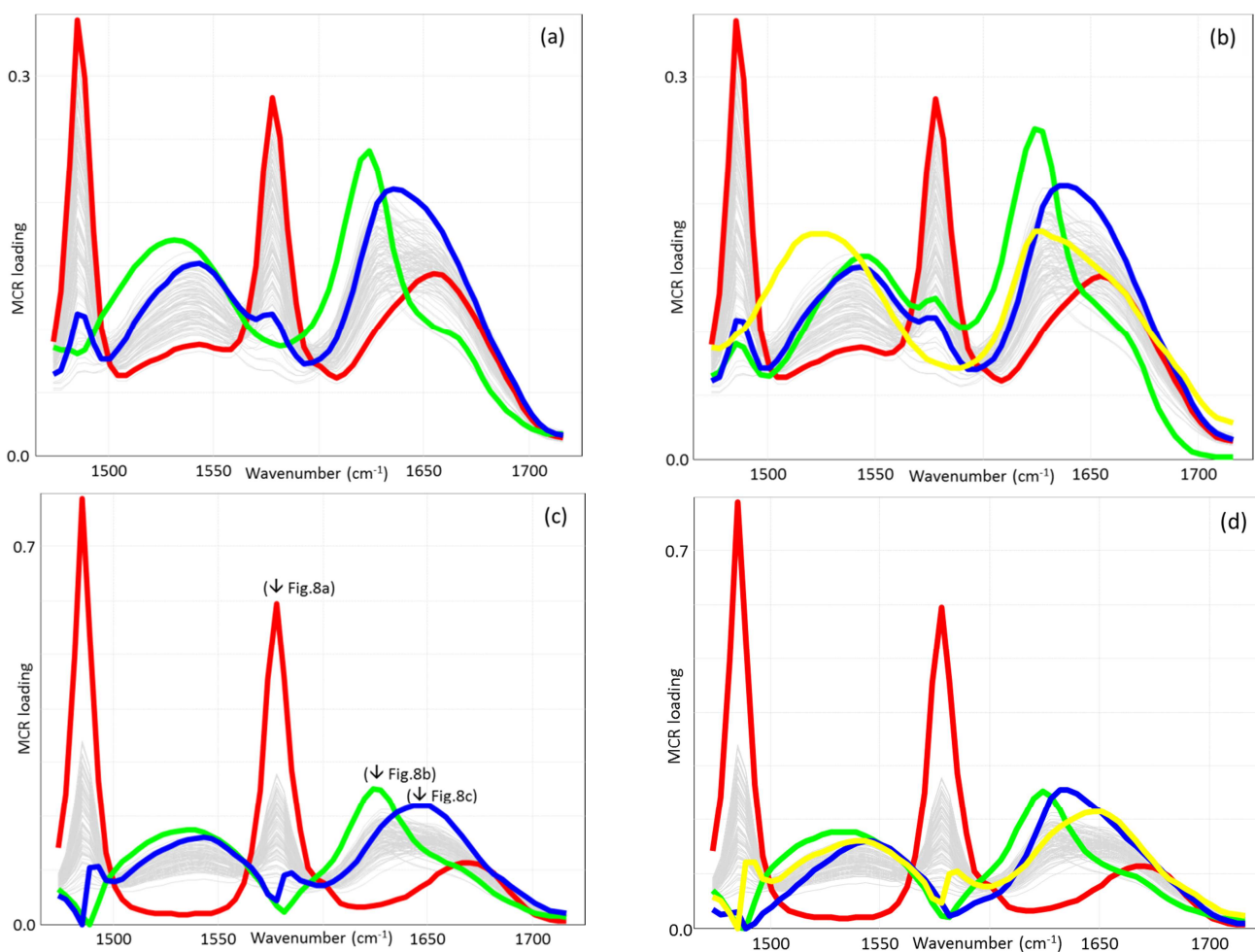


Figure 5 – Multivariate Curve Resolution. MCR models (N=100) with (a) three and (b) four factors, non-negativity; with (c) three and (d) four factors, non-negativity, equality constraint (PES loading).

By simple inspection of Figures 5a and 5b it remains challenging to determine the correct number of factors (three or four) to model this range. It can be observed in the figure that some of the peaks in the protein ranges behave differently from the normal Gaussian/Lorentzian profiles. It is further observed from Figure 5b that the PES related spectral loading stills models a wide range of the band associated with the amide (around 1660 cm^{-1}). In order to investigate this covariation into more detail one additional constraint is added. Membrane material (PES) that has a comparable structure (but potentially not 100% the original membrane due to vendor differences) has been measured under the same conditions as the fouled membranes and can be used as an equality constraint on the spectral loadings. This will force one of the MCR model factors to resemble the membrane material and the remaining factors are then forced to model the remaining features in the spectra (Figure 5c,d). The models containing the equality constraint exhibit improved loadings with regards to both three and four factors. The peak shapes of the MCR loadings now appear more natural Gaussian-like and the amide I band is split into three underlying peaks. At the same time we notice some weak artifacts underneath the PES peaks, possibly a consequence of the forced equality constraint with a not entirely identical membrane.

Investigation of the data shows that there is a difference in rank over the full spectrum. The two amide sections describe different structures of the residual protein; amide I ($1600\text{-}1700\text{ cm}^{-1}$) describes the secondary structure in the protein and has hidden below it the water bending band at 1640 cm^{-1} and the CLAC-like band at 1670 cm^{-1} , while the amide II band ($1500\text{-}1550\text{ cm}^{-1}$) section has fewer underlying peaks and mostly describes the antiparallel β -sheet structure at $1510\text{-}1530\text{ cm}^{-1}$ and the parallel β -sheet structure found at $1530\text{-}1550\text{ cm}^{-1}$. An MCR analysis of the amide II alone (Figure 6a) reveal that only two factors are needed to describe this range, one for the membrane

material and one for the residual fouling. The secondary structure information from this band seems to be towards higher wavenumbers i.e. more parallel β -sheet structure. The amide I range includes more individual structures and therefore at least three factors are required to model that specific section of the spectrum (Figure 6b). The model including three factors appears to be the most realistic as it exhibits the most natural peak shapes. It should be noted that such differences in rank across parts of the spectrum might give rise to overfitting and to difficulties in determining the appropriate rank of the system. Finally, the fat range - 1710-1770 cm^{-1} , Figure 6c - was included in the MCR modelling. This could potentially lead to an increase in rank because fat is an independent minor component in the residual fouling layer that does not correlate with the remaining peaks (Figure 3a). However this was not found to be the case as the factor that describe the amide peaks also describe the fat peak which indicate that the fat fouling does not occur independently from the protein fouling

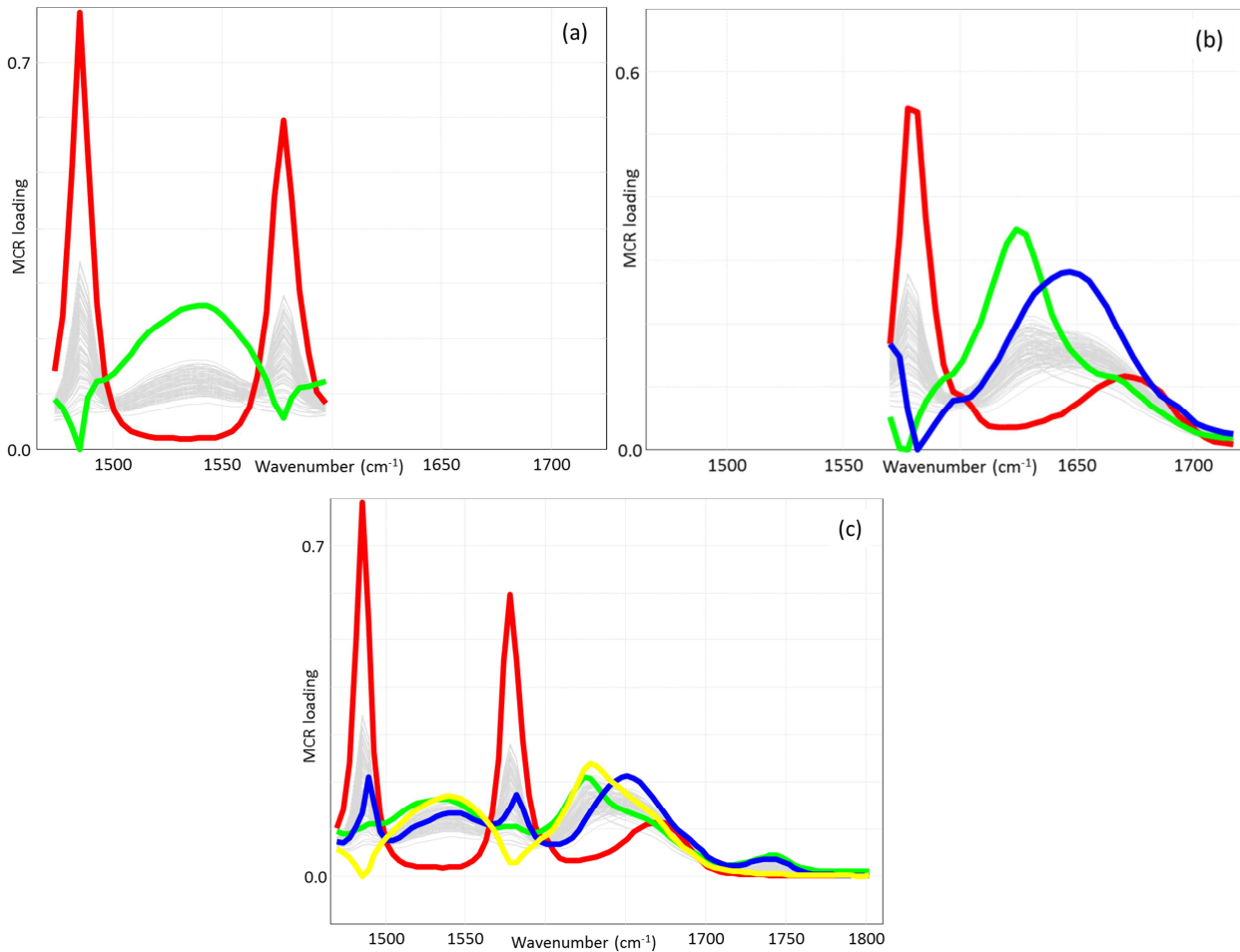


Figure 6 – MCR models (N=100) with (a) two factors for 1470-1600 cm^{-1} , (b) three factors for 1570-1710 cm^{-1} and (c) four factors for 1470-1800 cm^{-1} . All models use non-negativity and equality constraint (PES loading).

From the above it is obvious that the data contains several components that co-vary with different degrees (residual bound-moisture, fat, protein, PES and PES grafting) but also components used for grafting (CLAC's) would prove difficult to identify by utilizing only univariate data analysis. MCR often exhibits uniqueness challenges where the lack of uniqueness arises from the intrinsic ambiguities of different combinations of concentration and spectral profiles reproducing the original data with the same quality of fit. The most common way to avoid these ambiguities is by adding appropriate constraints in one or both directions, but at the same time these constraints can result in

overfitting and spurious interpretations. An alternate strategy is to merge a second data set with the original data set. The second data set has to describe the same problem from another viewpoint; this can be e.g. a different instrumental method (e.g. Raman spectra) or a different set of samples that has been produced under the same circumstances and describes the same issue such as a reaction with the same kinetics run e.g. at a different concentration [14]. In our investigation a large number of spiral wound ultrafiltration membrane have been sampled. One membrane originates from the same factory, but a different whey processing line and it has been in use for a longer period (2 years, 3 months). It can thus be anticipated that both aspects will make the residual fouling of the two UF membranes systems sufficiently different yet compatible. There are some dimensional differences between the two membrane cartridges, but nothing that is suspected to affect the residual fouling dramatically. This makes it possible to unite the two data sets to form one multi-set structure for further analysis. Figure 7a shows the two superimposed data sets illustrating that they indeed have the same chemical finger print, but different intensities (concentrations). The combined data set was then investigated without the equality constraint as the concatenated data set should eliminate the possibility of ambiguities. Thus only non-negativity is added in both the spectral loadings and the concentration profiles as it does not make sense for them to show negative values.

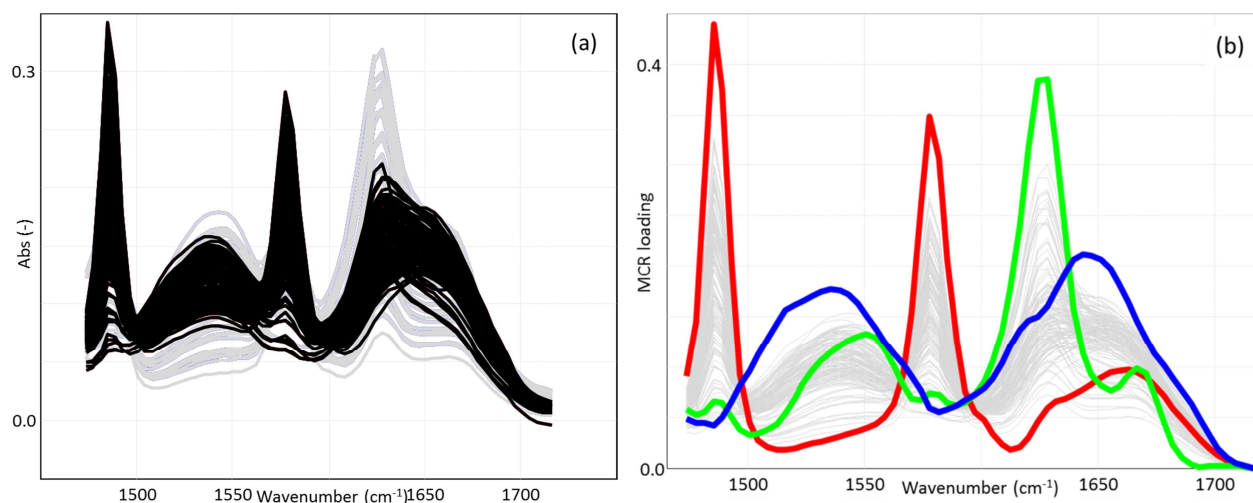


Figure 7 – The combined data set. (a) Data from two UF membrane systems: main data set ($N = 100$) and the assisting data set ($N = 36$); (b) MCR models ($N=136$) with two data blocks with three factors non-negativity.

The data set in the range $1470\text{-}1710\text{ cm}^{-1}$ was initially investigated with three factors included in the model (Figure 7b). However, parts of the loadings in the model exhibit non-Gaussian/non-Lorentzian/bi-modal shapes and in general this exercise did not improve the interpretation of the data. It turned out that the two different data sets and residual fouling UF membranes are too distinct to concatenate and analyze simultaneously. The same conclusion was reached with other data sets from different membrane systems.

Based on the loading results it was concluded that the most optimal number of factors is three, with non-negativity constraints applied in both the spectral and concentration direction, and an equality constraint applied to the first loading forcing it to resemble the virgin membrane known to be present in the samples (Figure 5c). Using the concentration profiles a polynomial surface response model for the three individual contributions is estimated:

$$c_i = b_0 + b_1\mathbf{DFF} + b_2\mathbf{DFC} + b_3\mathbf{DFF}^2 + b_4\mathbf{DFC}^2 + e_i \quad (3)$$

The concentration contour profiles in Figure 8 for the rank three model, estimating the composition over the membrane sheet area (see Figure 1), show how the two layers in the membrane and fouling system affects each other. The first score profile in Figure 8a originates from the membrane material (PES). The second score, shown in Figure 8b, contains information on the fouling layer, specifically the proteins, and shows the complete opposite behavior of the PES profile giving us evidence that it is indeed fouling material. The third score (Figure 5c) is shown in Figure 8c to have a less distinct profile in the Distance From Feed (DFF) direction, and a trend of higher scores (concentrations) as a function of distance from center tube (DFC). Where Figure 8a and 8b are essentially *counter images* which corresponds well with the notion higher residual fouling load equals less PES membrane material visible for the ATR-FT-IR, Figure 8c suggests that there is a relative higher residual fouling for a selected protein set at the edge of the membrane envelope, away from the central tube of the cartridge. The variation in the samples for each coupon is large which indicates an inhomogeneity in the samples which is consistent with the picture shown in Figure 1. There is an obvious large inhomogeneity in the individual coupons that originates from the pattern observed in the membrane; the concentrations shift over the membrane area but also considerable differences in concentration are caused where the spacers have been *rubbing* against the membrane.

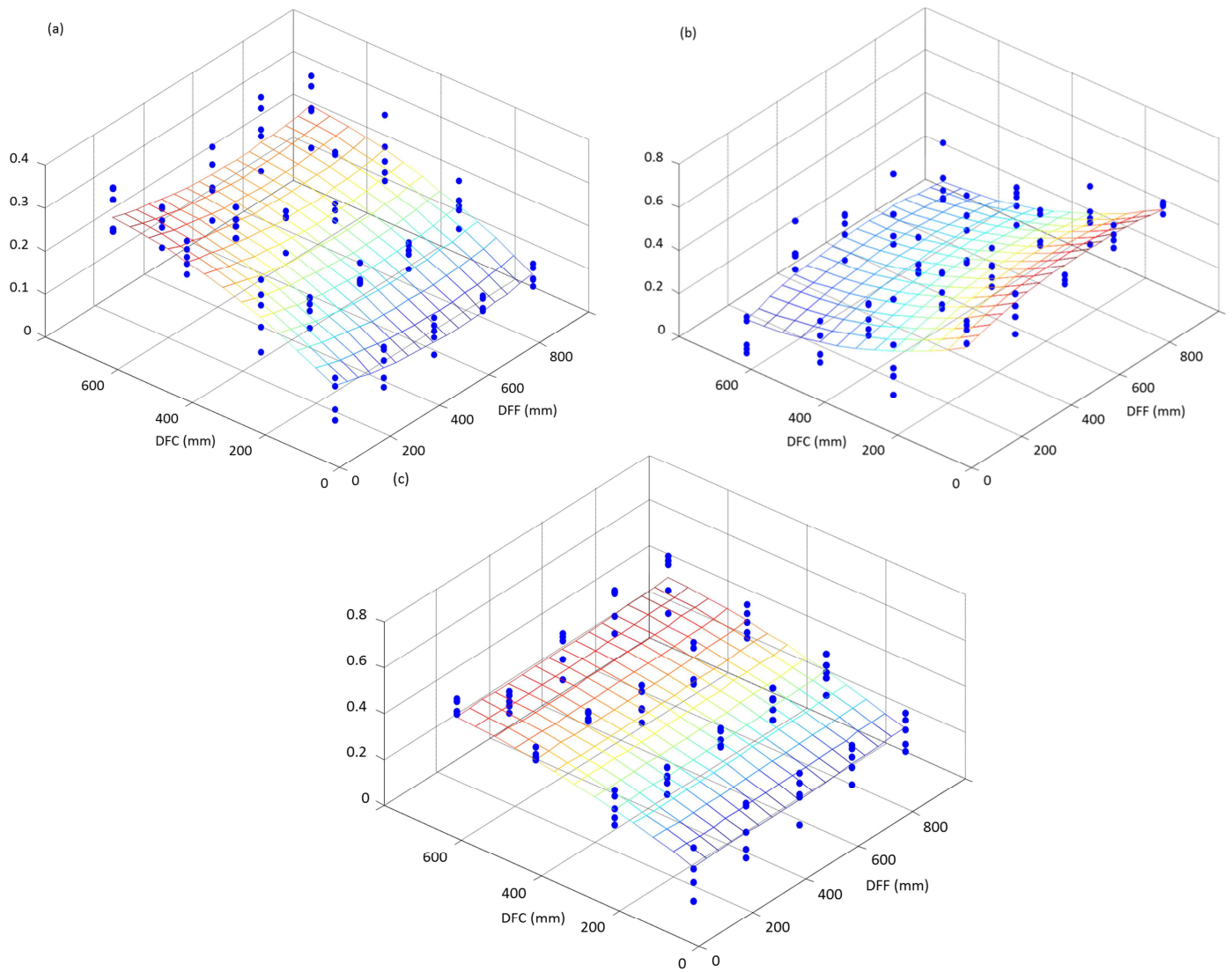


Figure 8 – MCR models (N=100). Contour plots of the scores from model made with data range 1470-1710 cm^{-1} , non-negativity constraint is applied in both directions and equality constraint is applied to the loadings (Figure 5c); (a) score 1, $R^2 = 65.0\%$; (b) score 2, $R^2 = 66.7\%$; (c) score 3, $R^2 = 53.6\%$.

4 Conclusions

When using traditional methods to describe an ultrafiltration membrane with IR it is common practice to calculate and use the height of the peak of interest. This is a tedious and sometimes

impossible method if you want information on several peaks. This study has shown that e.g. the amide I peak region contains several absorption bands besides the most common mentioned ones from Table 2. In the same region adsorbed water is present at 1640 cm^{-1} if the membrane had not been properly dried, but also possible evidence of CLAC is found around 1676 cm^{-1} which indicates that the membrane might have been subjected to grafting. The variation of absorption bands found under the amide I peak makes this peak difficult to investigate with univariate methods wherefore mostly the amide II is investigated in the literature using simple quantification methods. This problem can be solved by using multivariate methods such as PCA or MCR as these methods *average out* the insignificant features of a spectrum and enhances the important/*principal* ones. MCR finds and models the important factors resulting in an overview of several different peaks/loadings that describe the major different trends and has proved useful for this investigation to describe the residual fouling. In this study the underlying secondary structure information of the amide peaks has not been useful since no variation in protein secondary structure was observed. Nevertheless, an intrinsic rank difference was observed for the two amide sections (amide I; $1600\text{-}1700\text{ cm}^{-1}$, amide II; $1500\text{-}1550\text{ cm}^{-1}$) resulting in two choices for optimal factors: three factors are required to describe amide I plus membrane material while two factors are sufficient to describe the amide II region. This is another argument why (univariate) investigations of protein on ultrafiltration membranes are regularly performed on the amide II peak. Applying MCR to the ATR-FT-IR data has aided in determining several peaks in one calculation, identifying at the same time determine peaks that has not previously been described. The issue with the many co-varying components is overcome by applying MCR as it ensures that only the amide peaks are used in quantification. Using MCR we get an overview of the full fouling aspect and the potential pitfalls that are encountered with the ATR-FT-IR-method usually encompassed for this type of research.

5 Acknowledgement

The Danish Council for Strategic Research and the Danish Dairy Research Foundation is acknowledged for generous financial support to the project entitled *Applying PAT for optimization of water management* under the inSPIRe (Danish Industry–Science Partnership for Innovation and Research in Food Science) consortium (Copenhagen, Denmark).

6 References

- [1] T.H.A. Berg, J.C. Knudsen, R. Ipsen, F.W.J. van den Berg, H.H. Holst, A. Tolkach, Investigation of consecutive fouling and cleaning cycles of ultrafiltration membranes used for whey processing, *International Journal of Food Engineering*, accepted for publication (2014)
- [2] G. Brans, C.G.P.H. Schroën, R.G.M. van der Sman, R.M. Boom, Membrane fractionation of milk: state of the art and challenges, *Journal of Membrane Science* 243 (2004) 263-272
- [3] L. Bégoïn, M. Rabillier-Baudry, B. Chaufer, C. Faille, P. Blanpain-Avet, T. Bénézech, T. Doneva, Methodology of analysis of a spiral-wound module. Application to PES membrane for ultrafiltration of skimmed milk, *Desalination* 192 (2006b) 40-53
- [4] J. Kiefer, N.H. Rasul, P.K. Ghosh, E. von Lieres, Surface and bulk porosity mapping of polymer membranes using infrared spectroscopy, *Journal of Membrane Science* 452 (2014) 152-156
- [5] M. Rabiller-Baudry, M. Le Maux, B. Chaufer, L. Bégoïn, Characterisation of cleaned and fouled membrane by ATR-FTIR and EDX analysis coupled with SEM: application to UF of skimmed milk with PES membrane, *Desalination* 146 (2002) 123-128

- [6] S. Belfer, J. Gilron, O. Kedem, Characterization of commercial RO and UF modified and fouled membranes by means of ATR/FTIR, *Desalination* 124 (1999) 175-180
- [7] J. Schwinge, P.R. Neal, D.E. Wiley, D.F. Fletcher, A.G. Fane, Spiral wound modules and spacers; Review and analysis, *Journal of Membrane Science* 242 (2004) 129-153
- [8] J.M. Chalmers, P.R. Griffiths, *Handbook of Vibrational spectroscopy, Sampling Techniques*, volume 2, John Wiley & sons, LTD, 2002
- [9] J. Fontanella, R.L. Johnston, J.H. Colwell, C. Andeen, Temperature and pressure variation of the refractive index in diamond, *Applied Optics* 16(11) (1977) 2949-2951
- [10] R. Bauer, C. Rischel, S. Hansen, L. Øgendal, Heat-induced gelation of whey protein at high Ph studied by combined UV spectroscopy and refractive index measurement after size exclusion chromatography and by *in-situ* dynamic light scattering, *International Journal of Food Science and Technology* 34 (1999) 557-563
- [11] K. Kuriki, O. Shapira, S.D. Hart, G. Benoit, Y. Kuriki, J.F. Viens, M. Bayindir, J.D. Joannopoulos, Y. Fink, Hollow multilayer photonic bandgap fibers for NIR applications, *Optic Express* 12(8) (2004) 1510-1517
- [12] F.M. Mirabella, *Internal Reflection Spectroscopy: Theory and Applications*, CRC Press, 1992

- [13] W.H. Lawton, E.A. Sylvestre, Self Modeling Curve Resolution, *Technometrics*, 13(3) (1971), 617-633
- [14] A. de Juan, J. Jaumot, R. Tauler, Multivariate Curve Resolution (MCR), Solving the mixture analysis problem, *Analytical Methods* 6 (2014) 4964-4976
- [15] J. Jaumot, R. Gargallo, R. Tauler, Noise propagation and error estimation in multivariate curve resolution alternating least squares using resampling methods, *Journal of Chemometrics* 18 (2004) 327-340
- [16] M. Maeder, Evolving Factor Analysis for the Resolution of Overlapping Chromatographic Peaks, *Analytical Chemistry*, 59(3) (1987) 527-530
- [17] W. Windig, J. Guilment, Interactive Self-modelling Mixture Analysis, *Analytical Chemistry* 63 (1991) 1425-1432
- [18] L. Bégoïn, M. Rabiller-Baudry, B. Chaufer, M. Hautbois, T. Doneva, Ageing of PES industrial spiral-wound membranes in acid whey ultrafiltration, *Desalination* 192 (2006a) 25-39
- [19] F. Ran, X. Niu, H. Song, C. Cheng, W. Zhao, S. Nie, L. Wang, A. Yang, S. Sun, C. Zhao, Toward a highly hemocompatible membrane for blood purification via a physical blend of miscible comb-like amphiphilic copolymers, *Biomaterials Science* 2 (2014) 538-547

[20] J. T. Pelton, L. R. McLean, Spectroscopic Methods for Analysis of Protein Secondary Structure, *Analytical Biochemistry* 277 (2000) 167-176

[21] H.R. Keller, D.L. Massart, Evolving factor analysis, *Chemometrics and Intelligent Laboratory Systems* 12 (1992) 209-224

Paper III

J.K. Jensen, S.B. Engelsen, F. van den Berg

Review of ATR FI-IR as Investigative Tool and Quantitative
Method for Protein in Membrane Separation Systems

In preparation, intended for Journal of Applied Spectroscopy

Review of ATR FT-IR as Investigative Tool and Quantitative Method for Protein Fouling in Membrane Separation Systems

Jannie K. Jensen^{*}, Søren B. Engelsen, Frans van den Berg
University of Copenhagen, Faculty of Science, Department of Food Science, Spectroscopy & Chemometrics, Rolighedsvej 26, DK-1958 Frederiksberg C, Denmark

* Corresponding author: janniekj@food.ku.dk, +45 2272 4748

Abstract

The use of Attenuated-Total-Reflectance Fourier-Transform Infrared spectroscopy (ATR FT-IR) is a common tool for measuring (residual-)fouling on filtration membranes of different origin and purpose. This review aims at giving an overview of the numerous qualitative and quantitative investigations of membrane fouling made using ATR FT-IR with special emphasis on the following data analysis. The timespan of this review is from 1990 up to 2015 and it will cover the implementation of data analysis within the membrane investigations, where the most common way of using ATR FT-IR is for identification. The methods used to analyze the membranes are the result of the complex construction of not only the materials forming the membrane systems, but also the fouling and the cleaning, and even the geometry and flow in the membrane unit operations and the resulting fouling distribution. This review gives an overview of the different analytical methods used and will illustrate that the application of multivariate data analysis and large scale sampling can be very informative and beneficial. The review further stresses that there is a considerable gap between most research conducted in laboratory/pilot-scale and full-scale industrial investigations.

Introduction

Membrane filtration is a relatively new but growing (Holst et al, 2015) unit operation in the dairy industry, other food processors, medical product manufactures and water filtration industry (Wagner, 2001). The processes are used in a wide variety of separation and concentration steps and a major challenge is membrane fouling by proteins and other biomolecules from the feed streams. This demands regularly cleaning of the membranes to remove both the foulants deposited on the surface and/or inside the membrane material (Regula et al., 2014). Cleaning is a vital step in maintaining the permeability and selectivity of the membrane which in the end should lead to a plant that runs at almost optimal capacity throughout the production time, while at the same time

minimize risk of bacterial contamination - of utmost important to make a safe product and maintaining quality standards (Regula et al., 2014).

The cleaning performed at e.g. a full scale dairy filtration operation is complex and involves several consecutive steps. It is a Cleaning-In-Place (CIP) which infers that the membranes remain in their position (most often in the form of a Spirally Wounded Membrane Cartridge, SWMC) while all cleaning agents are pumped through the system. The CIP thus requires a lot of clean potable water, large volumes of several types of costly chemicals and formulations and, most importantly, a lot of time (6 or 7 hours of downtime is not uncommon) (Berg et al, 2014). The chemicals are almost always supplied by specialized companies with no (direct) relation to the dairy, and often these companies are involved in designing CIP programs (in cooperation with the equipment/hardware vendors and dairy managers). During downtime obviously no product is produced which makes cleaning an expensive, but unavoidable facet of membrane management. Cleaning in dairies is required approximately every 24 hours due to a rise in pressure in the membrane cartridges caused by the pores getting blocked with, mostly, protein but also fat and minerals buildup, plus for hygienic reasons. Taking all economic aspects into account it is of great importance to gain increased knowledge on the membranes, the fouling of the membranes as well as the cleaning that can aid in saving large sums of money. This financial interest explains the relative large number of researchers active in the area of membrane cleaning.

Reducing the downtime is the goal of many investigators and in order to achieve that the mechanisms of fouling and the interaction between fouling material and the membranes has to be better understood. To be able to control the parameters involved in the CIP process, it is useful to know where the adsorption primarily takes place during the filtration process (Pihlajamäki et al., 1998). To improve and optimize the CIP methods a better understanding of the analytical data recorded from the used membrane is also essential. Currently most of such data is used for identification of the foulants, residual fouling, membrane material, and grafting material. Only few studies are conducted on production size membranes to gain further knowledge on the mechanisms during fouling and cleaning. Many different data analytical techniques have been used to investigate different types of membrane related questions, but common for most of them is that they are analyzed with univariate data statistics and focused on the identification of functional groups. The use of chemometrics and multivariate data tools has the potential to augment the outcome of the

results when using spectroscopic methods. Minute differences in spectra or spectral regions are difficult to differentiate with the human eye and therefore a more data-driven tool can assist in emphasizing the important features of the investigation. The most common tools for extracting knowledge with regards to relative concentration are non-linear regression (Massart et al., 1997) and possibly multi curve resolution (MCR) (A. de Juan et al., 2014). The more visual tools are principal component analysis (PCA) (Bro & Smilde, 2014) for retrieving an overview of samples, finding outliers and clustering data. For determination of concentrations a partial least squares (PLS) regression is useful (Wold et al., 2001), while for classification of different samples e.g. soft independent of class analogy (SIMCA) can be used (Wold & Sjöström, 1977).

ATR FT-IR in membrane fouling research

Infrared spectroscopy is the direct absorption method for measuring molecular vibration and is a generally employed analytical method. The method builds on the fact that all molecules exhibit molecular vibrations and that they do it at their own specific frequencies. Infrared spectroscopy can be used for both identifying and quantifying molecules based on their vibrational modes. ATR FT-IR is a powerful tool in membrane investigations because it can aid in understanding the molecular compositions of many types of materials and foulants. It is a nondestructive method (at least at the analytical chemistry level) and can measure all (IR-active) components in the sample within the same spectrum. It is thus an intrinsically multivariate method offering the opportunity to use more complex mathematical/chemometric tools to explore and extract information.

IR is intrinsically difficult to measure due to the high absorbance levels of condensed materials, but this problem was largely solved when attenuated total reflectance was introduced. ATR offers an alternative solution to the sampling problems with ultra-thin liquid cells and sample dilution in KBr tablets. With the advent of the ATR sampling device all sample types including solid samples such as membranes can be placed directly on the IR-device under the condition of sufficient contact between the sample and ATR cell. This is important because the light penetration depends on the contact, the geometry of the optical device as well as the light properties of the sample (Lin et al., 2009). ATR spectroscopy requires total internal reflection and this happens when radiation moves through a material with high refractive index n_1 and impacts the interface with a material with a lower refractive index n_2 at an angle greater than the critical angle (Chalmers & Griffiths, 2002).

Sometimes it is necessary to take a third refractive index (n_3) into consideration; this is particularly important if you have inhomogeneous sample material (Figure 1).

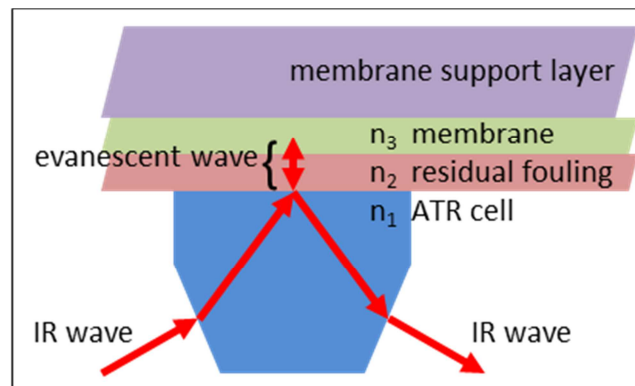


Figure 1 – Schematic overview of the breaking indices when measuring membrane samples by ATR FT-IR.

When working with inhomogeneous samples or, as in the case with membranes that are layered samples, quantification in ATR FT-IR might become a problem due to the large variations that are seen over a full membrane area. This issue is easily recognized in Figure 2a which shows the four corners of one membrane leaf (~965x900 mm) from a SWMC used whey ultrafiltration (Jensen et al., 2015a). The IR spectra shown in Figure 2c describe the inhomogeneity within one sample coupon (100x100 mm). The visual distortions from an originally flat sheet originate from the deformations caused by the retentate spacers imprinted over time, while the different levels of residual fouling originate from a difference in accessibility during production and cleaning. Figure 2b shows the spectral differences between the four leaf corners in Figure 2a where an obvious intensity difference is present, but also a slight shift is seen in the amide peaks.

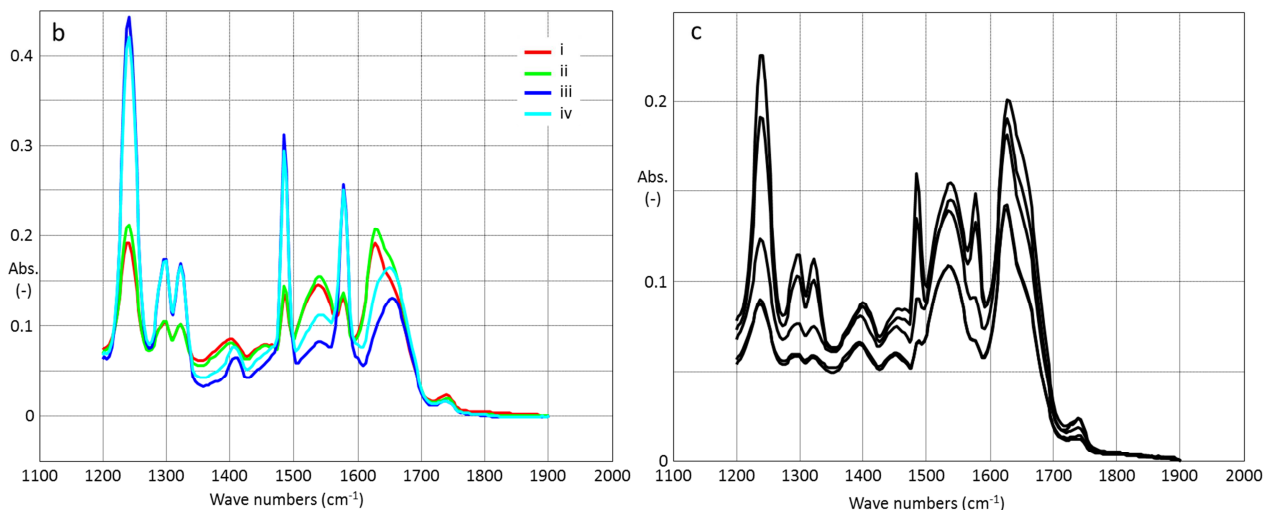
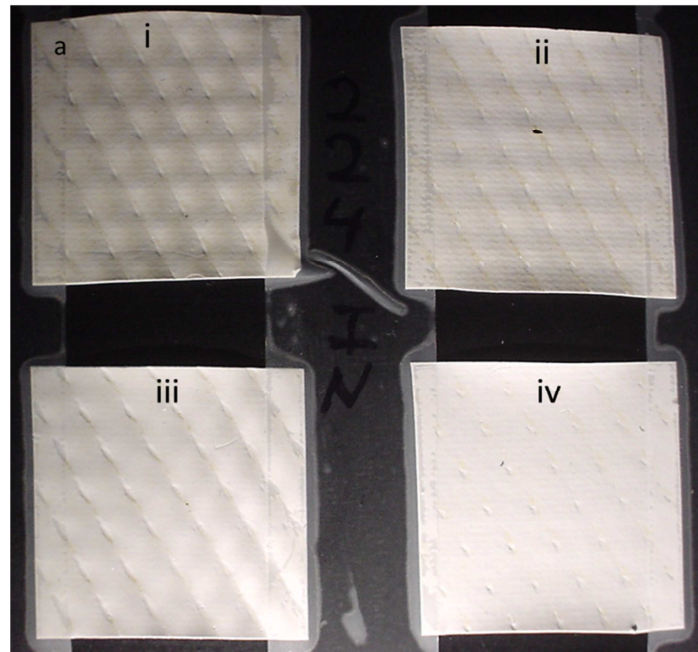


Figure 2 – a) samples representing the four corners of a SWMC leaf, b) representative sample for each leaf corner shown in (2a), c) five spectra from one single coupon showing the inhomogeneity issue.

The first layer in membrane investigations for the dairy and food industry is easily quantifiable providing that the light penetrates through the layer. Quantification of the second layer becomes more problematic because the volume of light hitting this part of the sample is unknown since some radiation is already absorbed in the previous layer (Figure 1). Moreover, the previous layer might have a varying thickness making the illuminated volume the limiting factor for the quantification.

Superimpose on this the inhomogeneity (Figure 2) and the result is a complex structure that is difficult to quantify.

Because of the limited penetration depth it is of great importance that the membrane is in close, controlled contact with the surface of the ATR device. This is one of the challenges of using IR for solid phase measurements. It is usually done by using a pressure-pin to squeeze the sample against the ATR crystal and which is in most cases installed on the ATR FT-IR interface. The pressure applied to the membrane is unfortunately difficult to control accurately even though some instruments have a simplified pressure gauge (Figure 3).

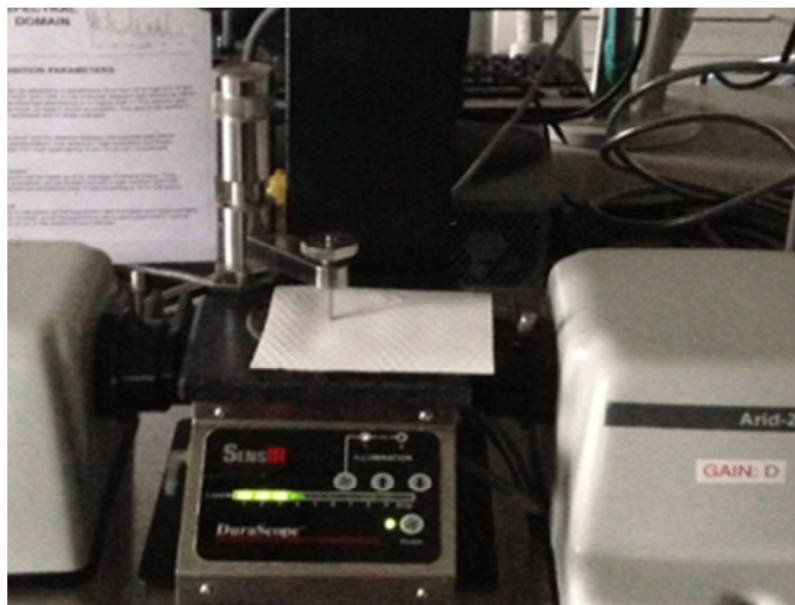


Figure 3 – Sample positioning in ATR measuring a membrane coupon extracted from a SWMC leaf, with the pressure applied indicated.

Segal et al (2011) stated e.g. that the recorded spectra can depend on the pressure applied to the membrane especially if there is a non-uniform distribution of the fouling (depth-wise). Further, by using the pin installed on the instrument with high pressures, the fouling layer is disrupted and changes in the concentration can occur. Kiefer et al. (2014) have suggested a potential solution to this problem where a rubber bung is placed between the metal pin and the membrane. The drawback is a decrease in the intensity of the spectra, but the central features of the spectra were

still visible and useable for further analysis. The pressure though is still arbitrary but this method did not break the sometimes fragile membrane and disturb the fouling.

Material

This review presents an overview of scientific publications using ATR FT-IR for the investigation of fouling in membrane systems used in food and pharmaceutical applications. As can be seen from the bibliometric analysis in Figure 4, the number of publications using ATR in combination with infrared spectroscopy is steadily inclining over recent years. Combining the search with specific membrane separation methods reduces the number of publications significantly, but it becomes obvious that infrared spectroscopy is a powerful analytical technique in membrane investigations. However, ATR instrument interfacing, with its specific strengths and weaknesses, has a limited but steady presence in modern investigations.

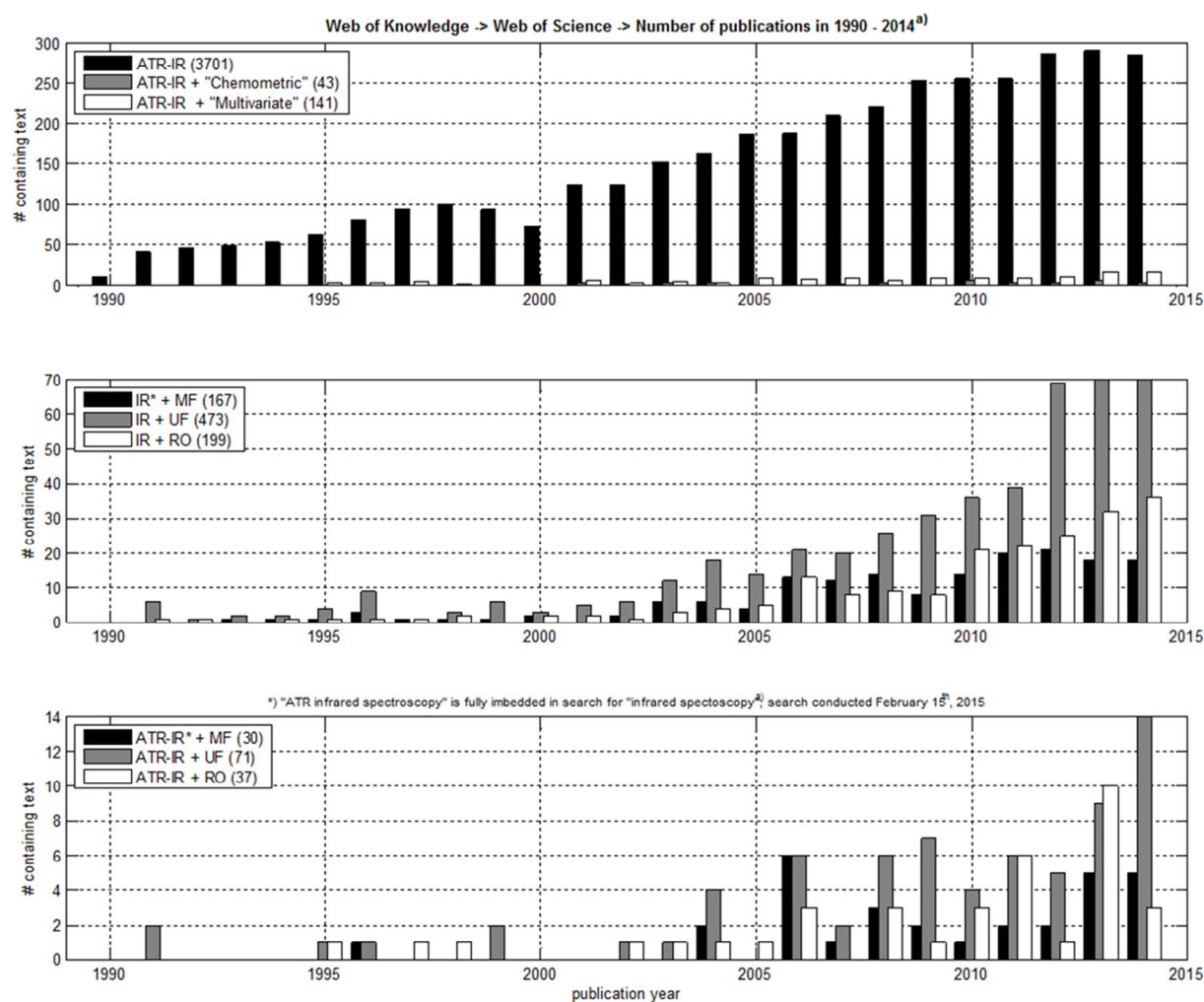


Figure 4 – development in the number of scientific papers published regarding ATR FT-IR

The identification of functional groups is the primary used data analysis with regards to ATF-FT-IR measurements; see e.g. Oldani & Schock (1989), Pihlajamäki et al. (1998), and Rabiller-Baudry et al. (2002). The functional groups present in membrane IR investigations vary largely and depend on the aim of the research. An array of other analytical techniques has been used in trying to describe the properties of the membranes and the mechanisms behind fouling and the method selected depend on the information required. Table 1 gives an overview of the type of membrane module, the analytical method(s) used, the data analysis performed and major findings. From this table it is obvious that ATR FT-IR is mostly used for identification and sometimes combined with complementary methods, in particular scanning electron microscope (SEM) along with more physical principles such as flux measurements and zeta potential to determine the effect of the cleaning of the membranes.

A large variety of membrane types and filtration units along with many different types of foulants have been investigated in the papers that are included in this review. Most of the membranes investigated are laboratory scale units such as *dead-end filtration*, *flat sheet planar modules*, *static conditioning* where adhesion to the membrane without any heating, stirring or pressure is applied, or so-called *circular vibrating houses* (VSEP). Only very few membranes from full scale real use in industry have been investigated, which is probably due the limitations raised by using publically available research, or possibly due to the problems that arise when trying to determine the true concentration of the residual fouling absorbed on the membrane, since classically controlled calibrations cannot be performed under process circumstances. A second hindrance is the costs involved when experiments are conducted with full-scale membrane SWMCs. To foul an industrial membrane in a representative manner in a laboratory setting requires special equipment and large volumes of fouling material (whey, BSA solutions or others process liquids), large volumes of water for cleaning and chemicals. Moreover, a lot of time is required as the membrane is only *properly* fouled after a certain period of usage, that is several production and CIP cycles (Berg, 2014).

The most common material used for ultrafiltration membranes are polysulfone (PSf) (Maruyama et al., 2001), polyethersulfone (PES) (Bégoin et al., 2006b) and polyacrylnitrile (PAN) (Segal et al., 2011). Other types of membranes have also been investigated including microfiltration membranes made of polytetrafluoroethylene (PTFE) (Maruyama et al., 2001) and polypropylene (PP) (Fontyn et al., 1991), polyamide for both nanofiltration (NF) (Delaunay et al., 2008) and reverse osmosis (RO) (Delaunay et al., 2008), and nylon membranes for filtration of oil/water emulsions (Gelaw et al., 2011). The fouling material can originate from many sources, most commonly from protein (BSA is often used as model molecule) (Bégoin et al., 2006b, Segal et al., 2011), oil and whey suspensions (Gelaw et al., 2011) but also characterization of membranes without fouling is a common theme (Fontyn et al., 1991, Pihlajamäki et al., 1998, Kiefer et al., 2014). Modification of the membranes is also a common theme, followed by the identification of the molecules inside the membrane matrix with IR in order to ensure that they have been properly attached, and the determination of the (change in) hydrophobic/hydrophilic properties. Shared by all investigations is that the spectra from the ATR FT-IR are used primarily for identification. Few researchers take the data analysis to the next level and use the chemical/quantitative information in the spectra

(Delaunay et al., 2008). One potential obstacle is that the producers of the membranes not always give the full recipe of the polymers used in the production and/or modifications of the basic ingredients. This limitation has been reported by several researches. There is common evidence of grafting material on the surface of unused/virgin membranes, but also on used membranes. So the differences in membranes can occur due to e.g. terminology problems (Belfer et al., 2000) where the producer identifies its membrane as polysulfone or a derivative, but in reality it has been subjected to grafting and is thereby significantly altered to a configuration that changes the properties and at the same time the IR-spectrum (Jensen et al. 2015b).

Table 1. Overview of the different literature sources.

Author (year)		Membrane module	Analytical method(s)	Data analysis	Findings
1	Oldani & Schock (1989)	Dead-end filtration	ATR FT-IR, ESCA, Contact angle measurement	Identification	Flux and retention depends on morphology and surface chemistry
2	Fontyn et al. (1991)	Static absorption (24h)	ATR FT-IR, XPS, FAB-MS	Identification, double difference method	Developed a topographic model of interactions with membrane, including hydrophobic interactions.
3	Pihlajamäki et al. (1998)	Laboratory scale	ATR FT-IR	Depth profiling, identification	Protein molecules absorb more inside pores
4	Zhu & Nyström (1998)	Laboratory scale	ATR FT-IR, flux, zeta-potential	Identification	pH and ionic strength affect the cleaning by changing charge of membrane and cleaning agent
5	Belfer et al. (1999)	Static and dead-end filtration	ATR FT-IR	Identification	Grafting changes the hydrophobicity of membranes. Water is bound to the surface due to functional groups. Broadened band is sign of hydration.
6	Belfer et al. (2000)	Dead-end filtration	ATR FT-IR	Identification	Membranes hold water in the pores even though they are dried. Terminology is a problem as producers of membranes does not tell the full story. Rehydration alters the spectra significantly
7	Maruyama et al. (2001)	Dead-end filtration	FT-IR	Deconvolution to determine height, width and position of peaks. Identification of alpha-helix, beta-sheets and turns	Amide I peak contains several structures alpha-helix, beta-sheets and turns. Gel-like deposit changes the structures of amide while the molecules attached to the membrane does not change as much
8	Rabiller-Baudry et al. (2002)	Static: Beaker glas Dynamic: Flat sheet planar module	ATR FT-IR, SEM-EDX	Double difference method	Membrane contribution depends on the thickness of the fouling. Detection limit is reached when measuring cleaned membranes.
9	Howe et al. (2002)	Dead-end filtration	ATR FT-IR, XPS	Identification, double difference method	90-95% of permeability of virgin membrane can be lost rapidly
10	Kimura et al. (2004)	Used industrial membrane, cut into smaller pieces used in laboratory scale	ATR FT-IR, Fluorescence (EEM), TOC, DOC, UV	Identification	Calcium is not contributing to irreversible fouling. Polysaccharides are responsible for irreversible fouling in water filtration.

			absorbance, Lowry, phenol-sulphuric acid method.		
11	Bégoïn et al. (2006a)	Industrial used membrane (8000h)	ATR FT-IR, SEM-EDX, SEM-FEG, AFM	Identification and quantification of protein Mapping of fouling using SEM-EDX (Ratio of peak 1538cm ⁻¹ /1240cm ⁻¹)	Fouling layer thicker at collector axis. High level of fouling at collector axis, decreases over length of membrane.
12	Bégoïn et al. (2006b)	Industrial used membrane (4 years)	ATR FT-IR, SEM-EDX, SEM-FEG, AFM	Mapping of fouling using SEM-EDX results. IR used for identification	Differences observed on the membrane are strongly connected to with the distribution of the fluid velocity in membrane. Fouling C+N+O = 99.6%, C+N = 59.3%, O = 40.3%
13	Delaunay et al. (2008)	VSEP, Plate and frame module, Industrial UF, industrial NF	ATR FT-IR, image analysis, CFD	Mapping of UF and NF, mapping deposit with regards to flow, using height ratio of peaks	Membrane mapping. Fluid velocity investigated with charcoal, spacer is important for full functionality.
14	Gelaw et al. (2011)	Dead-end filtration on nylon membrane	ATR IR-MS	SIMCA, PCA, Mahalanobis distance+residuals for outlier detection, variable selection (1800-1900cm ⁻¹)	SIMCA can classify new, fouled and cleaned membranes.
15	Segal et al. (2011)	Dead-end filtration	FTIR-PAS, UV	PLS calibration with BSA and polysaccharide	Disadvantage of IR: hard to replicate due to penetration depth and inhomogeneity.
16	Kiefer et al. (2014)	One membrane leaf	ATR FT-IR	Mapping of porosity	Porosity is key parameter and significantly influences behavior of a membrane in any given application.
17	Jensen et al. (2015a)	Industrial used membranes (4 membrane cartridges used for 5 months, 3 days to 2 years, 3 months)	ATR FT-IR	Mapping of residual fouling	Univariate data analysis is not sufficient to evaluate the full picture.
18	Jensen et al. (2015b)	Industrial used membranes (1 membrane used for 5 months, 3 days)	ATR FT-IR	Mapping of residual fouling	MCR is useful to evaluate and calculate the relative concentration of the residual fouling. The method includes relative concentration determination of both residual fouling and membrane material. ATR FT-IR exhibit problems with regards to layered samples.

Data analysis

The investigation of membranes often involves a spectroscopic method of some kind. These methods are multivariate by nature because of the multiple variables (e.g. wave numbers) measured. Unfortunately this is not fully exploited in many investigations. IR is specifically used for identification – assignment of different peaks and the description of the occurrence of some peaks and disappearance of others which is relevant when determining e.g. strategies for developing new molecular compositions where hydrophobicity/hydrophilicity is highly influential of the production and cleaning performances of the membrane. There is a general lack of multivariate data interpretation present in the current literature; only few authors have employed multivariate data analysis for modelling of the residual fouling concentration. Even fewer studies investigate industrial membranes, the only option to get actual insight into the production regimes, the flow and fouling during filtration processes. This lack of information probably originates from the fact that it is difficult to describe the flow in the membranes once they are extracted from the SWMC and dissected into smaller pieces in order to do measurements. Furthermore the concentration of the residual fouling is challenging to calculate and predict because a full mass balance is never available.

Delaunay et al (2008) e.g. describe the quantification of protein on a laboratory scale membrane, but also on a real-size UF membrane used in acid whey and skim milk powder processing and a NF membrane used for skim milk. It is investigated how the shear rate affects the deposit of protein on a membrane. This is initially done on a bench top scale in two different types of membrane modules: VSEP and a plate and frame module. From the bench top plate and frame module a model is derived for the flow and this model is visualized by means of a charcoal suspension. From this flow model it is evident that the spacers in the membrane modules are a necessity in order to keep the velocity of the flow constant over the entire membrane area. From the same measurements Delaunay and coworkers have modelled the quantitative deposition of protein over the membrane using ATR FT-IR. This determination was further developed to include an entire membrane leaf from a full scale NF module, but the mapping that emerged was unfortunately not the same as that they saw in the bench top experiment. The main reasons for the dissimilarity can be found from differences in flow and pressure/pressure drop and hours of usage. In order to calculate the concentration Delaunay et al (2008) used a relationship between the amide II peak (1520-1550 cm^{-1}

¹) and a peak from the membrane material at 1240 cm⁻¹ (PES). They subtract a baseline and multiply the intensities with a coefficient that corresponds to a certain type of membrane. The concentrations are then expressed according to a position on the original NF membrane creating a quantitative map of the residual fouling. The mapping was done on small scale filtration membranes. According to the authors, this protein mapping is a reliable technique for autopsy purposes of membrane cartridges in the dairy industry. In addition Delaunay et al (2008) used image analysis to determine the importance of spacers in the spiral wound membranes by investigating the flow in a small laboratory scale flat cell unit. Charcoal was used to mimic the deposits of fouling and to provide a visual impression of the distribution, and using this trick the authors could prove the importance of the spacers as the flow becomes laminar when they are utilized.

Segal et al (2011) were using another approach to determine the concentration of protein on a membrane using PLS. A PLS calibration from UV-VIS data (200-1100 nm) was made with two chemical components investigated: BSA and alginic acid (AA). The calibration was not initially performed on the membranes but rather on the feed, permeate and cleaning liquids. The PLS calibration was based on 140 different solutions ranging from 0-15 mg/l with regards to BSA and AA, 70 samples were used for the calibration and 70 samples were used for validation. The UV-VIS data was correlated to the total fouling and the irreversible fouling by computing a mass balance. The feed, permeate and cleaning solutions were measured with UV/VIS and using the PLS calibration the authors obtained an indication of the content of foulant in the solution and thereby an insight into the amount of fouling still attached to the membrane. Subsequently, the membranes were cut into smaller pieces and measured with photo acoustic spectroscopy (PAS) FT-IR (700-4000 cm⁻¹) and the concentration (target value) estimated with PLS on the feed, permeate and cleaning solutions correlates to that specific spectrum. The irreversible fouling was calculated as:

$$\text{irreversible fouling} = \text{total fouling} - [\text{BSA}(\text{cleaning solution})]$$

$$\text{total fouling} = [\text{BSA}(\text{feed})] - [\text{BSA}(\text{permeate solution})]$$

In the study the membranes are fouled using a dead-end filtration unit with an area of 50 cm² under a pressure of 2 bars. Obviously this procedure does not resemble closely an industrial production. Segal and coworkers also found that polysaccharides play a big role in cake layer depositing

because of the large and elongated structure of the molecules. This cake layer prevented the passage of BSA molecules and created a reversible fouling that could be removed by cleaning.

Gelaw et al (2011) have investigated a type of membrane that deviates from the common filtration membranes, namely a nylon based membrane used for filtration of a water (~90% (v/v)) and sunflower oil (~10% (v/v)) emulsion with ~1% (w/v) whey protein. The membranes were measured before use (virgin), when fouled and after cleaning using Fourier-Transform Infrared Microspectroscopy equipped with an ATR needle (ATR IRMS). The aim was to separate the different classes of spectra using soft independent modeling of class analogy (SIMCA) in order to differentiate between the virgin, fouled and cleaned membranes. Moreover the objective was to obtain qualitative information about the foulant residuals on the membrane after the application of five different cleaning protocols, where they focus on the functionality of Tween 20 (polysorbate 20). Variable selection was used to find the most significant regions of the spectra ($900-1800\text{ cm}^{-1}$) which included the amide regions from the whey and also the regions that correspond to polysaccharides (C-O-C in esters, 1099 and 1057 cm^{-1}) from the sunflower oil. Outlier detection was performed with sample residuals and Mahalanobis distances. It was concluded that the classification of the different cleaning methods and the fouling states of the membrane by SIMCA was a success and the authors accordingly recommended the use of more multivariate data analysis for gaining further knowledge in future experiments. Gelaw et al (2011) concluded that it has been proven that ATR FT-IR is useful for analyzing filtration membranes, but that the combination of ATR FT-IR and multivariate data analysis can easily be applied in the membrane field to extend the knowledge of the phenomena occurring on the membrane surfaces.

Maruyama et al (2001) used chemometric methods to evaluate the fouling material using single wavenumber variables (univariately). The purpose of the study was to determine the behavior of the protein denaturation during membrane fouling. The PSf and PTFE membranes were fouled with BSA and the fouling was lyophilized, removed from the membrane and measured with ATR FT-IR in the form of a powder. Lyophilization was utilized in order to remove any interfering water peaks from the spectra. The data analysis was performed on the amide I band ($1600-1700\text{ cm}^{-1}$) because of the intensity and position in the spectrum. Curve resolution was used to resolve the amide I peak, thereby being able to determine the position and height of the underlying peaks which provide information about the secondary structure of proteins (Byler & Susi,1986). The amide I peak was

fitted with Gaussian curves to determine width, position and height. The underlying peaks expected to be present under the amide I peak are α -helix ($1656\pm 1\text{ cm}^{-1}$), β -sheets ($1636\pm 1\text{ cm}^{-1}$) and turns ($1681\pm 1\text{ cm}^{-1}$). A second derivative method was utilized to extract data of the underlying phenomena ensuring that the correct peaks are investigated. Maruyama and coworkers concluded that the PS membrane (UF) does not affect the secondary structure of BSA while the PTFE membrane (MF) has an effect on the secondary structure; the content of α -helices decreases while the content of β -sheets increases, depended on the BSA concentration.

Another case where multivariate data analysis was used to extract information in membrane research is Bégoïn et al (2006a). In this case the data was not only collected with ATR FT-IR, but also with scanning electron microscopy with energy dispersive x-ray (SEM-EDX) which detects the elemental composition. The membrane was mapped from the results of the SEM-EDX. In this investigation they made the sampling from a membrane module used in the industry, using four different leaves from the same cartridge (referred to as number 1, 4, 5 and 7 with leaf number 1 being the inner leaf and 7 the outer leaf). It is important to keep in mind that a membrane module like this is spiral wound and it has no first/inner or last/outer leaf. The same authors also made a second reporting (Bégoïn et al 2006b) where this numeration terminology is used. It is stated in these publications that the differences observed in mapping are strongly related with the distribution of the fluid velocity in the spiral membrane. The later publication (Bégoïn et al., 2006b) is especially interesting in this context because here they measured a membrane that had reached its maximum usage in the industry, and by SEM-EDX extracted information on carbon (C), nitrogen (N) and oxygen (O) which originates from the fouling material, and sulphur (S) which originates from the membrane material. The information collected was used to map the relative relationship between (C+N)/S and the relative relationship between O/S which indicates how the residual fouling is distributed on the four different membrane leafs. ATR FT-IR was also measured and the findings in these results support the results of the SEM-EDX measurements. A deeper insight into the fouling of PES membranes was achieved by the use of modeling. The modelling shows that the membrane is most likely to foul at the center tube of the module which is visualized by graphics, making the results easy to interpret.

Conclusion

The data analysis used in the investigations of membranes has primarily been univariate with focus on the identification of relevant peaks and on the conformation of presence/absence of peaks before and after fouling. This is a pity since the IR spectra contain much more information which should be fully exploited. Calculating the precise concentration of the residual fouling should not be the only objective for a membrane investigation as it eliminates the possibility to investigate industrial/used membranes due to the impossibility to determine the precise compositions based on e.g. mass balances, the concentration calculations should rather aid in determining if a cleaning procedure is sufficiently effective and for that relative concentrations are adequate. In the case where fouling is modeled it is usually performed by calculating the *concentration* by computing the ratio between an amide peak and e.g. a *fixed* peak at 1240 cm^{-1} that originates from the PES membrane material.

ATR FT-IR measurements of membrane systems and fouling is mostly used for identification due to its powerful ability to measure even minute differences in sample composition, but so far the method has only been limited used to describe the membranes in correlation to flow, fouling or mapping. In contrast e.g. SEM-EDX and other methods are used for the mapping of the fouling because they extract atomic percentages that can thus be used mathematically with only few alterations. IR on the other hand needs more *advanced multivariate methods* to extract relevant information, but the data extracted from IR can be very useful as it describes the functional groups and to some extent their interaction, all in a relatively *soft* and non-destructive way which means less disturbance and biasing due to measurements. This larger demand for mathematical tools is probably one of the reasons why IR is still mainly used for classical identification only. The quantitative aspect requires more elaborate data handling and the multivariate nature of the IR measurements makes it a perfect candidate for a chemometric investigation.

A second aspect that emerged from this review is the need for more analysis on membranes that have been used in full scale industrial settings. Most investigations have been performed on systems that were fouled in minor laboratory scale units or dead-end filtration units for a very limited amount of time. The industrially used membranes are quite expensive and more difficult to handle, but better information on an industrial level is needed e.g. in order to explore new CIP strategies.

The membranes from a laboratory scale experiment do not offer sufficiently realistic insight into production scale fouling patterns and repetitive usage.

References

L. Bégoin, M. Rabiller-Baudry, B. Chaufer, M. Hautbois, T. Doneva, Ageing of PES industrial spiral-wound membranes in acid whey ultrafiltration, *Desalination* 192 (2006a) 25-39

L. Bégoin, M. Rabiller-Baudry, B. Chaufer, C. Faille, P. Blanpain-Avet, T. Bénézech, T. Doneva, Methodology of analysis of a spiral-wound module. Application to PES membrane for ultrafiltration of skimmed milk, *Desalination* 192 (2006b) 40-53

S. Belfer, J. Gilron, O. Kedem, Characterization of commercial RO and UF modified and fouled membranes by means of ATR/FTIR, *Desalination* 124 (1999) 175-180

S. Belfer, R. Fainchtain, Y. Purinson, O. Kedem, Surface characterization by FTIR-ATR spectroscopy of polyethersulfone membranes-unmodified, modified and protein fouled, *Journal of Membrane Science* 172 (2000) 113-124

T.H.A. Berg, Fouling and cleaning of membrane systems in the dairy industry – Towards optimization of micro- and ultrafiltration processes, PhD Thesis, Department of Food Science, University of Copenhagen (2014)

T.H.A. Berg, J.C. Knudsen, R. Ipsen, F.W.J. van den Berg, H.H. Holst, A. Tolkach, Investigation of consecutive fouling and cleaning cycles of ultrafiltration membranes used for whey processing, *International Journal of Food Engineering*, *International Journal of Food Engineering* 10 (2015) 367-381

R. Bro, A.K. Smilde, Principal component analysis, *Analytical Methods* 6 (2014) 2812-2831

D. Byler, H. Susi, Examination of the secondary structure of proteins by deconvoluted FTIR spectra, *Biopolymers* 25 (1986) 469-487

J.M. Chalmers, P.R. Griffiths, *Handbook of Vibrational spectroscopy, Sampling Techniques*, volume 2, John Wiley & sons, LTD (2002)

D. Delaunay, M. Rabiller-Baudry, J.M. Gozálvez-Zafrilla, B. Balannec, M. Frappart, L. Paugam, Mapping of protein fouling by FTIR-ATR as experimental tool to study membrane fouling and

fluid velocity profile in various geometries and validation by CFD simulation, *Chemical Engineering and Processing* 47 (2008) 1106-1117

M. Fontyn, K. van't Riet, B.H. Bijsterbosch, Surface spectroscopic studies of pristine and fouled membranes, Part II. Method development and adsorption mechanisms, *Colloids and Surfaces* 54 (1991) 349-362

T.K. Gelaw, A. Trentin, C. Güell, M. Ferrando, L.E. Rodríguez-Saona, S. de Lamo-Castellví, Attenuated total reflectance infrared microspectroscopy combined with multivariate analysis, a novel tool to characterize cleaning efficiency of organic microfiltration membranes, *Journal of Membrane Science* 376 (2011) 35-39

H.H. Holst, F. van den Berg and S.B. Engelsens, "Water reuse and saving in the food industry: A new frontier in food manufacturing", *New Food*, Volume 17, (2014) 49-52

K.J. Howe, K.P. Ishida, M.M. Clark, Use of ATR/FTIR spectrometry to study fouling of microfiltration membranes by natural waters, *Desalination* 147 (2002) 251-255

J.K. Jensen, N. Ottosen, S.B. Engelsens, F. van den Berg, Investigation of UF and MF Membrane Residual Fouling in Full-Scale Dairy Production Using FT-IR to Quantify Protein and Fat, *International Journal of Food Engineering* 11 (2015a) 1-15

J.K. Jensen, J.M.A. Rubio, S.B. Engelsens, F. van den Berg, Resolving ATR-FT-IR spectra of Protein Residual Fouling on Membranes using MCR, submitted (2015b)

A. de Juan, J. Jaumot, R. Tauler, Multivariate Curve Resolution (MCR). Solving the mixture analysis problem, *Analytical Methods* 6 (2014) 4964-4976

J. Kiefer, N.H. Rasul, P.K. Ghosh, E. von Lieres, Surface and bulk porosity mapping of polymer membranes using infrared spectroscopy, *Journal of Membrane Science* 452 (2014) 152-156

K. Kimura, Y. Hane, Y. Watanabe, G. Amy, N. Ohkuma, Irreversible membrane fouling during ultrafiltration of surface water, *Water Research* 38 (2004) 3431-3441

M. Lin, B.A. Rasco, A.G. Cavinato, M. Al-Holy, *Infrared Spectroscopy for Food Quality Analysis and Control*, Elsevier (2009), first diction, Editor Da-Wen Sun

T. Maruyama, S. Katoh, M. Nakajima, H. Nabetani. T.P. Abbott, A. Shono, K. Satoh, FT-IR analysis of BSA fouled on ultrafiltration and microfiltration membranes, *Journal of Membrane Science* 192 (2001) 201-207

D.L. Massart, B.G.M. Vandeginste, L.M.C. Buydens, S. de Jong, P.J. Lewi, J. Smeyers-Verbeke, Handbook of Chemometrics and Qualimetrics Part A, Elsevier (1997)

M. Oldani, G. Schock, Characterization of Ultrafiltration Membranes by Infrared Spectroscopy, ESCA, and Contact Angle Measurements, Journal of Membrane Science 43 (1989) 243-258

A. Pihlajamäki, P. Väisänen, M. Nyström, Characterization of clean and fouled polymeric ultrafiltration membranes by Fourier transform IR spectroscopy-attenuated total reflection, Colloids and Surfaces, A: Physicochemical and Engineering Aspects 138 (1998) 323-333

M. Rabiller-Baubry, M. Le Maux, B. Chaufer, L. Bégoïn, Characterisation of cleaned and fouled membrane by ATR-FTIR and EDX analysis coupled with SEM: application to UF of skimmed milk with PES membrane, Desalination 146 (2002) 123-128

C. Regula, E. Carretier, Y. Wyart, G. Ge´san-Guiziou, A. Vincent, D. Boudot, P. Moulin, Chemical cleaning/disinfection and ageing of organic UF membranes: A review, Water research 56 (2014) 325-365

Y. Segal, R. Linker, C.G. Dosoretz, Quantitative estimation of protein fouling of ultra-filtration membranes by photoacoustic spectroscopy, Desalination 271 (2011) 231-235

J. Wagner, Membrane Filtration Handbook, Practical Tips and Hints, Second edition, second revision, Printed by Osmonics (2001)

S. Wold, M. Sjöstrom, SIMCA, a method for analyzing chemical data in terms of similarity and analogy. In: Chemometrics: Theory and Application, American Chemical Society, Editor B.R. Kowalski (1977), 243-282

S. Wold, M. Sjöstrom, L. Eriksson, PLS-regression: a basic tool of chemometrics, Chemometrics and Intelligent Laboratory Systems 58 (2001) 109-130

H. Zhu, M. Nyström, Cleaning results characterized by flux, streaming potential and FTIR measurements, Colloids and Surfaces, A: Physicochemical and Engineering Aspects 138 (1998) 309-321

Poster I

C.B. Lyndgaards, J.K. Jensen, S.Knøchel, F. van den Berg

Process Water – Minimizing Industrial Water Use by In- Process Cleaning Diagnostics

Presented at the Danish Water Forum (DWF), GEUS, Copenhagen, Denmark (2012)

Process Water - Minimizing Industrial Water Use by In-process Cleaning Diagnostics

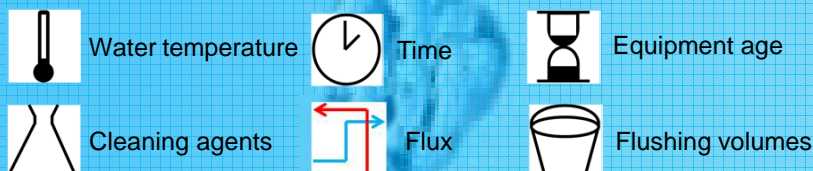
Christian B. Lyndgaard^{*)}, Jannie K. Jensen, Susanne Knøchel, Frans v.d. Berg
 Department of Food Science, Faculty of Life Sciences, University of Copenhagen, ^{*)} chha@life.ku.dk

Objective

To optimize cleaning efficiency in the food industry by:

- Develop of fast in-line cleaning validation sensors
- Evaluate cleaning factors by statistical design of experiments

Cleaning factors to be optimized:

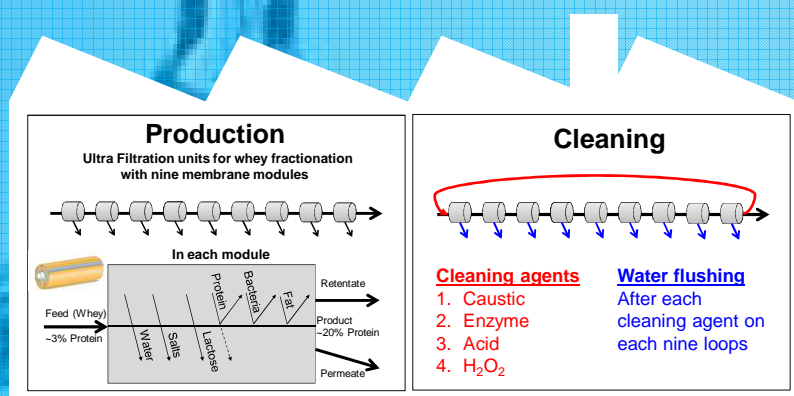


Case: Cleaning membrane unit

Fractionating dairy products by membrane ultra filtration (UF) plays an important role in manufacturing of many products for the food and ingredients industry. Cleaning of membranes has a large influence on the efficiency of the UF operation.

After a given amount of production time without cleaning the performance of the membrane modules will decrease and energy demand to maintain equal flux will become excessive.

The required Cleaning In Place (CIP) step cuts away a considerable time from the continues production capacity of a factory and a high CIP efficiency is thus of substantial economic importance.



Cleaning by recipe

Cleaning of UF membranes is recipe driven. A fixed program (often provided and decide by the equipment vendor) is used to guarantee chemical and microbiological cleanliness. This procedure does not take into consideration the long-term, on-site performance of the equipment nor the short-term production history.

Towards active control ...

Approach

In our research we investigate an active control strategy for CIP of UF facilities. The first step is to get a detailed overview of the chemical composition of residues removed in the different cleaning steps.

Sampling and measurements

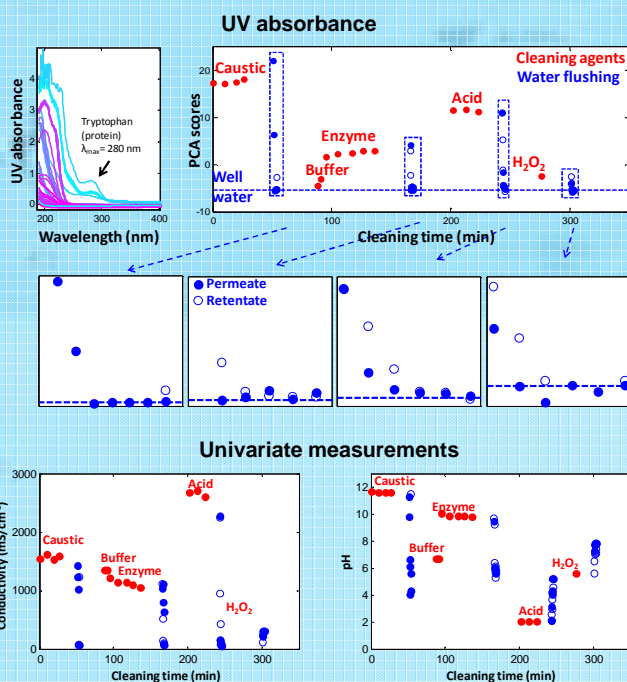
A large number of outlet grab samples from the permeate plus retentate side of a UF unit were analyzed by three potential sensor based monitoring methods which could work for automatic CIP control:

- > Absorption of ultraviolet light
- > pH
- > Electrical conductivity

Result

The multivariate response from UV absorbance were subjected to Principal Component Analysis and the development of the first score (a unit less pseudo-concentration) is showed in the figure (right). UV absorbance during the water flushings (zoom plots) appears to reach the level of well water very early during flushing. This suggests that water flushing could be terminated earlier in the particular cleaning process, which opens up for the possibility of reducing water consumption.

Methods for CIP monitoring



Det Strategiske Forskningsråd og Rådet for Teknologi og Innovation står bag initiativet og bevillinger til inSPIRe. Industri og fonde bidrager ligeledes med bevillinger til inSPIRe..

Poster II

J.K. Jensen, F. van den Berg

Mapping of UF Membrane Residual Fouling in Full Scale Dairy
Production using FT-IR to Quantify Protein and Fat

*Presented at the 13th Scandinavian Symposium on Chemometrics (SSC13), Stockholm,
Sweden*

Mapping of UF Membrane Residual-Fouling in Full Scale Dairy Production using FT-IR to Quantify Protein and Fat



Jannie K. Jensen^{a,*}, Frans van den Berg^a

^a University of Copenhagen, Science, Department of Quality and Technology, Rolighedsvvej 30, 1958 Frederiksberg C

* Corresponding author: janniekj@life.ku.dk

Abstract

The residual-fouling present on spiral wound polyethersulfone after cleaning-in-place of full scale production ultrafiltration membranes was investigated with special interest in protein (amide I and amide II) and fat residue. The residual-fouling was determined by ATR-FT-IR where three spectral regions were used: amide I (1500-1515 cm^{-1}), amide II (1645-1670 cm^{-1}) and fat (1720-1760 cm^{-1}). Each of the peaks found in these spectral regions was fitted by Cauchy-Lorentz or Gaussian distributions via non-linear regression in order to quantify the area under the peak. This number can be used in further statistical calculations, regardless of varying spectral backgrounds. ANOVA is used to evaluate the significance of the four factors affecting the model (leaf inside a cartridge, inside/outside membrane layer, Distance From Feed/DFC, and Distance From Center/DFC). DFF, DFC and DFC² turned out to be statistically significant factors in the residual-fouling response-surface models of the membranes. Evaluating the contour plots of amide I, amide II and fat from the experiments similar characteristic patterns expressed are found regardless of the membrane and the fouling agent.

Introduction

The dairy filtration industry uses considerable volumes of water every day for cleaning in order to maintain the required hygienic standards and to keep their operations running at satisfactory capacity. This translates into a large use of resources in the form of potable water being consumed and in production downtime while cleaning-in-place (CIP) takes place.

After CIP this water it is led back to the waste management facilities which, depending on the state of the water, can be a costly and energy demanding process.

In the Danish dairy industries a substantial effort is made to minimize the use of water and time in cleaning. This research includes increased knowledge on the state of the ultrafiltration (UF) membrane cartridges that are routinely used in the milk powder production from whey.

Conclusion

It is possible to identify a characteristic pattern of residual-fouling for the UF membrane cartridges investigated. The DFF and DFC directions have a significant influence on the findings in all the ANOVA investigations performed on amide bands. The concentrations of both amides are highest at the center tube and decreases towards the glued edge along the DFC direction. Similar results have been presented by Schwinge et al (J. of Membrane Science 242, (2004) 129-153). ATR-FT-IR analysis is discriminatory in the sense that it can differentiate two different types of residual-fouling in the layer on chemical (IR finger printing) rather than physical (thickness) grounds. The staining for proteins as applied to the membranes aided in describing and understanding the residual fouling on the membrane and helped identify the inhomogeneity that can cause large variation in the measurement results.

Processing of whey

Sweet whey

- Byproduct when making rennet types of hard cheeses.
- Initial total true protein (TTP) concentration around 0.54% (w/w) and a lactose concentration of 4.05% (w/w).
- After filtration the average TTP content of the retentate and permeate is 22.76% (w/w) and 0.03% (w/w), respectively.
- The lactose concentration also decreases during filtration to averages of 2.37% (w/w) and 3.94% (w/w) for retentate and permeate

24h production

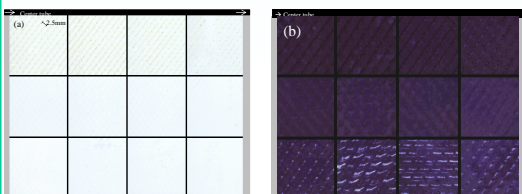
Cleaning started

CIP cycle (6-7h)

- Flushing – removes free material and particles
- Caustic – removes layer and unfold protein for enzymatic cleaning
- Flushing
- Enzyme – removes proteins attached or integrated in the membrane
- Flushing
- Acid – removes minerals
- Flushing
- Hydrogen peroxide – disinfection
- Flushing

Membranes extracted from process line (app. 1 year in use)

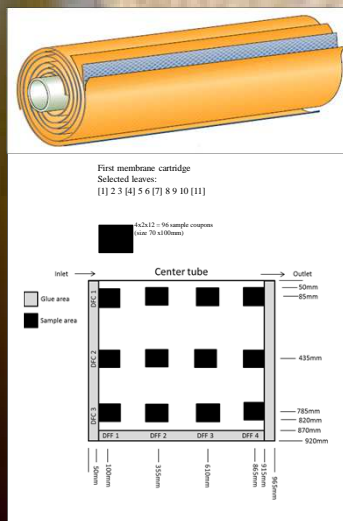
Membranes contains residual fouling
(a) No staining (b) Stained fouling



Materials and methods

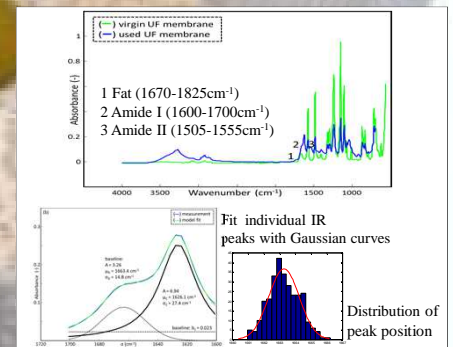
Membrane leaves from a whey processing are cut into coupons that is considered our sample unit for the experiment.

The membrane is an ultrafiltration cartridge, and membrane sheet material is polyethersulfone. The unit consists of 11 leaves with an inside/outside layer. Cutting the membrane into coupons creates 96 samples where triplicate measurements at random positions are performed on each object.



Data analysis

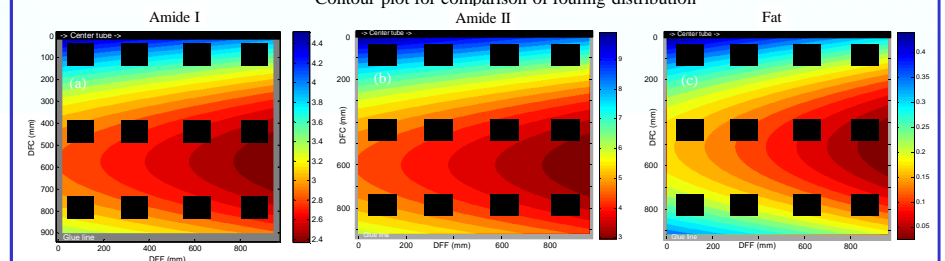
Determine peak area by non-linear regression in IR spectra for protein (amide I and amide II) and fat. For the data analysis of the FT-IR measurements three specific regions of the spectra that are known to be influenced by the residual-fouling constituents are compared:



Determine area under curve as an indirect indicator for concentration

ANOVA determines the important factors creating a surface response model on maximum values

Contour plot for comparison of fouling distribution



**SPECTROSCOPY AND CHEMOMETRICS RESEARCH GROUP
DEPARTMENT OF FOOD SCIENCE
FACULTY OF SCIENCE, UNIVERSITY OF COPENHAGEN
PHD THESIS 2015**

JANNIE KROG JENSEN

Investigation of Filtration Membranes from the Dairy Protein Industry for Residual Fouling using Infrared Spectroscopy and Chemometrics



Infrared spectroscopy is one of the vibrational analytical methods. It measures and quantifies the vibration and is particularly sensitive towards the functional groups in the molecule. It provides information on chemical structure and has several other advantages such as being non-invasive, fast and requiring no or minimal sample preparation.

The main aim of this thesis work is to characterize the residual fouling on ultrafiltration and microfiltration real size production membranes with infrared spectroscopy. By investigating the infrared spectroscopic data it became evident that the method has some pitfalls when looking at inhomogeneous, layered, (semi-) solid samples such as the filtration membranes.

To provide a better overview of the residual fouling Multivariate Curve Resolution is utilized. The MCR method improved the interpretation of the models considerably compared to alternative methods. However, it also became evident that the penetration depth of the infrared beam creates additional complexity when measuring semi-solid layered samples.

In conclusion, the research in this dissertation has shown that the use of infrared spectroscopy in combination with multivariate data analysis improved the understanding of the residual fouling on real size production membranes and can assist in the design of new membranes, membrane grafting and membrane cleaning procedures in industry.